A STUDY OF LIQUIDS IN HIGH POWER LASER SYSTEMS

A.C.Selden

Thesis submitted for the degree of Doctor of Philosophy at the University of London.

June 1970

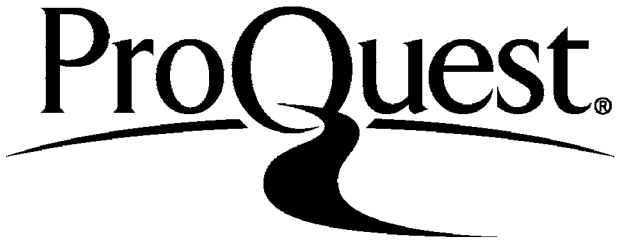

ABSTRACT

The influence of liquids in the laser beam on the emission and propagation characteristics of intense pulsed neodymium lasers is described. Results are presented on Q-switching by a thermal effect in organic solvents, on basic self-modulation and mode-locking processes in an oscillator, and on the transmission and amplification of picosecond light pulses in an inorganic liquid laser.

Mary, Julian, Clive and Sean

PREFACE

The present study has its origins in the continuing development of high power pulsed neodymium lasers, which at the time of writing can produce single pulses of light of peak power 10^{10} to 10^{13} watts and duration 10^{-9} to 10^{-11} seconds[8,79,88,128]. The corresponding energy content of these powerful light pulses is of the order 10 to 100 joules[126] and will no doubt be increased to the kilojoule region in the near future. The main motivation behind this development in lasers is that it offers a clean way of producing very hot dense plasma for use in thermonuclear fusion experiments, sufficiently hot to release neutrons from nuclear reactions induced by the extreme irradiance at the laser focus[127].

The generation of such intense light pulses requires a powerful laser system consisting of an oscillator and a high gain amplifier chain. The oscillator produces a pulse of suitable duration but relatively low energy which is directed into the laser amplifier. Here it grows by stimulated emission from the prepared population inversion, reaching energies of tens of joules and peak powers of at least 10^{10} watts, as noted above. The pulse width is continually reduced as a result of gain saturation, and the intensity increases to the point where the pulse depopulates the inversion in a time comparable with the inverse spectral bandwidth, which is $\sim 10^{-12}$ sec. for a typical solid state

laser. Thus in an infinite amplifier the propagating pulse approaches a steady state, the 'π pulse' or 'limit pulse', whose width is of the order of the inverse bandwidth of the amplifying medium and whose peak intensity is set by the dipole moment of the transition and the scattering losses[44,45].

The study of a high power laser system can be divided into two separate parts, one concerning the laser oscillator, the other the laser amplifier, in which the former may serve as a convenient signal source for determining the response of the latter. Liquids can enter into both aspects of such a study, and it this observation which provides the framework of the thesis.

The reason liquids are of special interest in laser research is that they exhibit a large number of interactions with light, most of which are either inherently non-linear or become so through stimulated processes occurring above some well defined threshold power or intensity. Once this is reached a co-operative interaction ensues between the liquid and the radiation field, and it grows at an exponential rate until saturation sets in. Because of this self-acting property of the system quite a small coupling results in an ultimately large effect, and growth is rapid because of the high propagation velocity of the electromagnetic field and the limited dimensions of the interaction region. If a liquid and a laser oscillator are allowed to interact by exchanging energy with the radiation field, quite dramatic effects, such as powerful Q-switching of the laser[19,40] are observed.

We therefore begin by reviewing optical effects in liquids (Chapter I), a field revolutionised by the advent of the laser, with particular emphasis on those active phenomena which are most relevant to the behaviour of laser systems incorporating liquids. In Chapter 2 the principles and practice of mode-locking are discussed as a means of generating ultra-short light pulses of duration 10^{-11} to 10^{-12} sec., since it is these which are of interest in very high power laser systems. This is followed in Chapter 3 by a short review of the neodymium inorganic liquid laser, a broad band high gain material which may replace neodymium glass in high power systems and thereby obviate the damage problem associated with the use of solid state lasers[114].

The next three chapters are concerned with the results and interpretation of some experimental studies of lasers and laser-liquid interactions. It is shown in Chapter 4 that many common organic solvents Q-switch the neodymium laser, a finding interpreted in terms of the formation of thermal phase gratings in weakly absorbing liquids. The influence of dielectric plates on the emission of a laser oscillator, and the relevance of this for studies of mode-locking are discussed in Chapter 5. Finally, in Chapter 6, we describe the performance of the neodymium liquid laser in amplifying picosecond pulses generated by a mode-locked neodymium glass oscillator. A summary and evaluation of the results is given in a short concluding chapter (Ch.7), together

with some remarks on applications and guide lines for further research.

Many, possibly all, laser phenomena can be considered as different aspects of the principle that stimulated emission is self-optimising, a principle originally applied to observations of spontaneous mode-locking[104], where the phases of the laser modes appear to adjust themselves to minimise losses and maximise the gain by stimulated emission[105]. In this way it should be possible to achieve a general description of laser behaviour. This self-optimising ability is illustrated in the growth of modes in the cavity of a laser oscillator, and its origin may perhaps be understood by considering the dynamic processes involved. The gain associated with stimulated emission causes the excited radiation modes to grow in intensity at the expense of the population inversion, the more intense ones successfully competing with the weaker ones and thereby narrowing the emission linewidth to a small fraction of that observed for normal fluorescence[66]. This compression of the radiation into relatively few modes of high intensity is an important feature of stimulated emission and leads to extreme brightness of the radiation field, many orders of magnitude greater than that obtainable from thermal sources of comparable energy. This self-brightening of a radiation field through its interaction with an inverted population represents a temporary reversal of entropy flow brought about by preparing the radiation source in a state of negative temperature, the

thermodynamic consequences of which are just those observed.

It is a pleasure to acknowledge the very real support and encouragement of Dr. G.Magyar during the greater part of this work and to thank both him and Dr. J.Katzenstein of Culham Laboratory for the many fruitful discussions and constructive arguments we have had on the finer points of it. I also wish to thank Professor S.Tolansky for his able supervision and encouragement toward precise statement of results. I am grateful to Royal Holloway College for academic support, to the UKAEA for a fellowship and for the opportunity to use the extensive facilities of Culham Laboratory, to Dr.D.E.Evans and Mr.M.J.Forrest and other members of Culham staff for discussions, and to Mr.F.Hudswell and Miss B.Maude of AERE Harwell for preparing the liquid laser solutions. Finally my appreciation to my family for their forebearance and understanding over a period of several months encroachment on their leisure, and to the young governor of Thebes under whose pale gaze much of this thesis was vritten.

CONTENTS

About nature consult nature herself.

Francis Bacon

CHAPTER I Optical effects in liquids

I.I Introduction

Liquids are frequently used to provide certain controlling and selective functions in high power lasers, and offer a simple and versatile means of introducing active material e.g. organic dyes, into the system for these purposes. They conveniently divide into two classes: I) the common organic solvents 2) certain inorganic solvents suitable as laser host media. Because the chosen liquid is incorporated in the active system and is traversed by the intense optical beams generated by the laser, it is necessary to consider what effect this may have on the character of the light emitted.

The interaction of light with liquids takes place through the scattering of light from various fluctuations in the liquid medium, through field effects which distort the liquid from its equilibrium state, and through molecular scattering. Most of the physical processes involved in such interactions are well known optical and field effects observed originally with low intensity incoherent light and weak fields, but with the advent of the laser the magnitude of such effects is greatly increased, and for sufficiently intense coherent light stimulated processes are generated, thus enriching the study of optical effects in liquids. Briefly, these arise through the coherent generation of disturbances in the liquid medium by the conversion of electromagnetic energy into those statistical fluctuations already present and having the correct wave vector relations

with the incident electromagnetic field. The result is an exponential growth in amplitude and a significant exchange of energy between the two fields, many orders of magnitude greater than for the incoherent processes observed with low intensity incoherent thermal light. The existence of stimulated effects is important in two ways, firstly in making possible the detailed study of liquid optical properties, and secondly in affecting or even controlling the nature of laser generation and emission in a practical system. This second aspect is the one with which we are concerned. It also divides naturally into two parts, the first involves studying the behaviour of the laser oscillator, where liquids introduce novel effects, the second arises from the use of a liquid medium as the host material of a high power laser amplifier (Chapters 3 and 6).

The chief optical effects germane to the problem of high power laser systems are:

Rayleigh scattering of light by thermal and molecular fluctuations in the liquid, in which the frequency of the scattered light is essentially unchanged

Mandel'shtam-Brillouin scattering of light by density fluctuations (sound waves)

Raman scattering by optical excitation of molecular energy levels

Optical Kerr effect - polarisation of the liquid by the optical field

Electrostriction - density increase in high field regions

by mass transfer (molecular streaming)

Thermal effects - build up of temperature and density fluctuations in optically absorbing liquids.

I.2 Optical scattering in transparent liquids

It is clear that light incident on a liquid can be scattered by a number of processes, some of which are random fluctuations in the properties of the liquid considered as a classical fluid, and others which occur through the actions of molecules, either through random fluctuations in their orientation and position, or through changes in their internal energy. In the case of inelastic scattering the scattered light suffers a frequency shift to either a higher or a lower frequency, depending on whether a nett gain or loss of energy occurs, and the scattering spectrum associated with monochromatic incident light is therefore symmetric about the incident frequency. Such a spectrum[I] is reproduced in Fig. I.Ia). The central component corresponds to Rayleigh scattering[2] from thermal and molecular anisotropy fluctuations[3]; the latter are due to Brownian motion of the molecules in the liquid and their vibration in the field of neighbouring molecules[I,4]. The frequency is essentially unchanged so that the line is symmetric about zero frequency shift, its width being determined by the decay of entropy fluctuations due to thermal diffusion in the fluid[3,5], and the extent of the wings by the damping of molecular anisotropy fluctuations[4]. The characteristic

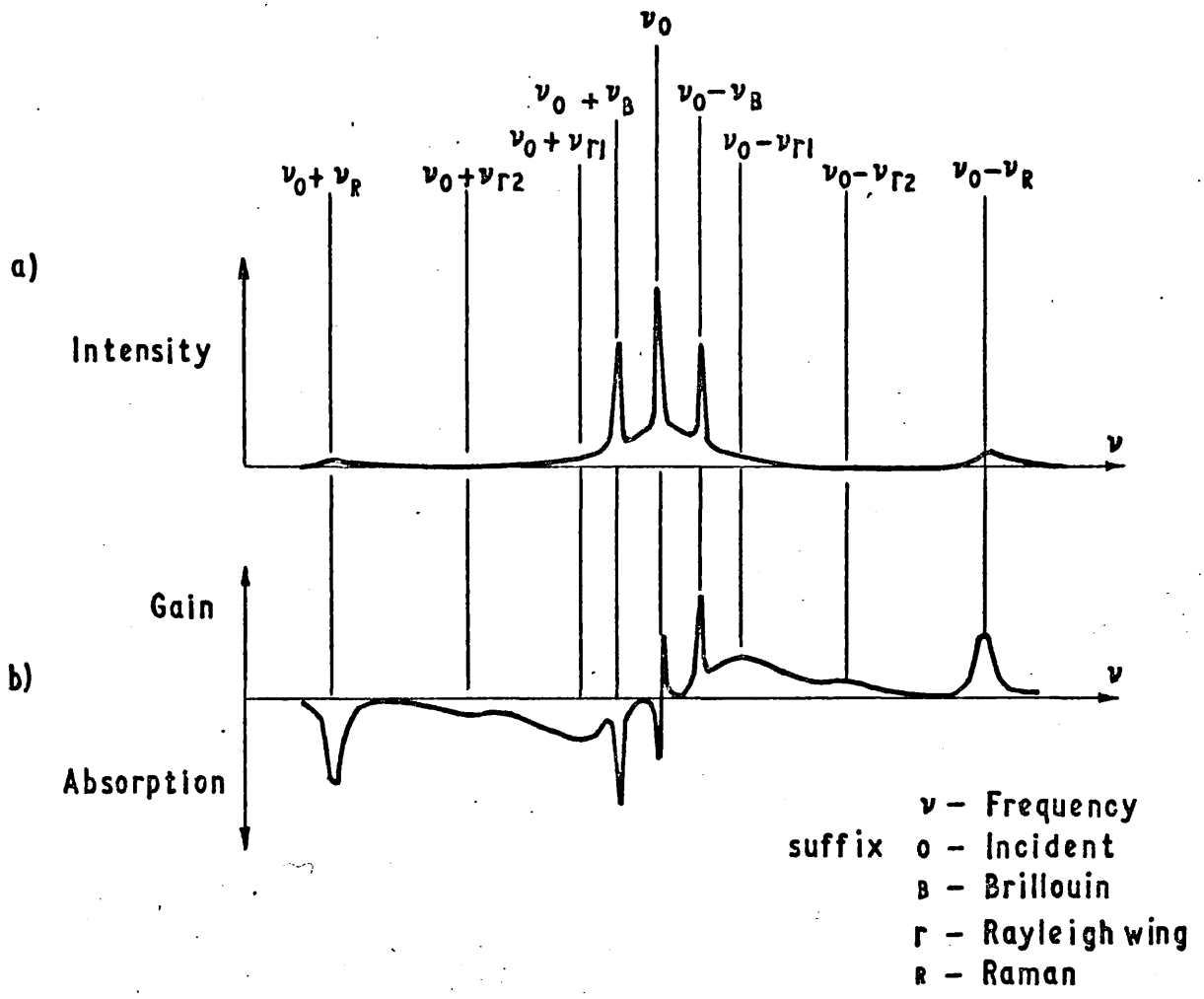

Fig. 1.1 a) Spontaneous and b) stimulated scattering spectra for a pure liquid (from ref.1).

decay times are 10^{-7} to 10^{-8} sec. for thermal diffusion damping[1,6] and 10^{-12} to 10^{-13} sec. for molecular damping[4,7], corresponding to a width 10^{-3} cm^{-1} for the Rayleigh central component and an extension 150 cm^{-1} for the wings, for scattering in the visible part of the spectrum. For spherically symmetric molecules, such as CCl_4, there can be no scattering due to anisotropy fluctuations[1,4,15,16].

Equally spaced on either side of the central Rayleigh line are the pair of lines known as the Brillouin doublet[3,5] which result from scattering by density fluctuations propagating in the fluid with the velocity of sound. The frequency shift of the light scattered through an angle θ is[3]:

$$\nu_B = \pm 2\nu_L \frac{v}{c'} \sin \tfrac{1}{2}\theta \qquad (1.1)$$

where ν_L is the frequency of the incident light, v the velocity of sound and c' the velocity of light in the liquid. The amount of this shift is generally in the range 0.1 to 0.5 cm^{-1} for backward scattering ($\theta = 180^\circ$) in common liquids.[9] The width of the Brillouin lines is determined by the attenuation of hypersound, and is of the order 10^{-2} cm^{-1} [10].

Finally, we consider Raman scattering[11], whereby an incident photon is inelastically scattered by a liquid molecule, and gains or loses energy according to whether it causes the molecule to make a transition to a lower or a higher energy level. Only the vibrational bands are normally observed in liquids, and the corresponding frequency shifts in the scattered

light range from 200 to 3000 cm^{-I} approximately. These are characteristic of the molecular vibration states and not of the incident light, the shift being independent of the incident wavelength. Since in thermal equilibrium there are a larger number of molecules in the ground state, the intensity of the Stokes shifted i.e. lower frequency Raman band is greater than that of the anti-Stokes band (higher frequency). The bands are however still symmetrically disposed about the central Rayleigh line, with an overall intensity IO^{-3} of the Rayleigh scattered light(I2).

Turning now to stimulated scattering, we can construct an analogous spectrum(I) showing the nett gain or absorption associated with the different scattering processes (Fig. I.Ib), where now the scattered intensity can assume large values under stimulated emission, approaching that of the incident intensity. Stimulated scattering from liquids thus assumes importance in high power laser systems containing them.

Observation of stimulated scattering with a giant pulse laser as the light source is used extensively in determining liquid parameters. Cho et al.(I3) and Foltz et al.(I4) have used stimulated Rayleigh wing scattering (SRWS) to measure molecular re-orientation times in benzene derivatives by relating the frequency shift of the scattered light to viscosity and temperature. As with all stimulated processes SRWS has a distinct threshold intensity, withaa minimum at a frequency shift $\frac{1}{\tau}$, where τ is the anisotropy relaxation time(I5).

Intense stimulated scattering of the central Rayleigh component (SCRS) occurs in certain liquid mixtures due to concentration fluctuations, which are enhanced by interaction with the incident light[16].

The velocity of hypersound in liquids and glasses has been found from the observed frequency shift of the stimulated Brillouin back-scattered light[9]. A series of lines equally spaced in frequency is observed when monochromatic light from a powerful laser is focused in the liquid sample. These are attributed to optical mixing, where the first order Brillouin shifted line is amplified in the laser until it is sufficiently intense to excite its own stimulated Brillouin scattering, with an equal shift in frequency, and so on, the process being limited only by the spectral width of the laser gain. This stepwise progression to lower frequencies has been used as a delayed pulse transmission switch in a Q-switched laser[17]. High stimulated Brillouin gains of e^{25} are possible[1] and can produce a 'liquid mirror' effect, with up to 90% of the incident laser light being reflected[18]. This effect can be used as a means of self Q-switching a laser by incorporating the liquid cell in the oscillator cavity at the focus of a lens to increase the incident intensity. As stimulated emission in the laser increases, stimulated Brillouin backward scattering of the light also increases and results in a dynamic reflectivity process which builds the laser emission rate to very high levels, such that the inverted population is rapidly depleted and a giant pulse generated. 100 MW pulses

with 25 ns. half-width are reported using this technique[19].

Stimulated Raman scattering was first observed[20] in the cavity of a giant pulse ruby laser Q-switched by means of a nitrobenzene Kerr cell, which emitted about 20% of the total laser energy at the Raman shifted wavelength of 7670 Å. It was soon shown that SRS could be produced in a number of benzene derivatives and compounds with a frequency shift appropriate to the molecular species involved, and with the common feature of a sharp threshold dependent on the incident intensity and the length of the liquid cell[21]. As with SBS, SRS gives rise to strong back reflection, and even amplification, of the incident light under appropriate conditions[22]. Since the large Raman shift moves the scattered frequency well outside the laser amplification bandwidth, the effect can be used to control the rate of emission in an oscillator cavity by depleting the cavity photon density available at the laser emission wavelength. In this way smooth pulses up to 3 μs. long can be produced[23].

I.3 Field effects

In addition to pure scattering effects initiated by fluctuations in the liquid are those produced by the electric field of the incident light, which distorts the medium. Under the action of an applied electric field an isotropic dielectric becomes optically bi-refringent, with the principal axis coinciding with the direction of the field. This is the Kerr effect[24]. The principal value of the dielectric tensor in

the field direction takes the form:

$$\varepsilon_{\parallel} = \varepsilon_{o} + \alpha E^{2} \qquad (I.2)$$

where ε_{o} is the scalar dielectric constant, E is the applied electric field and α the polarisability of the medium. If the electric field is that of an incident light beam we may call this the optical Kerr effect, where E^2 is averaged over many cycles of the optical frequency owing to the relaxation time of the order of 10^{-11} sec. for molecular re-orientation and re-distribution in the liquid. Thus the magnitude of the optical Kerr effect is proportional to the intensity of the incident light. One practical consequence of the resultant increase in refractive index is the formation of several intense filaments from an initially uniform beam of light by the phenomenon of self-focusing[25,26]. This occurs when the refractive index change induced in the liquid is sufficient to counteract the tendency of the beam to spread by diffraction. When the power in the indident beam exceeds the critical value[26] the beam diameter decreases with distance travelled and the beam becomes self-trapped[27]. The greatly increased intensity enhances stimulated scattering effects and reduces the threshold power required for their observation. This has been shown in the case of stimulated Raman scattering for example[28]. Self-trapping results in filaments of only a few microns diameter with intensities greater than 10^{9} W.cm^{2}[29]

Up to 90% of the light in the trapped filament is converted to the Raman shifted frequency. The filaments have a limited lifetime of the order of 0.5 ns., after which instability sets in and electric breakdown[30] and expansion of the channel at the shock velocity occur[31]. This would set an upper limit to the power in a liquid laser amplifier, beyond which catastrophic collapse and subsequent expansion would cause the loss of the beam. However, the effect depends on the optical polarisability of the medium and on the laser pulse duration. It is less important for pulses shorter than the molecular relaxation time i.e. for picosecond pulses[35], when only the electronic polarisability has a sufficiently rapid response[49].

Anisotropic molecular liquids, especially the benzene derivatives and carbon disulphide, have the largest optical Kerr coefficients. Hellwarth[32] gives an extensive table of the intensity dependent part n_2 of the refractive index, expressed as:

$$n = n_o + n_2\overline{E^2} \qquad (I.3)$$

where n_o is the refractive index for zero field, and the bar denotes the time average of E^2 taken over a period comparable with the molecular relaxation time. Although this intensity dependent refractive index cannot follow the light frequency it is fast enough (10^{-11} sec.) to respond to the instantaneous intensity of a giant pulse laser emitting on

the nanosecond time scale. For such a pulse propagating in a liquid the peak of the pulse will slow due to the induced increase of refractive index, and the trailing edge will catch up to create an 'optical shock' with a limiting width set by dispersion and the response time of the medium[33]. For pulses whose duration is comparable with the relaxation time of molecular anisotropy fluctuations the pulse envelope suffers distortions of amplitude and phase[35,65] such that it is theoretically possible to compress the pulse to 10^{-14} sec. duration by imposing a linear frequency sweep[65].

A second field effect is electrostriction, a process by which polarised molecules are drawn to high field regions, thus increasing the local density and striction, or pressure, in the medium. This is the means by which the light field couples with the liquid in stimulated Brillouin scattering, and since mass transfer is involved, the pressure front propagates with the velocity of sound. Electrostriction is therefore an inherently slower process than the optical Kerr effect, and is usually less important on the 10^{-8} sec. time scale associated with the evolution of a Q-switched laser pulse[34]. However, the mass transfer time associated with self-trapped filaments a few microns in diameter is only 10^{-9} sec., and electrostriction may therefore be important in the final stages of their formation and ultimate disruption by electrostrictive over-pressure[31]. As in the Kerr effect, the increase in refractive index caused by electrostriction is proportional to the light intensity[34].

I.4 Effects in absorbing liquids

Optically absorbing liquids or solutions are subject to thermal effects arising from direct absorption of energy from the incident light, and the resulting increase in the local temperature and density. These are essentially time integrated effects, and are limited by thermal diffusion.

An effect which is important on the millisecond to one second time scale is gross refractive index change due to heating. This distorts the propagating beam, and is caused either by optical pumping, as in the liquid laser[110], or by direct absorption from the laser beam, an effect known as thermal blooming[36] because the refractive index decreases with intensity and the beam consequently diverges.

On the microscopic scale there are stimulated optical scattering effects in absorbing liquids, which are driven by absorptive heating, the two main ones reported in the literature being stimulated thermal Rayleigh scattering (STRS) and stimulated thermal Brillouin scattering (STBS). STRS, predicted by Herman and Gray[37] and observed by Rank et al.[38], occurs in the anti-Stokes wing of the thermal Rayleigh component, and is blue-shifted by an amount $\frac{1}{2}(\Gamma_L + \Gamma_R)$, where Γ_L is the laser linewidth, and the spontaneous Rayleigh linewidth $\Gamma_R = 2k^2D$, where D is the thermal diffusivity of the liquid and k the wave number of the incident plus scattered light field. For typical liquids and visible wavelengths $\Gamma_R \sim 30$ MHz, so that the frequency shift of the back-scattered

light is well within the longitudinal cavity mode spacing c/2L of a pulsed solid state laser, for which c/2L = I50 MHz for a cavity length L of I metre. In contrast to electrostriction and molecular alignment effects the refractive index is decreased in high field regions due to absorptive heating and thermal expansion of the liquid[37]. Theory predicts a critical absorption coefficient $\alpha_{cr.}$ above which STRS has a lower threshold than ordinary stimulated Brillouin scattering (SBS) and successfully competes with it. Observed values of $\alpha_{cr.}$ lie in the range 0.04 to 0.3 cm^{-I}, and observed frequency shifts in the range 0.002 to 0.0I cm^{-I}. A reflectivity of approximately I0% due to STRS is reported[38]. On a time scale too short for thermal fluctuations to produce density changes in the liquid, direct observation of scattering from entropy fluctuations in an absorbing liquid becomes possible[39]. This is observed with picosecond ($I0^{-I2}$ sec.) light pulses.

The density wave equation for an absorbing liquid contains two driving terms, one due to electrostriction, which leads to the well known stimulated Brillouin scattering for a non-absorbing liquid, and an absorptive heating term giving rise to an additional scattering, STBS[47]. This extra scattering distorts the Lorentzian gain profile obtained for SBS, with an increased maximum red-shifted by approximately $\frac{1}{2}\delta\nu$ with respect to the peak gain frequency shift $\nu = \nu_B$ for zero absorption, where $\delta\nu$ is the full width at half-maximum of the Brillouin line and ν_B is the Brillouin frequency shift characteristic of the liquid. The red shift

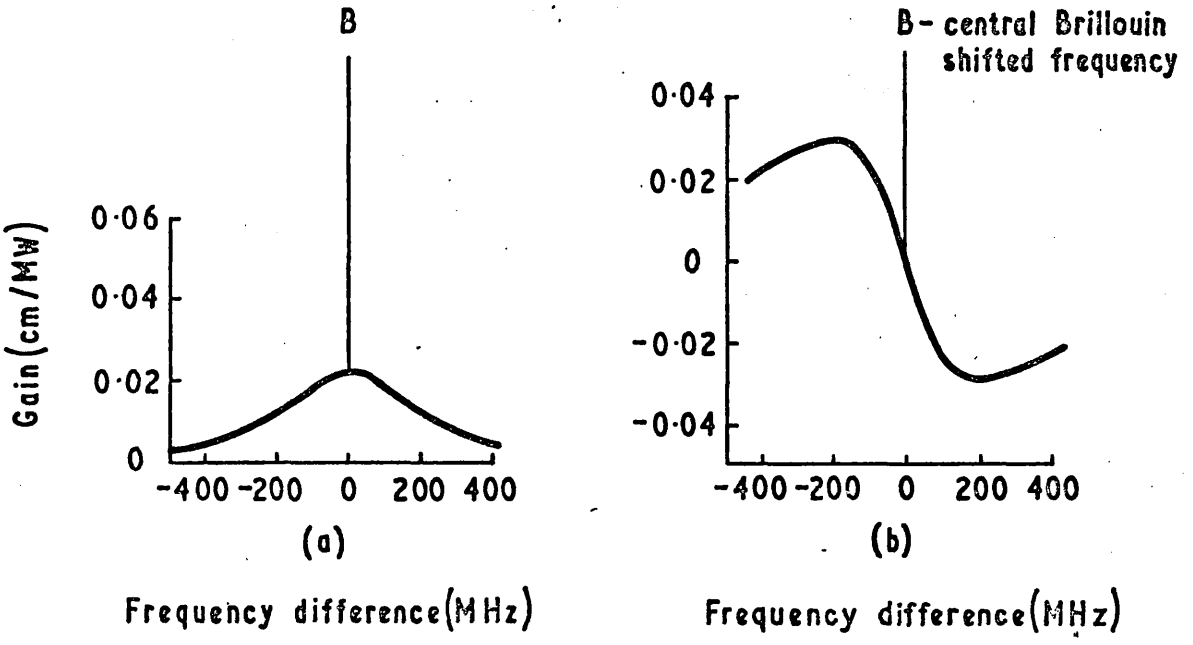

Fig. 1.2 Gain profiles for stimulated Brillouin scattering in liquids.

a) Transparent liquid

b) Thermal component of gain for an absorbing liquid, absorption coefficient 0.83 cm^{-1} (from ref. 47)

$\delta\nu$ amounts to -100 to -200 MHz in common liquids. There is a corresponding blue-shifted loss, of similar frequency shift and magnitude, due to the conversion of Brillouin-Stokes photons back to incident laser photons by addition of energy from thermal fluctuations. Thus the stimulated Brillouin scattering is quite distinct in the two cases (Fig. I.2).

I.5 The four-wave formalism

Having surveyed the main linear and non-linear optical effects in simple liquids relevant to laser physics, we may note that Bloembergen[42] has shown that all the non-linear effects may be formally described in terms of the interaction of four electromagnetic plane waves coupled by the non-linear susceptibility tensor χ_{ijkl} of the medium, which gives rise to a non-linear polarisation cubic in the electric field amplitude. However, we have seen that though formally similar, the non-linear optical effects described are physically distinct. Where the formal similarity is significant is in the formation of periodic phase gratings arising from a modulation of the refractive index due to the four-wave interaction in the liquid. This is a necessarily general description, and because the phenomenon is important to the understanding of laser Q-switching and liquid diffraction it is discussed more thoroughly in Chapter 4.

I.6 Relaxation time constants

The various non-linear optical effects have characteristic response times associated with them by the nature of the physical processes involved. For incident light pulses of short duration those non-linear effects characterised by longer response times are diminished because the coupling of the electromagnetic field to the liquid medium is decreased. For very short times several of the non-linear processes cease to operate. We have seen this already for STRS on the picosecond time scale. Table I.I shows the magnitude of these characteristic times for simple liquids. Clearly these are important for pulse propagation in a liquid laser amplifier (Chapter 6), where we desire to minimise non-linear losses for light intensities approaching 10^{10} W.cm^{-2}. Since many experiments on non-linear optics are made with 10^{-8} sec. pulses at intensities of the order of 10^{8} W.cm^{-2}, under which conditions appreciable interaction with the liquid takes place, the intense light pulses to be amplified in a liquid laser must be of shorter duration than this. Except for rather low viscosity liquids, such as carbon disulphide, with a rotational relaxation time of 2 psec.[7,48], Table I.I shows that pulses a few picoseconds long only interact with a non-absorbing liquid through polarisation of the electrons and molecular anisotropy fluctuations. The electronic Kerr coefficient is smaller by a factor of 10^{3} than that due to re-orientation of anisotropic molecules[34], and the self-focusing threshold

TABLE I.I

Characteristic relaxation times for non-linear optical effects in simple liquids

Optical Effect	Mechanism	Relaxation time, sec.	Frequency shift, cm^{-1}
Rayleigh scattering (centre line)	Thermal fluctuations	10^{-7}	10^{-3}
Rayleigh wing scattering	Anisotropy fluctuations	10^{-12}	100
Mandel'shtam-Brillouin	Density fluctuations	10^{-9}	0.1
Raman	Molecular excitation	10^{-11}	1000
Kerr	Molecular re-ordering	10^{-11}	
	Electronic polarisation	10^{-15}	
Electrostriction	Acoustic wave	10^{-9}	

is increased by a similar factor[49]. Stimulated Rayleigh wing scattering may become an important loss mechanism at sufficient intensity, though the threshold may be high. Ideally, picosecond SRWS could be very much reduced by employing laser liquids with isotropic molecules. Thus it is clear

that the amplification of picosecond pulses in a liquid laser is of practical significance, and this fact provides the departure point for the experimental investigation described in Chapter 6.

CHAPTER 2 Laser mode-locking and the generation of ultra-short pulses

2.I Definition of mode-locking

The electromagnetic field in a laser oscillator may be written as the sum of the resonant cavity modes, where each mode corresponds to a standing wave in the cavity. For an empty cavity with perfectly reflecting walls and a length large compared with the wavelength of light, the longitudinal modes are a set of sine waves with a constant frequency difference between any adjacent pair given by:

$$\Delta\nu = c/2L \qquad (2.I.I)$$

where L is the cavity length and c the velocity of light. In a dielectric medium dispersion causes variations of phase across the mode spectrum, and in an active medium the nature of the stimulated emission process and the presence of losses in the cavity give rise to frequency pulling and pushing effects which shift the mode frequencies away from the resonances of an empty cavity[43]. However, these frequency variations are usually small compared with $\Delta\nu$, and are more important to the consideration of the physical processes responsible for mode-locking than to an elementary understanding of the phenomenon. It will be assumed in the following therefore that the mode frequency difference is constant.

The effect of variations in $\Delta\nu$ is discussed later.

Consider a laser oscillator which generates a number of modes simultaneously. We will call this multi-mode operation. If the phases are randomly distributed the emission consists of statistical fluctuations in intensity. If, however, the phases are ordered in some way then the intensity shows a periodic behaviour with a fundamental period $2L/c$, the reciprocal of the mode frequency difference. In particular, the superposition of $2N+1$ modes with equal amplitude and zero phase produces a periodic train of pulses with a repetition period $2L/c$, peak intensity $(2N+1)^2 I_o$ and pulse width $3L/\pi cN$, where L is the cavity length and I_o the intensity of a single mode[50]. This temporal interference phenomenon has an intensity function very similar to that of a diffraction grating[50], its closest spatial analogue. In general the phase condition required for periodic pulsing is that the phase difference of any pair of modes be zero or an integral multiple of 2π, for all modes.

2.2 Experimental observation

Internal cavity loss modulation of a laser oscillator at the mode frequency difference promotes phase-locking of the longitudinal modes[50,53]. Hargrove, Fork and Pollack[51] achieved mode-locking of the helium-neon gas laser by means of acoustic modulation in the cavity. They found a narrow locking range for the modulation frequency, $10^{-5}\Delta\nu$, and a well-defined mode-locking threshold. Crowell[52] observed

mode-locked pulse widths of 0.5 ns. and 0.25 ns. for the helium-neon and argon ion lasers respectively. Deutsch[54] obtained mode-locked pulse trains from a ruby laser internally modulated with a KDP Pockels cell, and found a locking range of 8 mm. for the allowed variation in cavity length, for L=I metre. Mocker and Collins[55] mode-locked a ruby laser using cryptocyanine, a photo-sensitive dye with saturable absorption[56], a possibility for which Deutsch had indicated preliminary evidence[54]. With a relaxation time shorter than the cavity transit time L/c, the dye modulates the cavity loss at the longitudinal mode frequency difference because it is driven by the beat frequency of the modes themselves. This passive or self mode-locked behaviour has the advantage of automatic adjustment to the beat frequency, dispensing with the need for careful frequency tuning and cavity length control[5I,55]. Neodymium lasers were also first mode-locked with acoustic modulators. In the case of Nd:YAG a pulse width of the order of 80 ps. was obtained[57]. For neodymium:glass a detection-limited width < 0.5 ns. was observed, with a fine adjustment of cavity length in the range 0.02 to 0.05 mm.[58] Subsequently, passive mode-locking was achieved with a saturable absorber[59], with upper and lower limits on pulse width of 0.I5 ns. and 0.2 ps. from photo-detection and spectral width measurements respectively[60]. The liquid laser Nd:$SeOCl_2$ can also be mode-locked using a saturable dye.[6I]

Mode-locking the neodymium:glass laser with a saturable absorber combines the functions of Q-switching and mode-locking

in a simple passive element, and provides a means of generating ultra-short optical pulses of high peak power[60] with application to non-linear optics[39,48,49]. The 300 Å spectral width of the neodymium:glass emission band[64] makes the generation of 10^{-13} sec. duration pulses theoretically possible by mode-locking the entire emission spectrum. Mode-locked pulse trains with 180 Å spectral bandwidth[60] and picosecond pulses with sub-picosecond (2.10^{-13} sec.) components have been reported[62,63]. Since the pulse spacing is equal to twice the cavity transit time it can be adjusted simply by changing the optical path length. Pulse repetition periods up to 71.5 ns. have been obtained in this way, by inserting an optical delay line in the laser cavity[86]. Selection of a single pulse from a periodic pulse train is also possible, using a fast Pockels cell switch[79]. In this way an optical pulse of 10^{-11} sec. duration and a few millijoules energy is obtained, which may then be amplified by a laser amplifier chain to energies in the tens of joules range with peak power of the order of 10^{12} watts[88].

2.3 Picosecond pulse measurement

Since the short pulses generated by mode-locked solid state lasers are only a few picoseconds long due to the broad spectral bandwidth available for mode-locking, they are too short to be measured by photo-electric detectors. Indeed they provide a practical means of testing the pulse response

of such devices[71].

Instead picosecond pulsewidths are determined indirectly from intensity correlation measurements. These are conveniently done using multi-photon processes, particularly two-photon interactions which depend on the square of the incident intensity and thus give a measure of the second order intensity correlation function $G(\tau) = \int I(t)I(t+\tau)dt$. By directing a pair of short light pulses at a suitable crystal and observing the intensity of the second harmonic light as a function of the delay between the two pulses, their intensity correlation may be obtained[22,67]. Auto-correlation, the intensity correlation of a pulse with itself, can be done by recombining two beams derived from the same source by means of beam splitters. If pairs of pulses obtained in this way are recombined with a fixed delay, and the second harmonic signal examined for each pair, systematic variations of pulse characteristics in a long pulse train can be studied[83]. Intensity correlation of a narrow pulse with a broad pulse can be used to obtain the intensity profile of the broader pulse[84,85]. Since the free space velocity of light is approximately 3.10^8 m/sec., delay steps of 10^{-12} sec. require space increments of 0.3 mm. Thus auto-correlation in the picosecond range is feasible.

An elegant and experimentally simple method of performing intensity correlation is by means of two-photon fluorescence, TPF[68]. Here fluorescence is excited in a suitable dye by the simultaneous absorption of two photons, with an intensity

proportional to the square of the incident intensity. By reflecting a beam containing short light pulses back on itself from a mirror immersed in the dye solution, the reflected pulses are made to cross successive incoming ones, thus producing stationary overlap regions of locally high intensity which excite TPF in the dye more strongly than in the intervening spaces. The second order intensity correlation function is recorded photographically as a series of bright spots or bands superimposed on a background trail of about half the intensity[68]. This background may be nearly eliminated by interfering a strong beam at the laser wavelength with the weaker second harmonic[69]. The display can be magnified by collinear propagation of the fundamental and the second harmonic, using optical dispersion of the solvent to produce a steadily increasing delay and decreasing intensity correlation, such that the fluorescence intensity decreases at a rate dependent on pulse width[69]. The resolution limit of two-photon fluorescence measurement (TPFM) is estimated as 10^{-13} to 10^{-14} sec., and pulse widths in the range 1 to 3 ps. are found for the neodymium:glass laser, using this technique[68,69].

The dibenzanthracene dye originally used for TPFM[68] requires two-photon excitation by the second harmonic of the neodymium laser. A more convenient dye for TPFM is rhodamine 6G[70,71]. This has absorption bands at the second harmonics of the neodymium and ruby lasers, and can be used directly for TPF studies with the fundamental frequency of either[71,72]. The fluorescence lies in the yellow and the emission is brighter than for dibenzanthracene[71].

The analysis of TPF intensity records is not quite straightforward because random phased light with the same spectral bandwidth as the mode-locked laser emission produces a TPF pattern with similar structure[73]. Only the intensity ratio between the peaks and the background fluorescence differs in the two cases. For perfect mode-locking i.e. equi-phased modes, the ratio is 3, for random phase it is I.5[73]. The whole range of intermediate intensity ratios is possible, depending on the particular phase relations obtaining under the actual experimental conditions[74,76]. The observed TPF structure for random phase[74] reflects the two-photon correlation structure inherent in apparently unstructured thermal light, as demonstrated in the experiments of Twiss and Hanbury Brown[75].

The observed TPF structure for the mode-locked ruby laser gives good agreement with the pulse width inferred from the spectral bandwidth[72]. In the case of the neodymium glass laser the pulse width obtained from the TPF intensity pattern is often at least ten times[71] that expected from the observed spectral bandwidth, $\sim$3 ps. instead of $\sim$0.3 ps., and the contrast ratio frequently lies in the range I.6 to 2[74,79,80], indicating imperfect mode-locking[76,77] or possibly a frequency sweep across the bandwidth[78]. It is only by combining high resolution with accurate means of determining contrast ratio that sub-picosecond components representing the full spectral bandwidth are observed[62,63].

Because of the inherent symmetry of the TPF intensity correlation[73]; these fine structure components are recorded as a narrow spike only 50 to 75 microns wide superimposed on a broad base 10 to 20 picoseconds long. The intensity ratio for the spike reaches the theoretical value of 3, that of the broader base being in the region of 2[62,63]. Similar results are found for the third order intensity correlation using third harmonic generation in fuchsin dye[129]. When this fine spike is not resolved it is the broader part of the TPF intensity structure with reduced contrast ratio which is recorded[68,71,74,79].

A further effect of the symmetry of the second order correlation function is that only the pulse width and not its shape can be deduced. However, the third order correlation will reflect an asymmetry present in the pulse[81], and in principle three-photon experiments should be sufficient to recover the time dependence of laser intensity[87].

All intensity correlation methods of determining picosecond pulse duration are inferential, as we have seen, but are necessary because combined photo-detection and oscilloscope systems are not fast enough to display such short pulses directly. However, some electron-optic camera systems have a resolution of 10^{-11} sec., within an order of magnitude of the pulse width, and are certainly fast enough to display complex groups of picosecond pulses[82]. Such observations are direct records of intensity, and are a means of resolving ambiguities in the temporal behaviour of laser emission which can occur in the interpretation of spectral and

TPF intensity data.

2.4 Theory of the mode-locked laser

The theory of mode-locking rests on the observation that the periodic pulse train emitted by a mode-locked laser oscillator may be resolved into an intensity sum whose Fourier components are the normal modes of the cavity. Therefore a theory is required which can explain how the phases of the generated modes become ordered. Since the set of phase-locked oscillating modes is equivalent to a short pulse propagating in the cavity at the corresponding group velocity, in the sense that the electromagnetic fields are equivalent, the problem can be analysed in terms of either. Where the oscillating bandwidth is narrow and relatively few modes are involved, as in the gas laser, the analysis can be carried through in terms of mode interactions, notably in the work of Lamb[43]. Such analysis is complex for more than a few modes however, and it is more convenient for solid state lasers, in which $\sim 10^4$ modes can be oscillating simultaneously, to treat the propagating pulse model. Where the mode picture remains useful is at the beginning of generation, when the interference of the few initial modes gives rise to short intensity fluctuations from which the intense pulse ultimately develops[89,90]. Those treatments in which the mode analysis for solid state laser mode-locking is carried through rely on perturbation theory[91] and computer analysis[90] to solve the set of non-linear coupled differential equations involved.

Consider first the action of a dye mode-locked laser, in which the generation of m equal amplitude random phased modes produces intensity fluctuations of duration $\sim T/m$, where T is twice the cavity transit time, and intensity β times the noise level, with probability $e^{-\beta}$. These intensity fluctuations are selectively transmitted by the saturable absorber, because of its intensity dependent transmission, and amplified in the laser medium. The absorption is progressively reduced to the point of saturation, thereby Q-switching the laser and generating an intense pulse by gain saturation of the amplifying medium[89,90]. Part of the pulse energy is transmitted by the output mirror at the completion of each double pass in the cavity, thus producing the familiar periodic pulse train with a repetition period $T = 2L/c$, the reciprocal of the longitudinal mode spacing (2.I.I).

In the case of cavity loss modulation by an externally driven element, such as an acoustic modulator[5I], beats develop between modes and lead to ordering of phase[43], with the same end result of short pulse generation[92]. However, the two pictures are equivalent, because in the case of mode-locking by a saturable absorber the effect of beats between modes is to modulate the transmission at the mode difference frequency c/2L (2.I.I), thus providing the same mechanism of cavity loss modulation[7I].

Multiple pulsing, with a repetition frequency equal to an integral multiple of the fundamental cavity frequency c/2L, is observed with the saturable absorber placed at an

intermediate position within the laser cavity. In particular, if the dye cell is placed at a distance $x_m = L/m$ from one end, where m is an integer, the pulse repetition frequency is $mc/2L$ [93,94]. Fleck[90] explains this phenomenon in terms of pulse overlap at the saturable absorber. When this occurs, the local intensity is greater and transmission is enhanced. Thus loss modulation develops at a multiple of the cavity frequency.

In order that the saturable absorber be suitable for mode-locking it must have a sufficiently fast relaxation to respond to beats between adjacent longitudinal modes. The condition is $T_s < L/\pi c$, where T_s is the recovery time of the absorber and L is the cavity length[91]. This condition is highly satisfied for the neodymium laser mode-locking dyes, for which $T_s < 10^{-11}$ sec.[95] and $L/\pi c \simeq 10^{-9}$ sec. (for a one metre cavity). In the case of the ruby laser however, the phthalocyanine Q-switching dyes do not satisfy the condition and do not mode-lock, whereas cryptocyanine, for which $T_s \sim 10^{-11}$ sec., does[55,72,96].

In reviewing the theory of the mode-locked solid state laser it has been implicitly assumed that the medium is dispersionless. As already indicated (Sec.2.I), the dispersion of a real dielectric medium causes a variation of phase with mode number. Classically, the refractive index as a function of wavelength can be expanded as a Taylor series of terms involving the first, second and higher order derivatives, corresponding to linear, quadratic and higher index terms in

the expression for the phase. It is the quadratic phase term which is responsible for dispersion in the group velocity and the resultant pulse broadening[97], and it is this term which is equivalent to a linear frequency sweep[III]. (See Appendix II). When a large positive frequency sweep is imposed on the mode-locked laser emission[98,99] the resulting broad pulses can be compressed to the sub-picosecond range by passing them through a grating pair[78]. Random variations in phase about the quadratic distribution do not affect the pulse shape, but the average intensity of random emission between pulses is increased[III].

2.5 Intensity fluctuations and self-modulation

In the theory of laser mode-locking by a saturable absorber it is shown that short intensity fluctuations arise from the interference of several random phased modes[89,90]. Although these fluctuations have a probability distribution characteristic of a random interference process, they are nevertheless periodic with the cavity period precisely because it is the cavity length which determines the mode frequency spacing, as we have seen earlier (Sec. 2.I). The average time interval for the occurrence of an intensity fluctuation spike β times the average intensity is[100]:

$$\tau \simeq \frac{T}{m} e^{\beta} \qquad (2.5.I)$$

where m is the number of oscillating modes and T is the cavity double transit time. By imposing the condition that this spike occur within the period T it is seen that $\beta \sim \ln m$, and for a solid state laser with $m \sim 10^4$, intensity fluctuation spikes ~ 10 times the background intensity and duration $\sim 10^{-12}$ sec. are possible. The laser therefore emits periodic trains of sharp pulses superimposed on $\sim 10\%$ background noise, with pulsewidths the order of the inverse spectral bandwidth[100,101]. This type of emission has close similarities to that emitted by mode-locked lasers, and is observed as spiking or beats on fast oscilloscope displays and as picosecond pulses in TPF intensity records of both Q-switched and free-running lasers[102]. Where the emission of the laser with a large number of random phased modes differs from that of the ideally mode-locked laser is in the energy distribution. In the latter virtually all the energy is contained in the ultra-short pulses, which consequently have peak powers $\sim m$ times the mean power emitted (the mean being obtained by averaging over T). For random phased modes, the peak power of the intensity fluctuations is only $\sim \ln m$ times the mean, and almost all the energy is in the background noise. For $m = 10^4$, the ratio of peak powers of the spikes in the mode-locked and random phase cases is $\sim 10^3$. This is also the ratio of the background energy to that of the spikes for random phase emission.

The amplitudes and phases of the laser modes are not completely independent however, because they interact through the non-linear gain of the amplifying medium. Thus the emission

is not simply a linear superposition of a set of independent modes; rather the amplitude and phase of a growing mode are dependent on the state of those already present. For a small number of modes such interactions produce significant phase locking, as Lamb shows in his three-mode analysis of the gas laser[43]. Observation of intensity beats with solid state lasers[103] is similarly explained by showing that beats between three modes modulate the laser transition at the difference frequency $\Delta\nu$, and that the gain and emission rate are therefore phase dependent. The optimum phase relations are such that maximum intensity modulation occurs with the laser medium at one end of a cavity with external mirrors[104]. The case of a large number of modes can be treated on assuming that the optimum phase condition is that whichmaximises the emission. The analysis shows that the probability of spontaneous mode-locking increases with decreasing mode spacing i.e. at longer cavity lengths[105]. Thus a pulsed solid state laser can be expected to show spontaneous mode-locking under appropriate conditions.

It can be shown in general that optical inhomogeneities present in the laser cavity induce phase-locking[106], including the special case of the active medium at one end of the cavity. These inhomogeneities can take the form of spatial variations in excitation density (inhomogeneous pumping), in active atom density (discontinuity in laser medium), and in loss by absorption or scattering, and they induce the ordering of phase in such a way as to maximise the overall emission. The

laser modes tend to oscillate in phase at points of high excitation, thus increasing the induced emission, and out of phase at points of high damping, thus diminishing the absorption loss[106].

Such considerations are relevant to the experimental observations on spontaneous modulation of lasers with multiple plate reflectors, as described in Chapter 5.

CHAPTER 3 The liquid laser

3.1 Introduction

The neodymium inorganic liquid laser is of interest as an alternative to neodymium glass in the development of high power, high radiance laser systems because it avoids the problem of permanent material damage suffered by glass under the action of intense light pulses[114], and the required volume of homogeneous material is readily provided. Further, it is a high gain laser medium with a similar emission wavelength and spectral bandwidth to neodymium glass[107,108], it can be circulated for cooling purposes[109], an advantage on large systems because of the slow recovery from thermal distortions induced by optical pumping[110], and it has in principle a low intrinsic scattering loss since small particle impurities can be filtered off, leaving a pure liquid medium. A study of the liquid laser as a picosecond pulse amplifier is described in Chapter 6. Here we consider its development and laser properties.

3.2 Development

All rare earth ions, the lanthanons, have an incomplete inner electron shell in which optical transitions take place, and which are to a first approximation shielded by the outer completed shells from the ion's external environment. The

main features of rare earth spectra are independent of the environment to a similar degree; it is the linewidth and excited state decay time which are influenced by the local field of the host material[II7]. This independence has been thoroughly exploited in the development of rare earth lasers, and the Nd^{3+} ion has been found especially versatile, exhibiting laser action in a wide range of crystals[II6] and glasses[64, II4,II5]. Neodymium glass is interesting in the context of liquid lasers because it demonstrates that laser action is possible for an assembly of Nd^{3+} ions embedded in an amorphous medium. The emission spectrum is a broad band containing an assembly of spectra characteristic of each group of ions in its own local field, spatially averaged over the total volume. This is known as inhomogeneous broadening because of the heterogeneous environment, while within the broad band the narrower spectral profile due to thermal broadening by lattice vibrations of ions in one particular site is described as being homogeneously broadened. Here the ions are swept over the linewidth at the vibrational frequency of the lattice, $\sim 10^{13}$ Hz, and so the homogeneous broadening represents a time averaged rather than a spatially averaged emission profile[II8]. The difference in a liquid medium is that the ions are free to move in an environment which is no longer rigid but rapidly changing. Thus the inhomogeneous broadening characteristic of the solid becomes a time averaged homogeneous broadening in the liquid. Otherwise the emission remains broad band because of the amorphous nature of the liquid medium[II2].

The problem with the neodymium liquid laser is to find a solvent which does not quench the fluorescence. In crystals and glasses Nd^{3+} ions in the metastable excited state have a lifetime of 10^{-4} to 10^{-3} sec., and decay by spontaneous emission of radiation with high quantum efficiency(II9), an ideal requirement for laser media. However, in liquids the quantum yield of fluorescence is generally low, being only $\sim 10^{-5}$ in water for example(II2). This low yield is due to the rapid quenching of the excited state by non-radiative transfer to the vibrational energy levels of the liquid molecules. The quenching is greatest in hydrogenous media, since these have the highest vibrational frequencies. By replacing light atoms in the liquid molecule with heavier ones, the vibrational energies are reduced and the quantum yield of fluorescence enhanced.

In addition, a suitable liquid must have a large enough dielectric constant to dissolve neodymium salts at the required concentrations for lasers, and must be transparent over the spectral range of the absorption and emission bands of the laser ion(I07). Both the non-aqueous solvents selenyl and phosphoryl chloride(I20) meet the laser requirements, and both are used in neodymium liquid lasers(I07,I08). The addition of metal chlorides, such as $SnCl_4$, $ZrCl_4$, increases the solubility of the rare earth salts, and an optimum volume ratio of the two liquids can be chosen with respect to solubility and stability of the laser solution at the chosen operating temperature, usually 20 to 25°C (II3). Phosphoryl chloride is

less toxic than selenyl chloride, and the pure solvent is completely colourless. Its use in a liquid laser amplifier is described in Chapter 6.

3.3 Laser properties

First we consider the spectroscopy of the Nd^{3+} ion in phosphoryl and selenyl chloride (Fig. 3.I), since it is this which largely determines the stimulated emission characteristics of the medium. The fluorescent emission of neodymium selenyl chloride solution is centred at I.055 micron, and has a width of I60 Å and an exponential decay time between II0 and 230 μs., depending on how anhydrous the solution is. The principal absorption bands lie in the 0.5 to 0.6 micron and 0.7 to 0.9 micron regions[I07,II0], and the stimulated emission cross-section is approximately $I0^{-I9}$ cm^2 [I2I], a value intermediate between those of neodymium glass and neodymium YAG. The spectroscopy of neodymium phosphoryl chloride is very similar to that of the selenyl chloride, with a 200 Å emission bandwidth centred at I.053 micron wavelength, and a reported lifetime of 70 μs.[I08,I22] The stimulated emission cross-section is also approximately $I0^{-I9}$ cm^2 [I23]. The absorption bands give the solution a lilac colour, and the liquid is less viscous than selenyl chloride for a similar neodymium concentration.

These liquid laser solutions are corrosive and hygroscopic; in addition selenyl chloride is toxic. It is therefore necessary to seal the solution in a suitable glass vessel, to protect

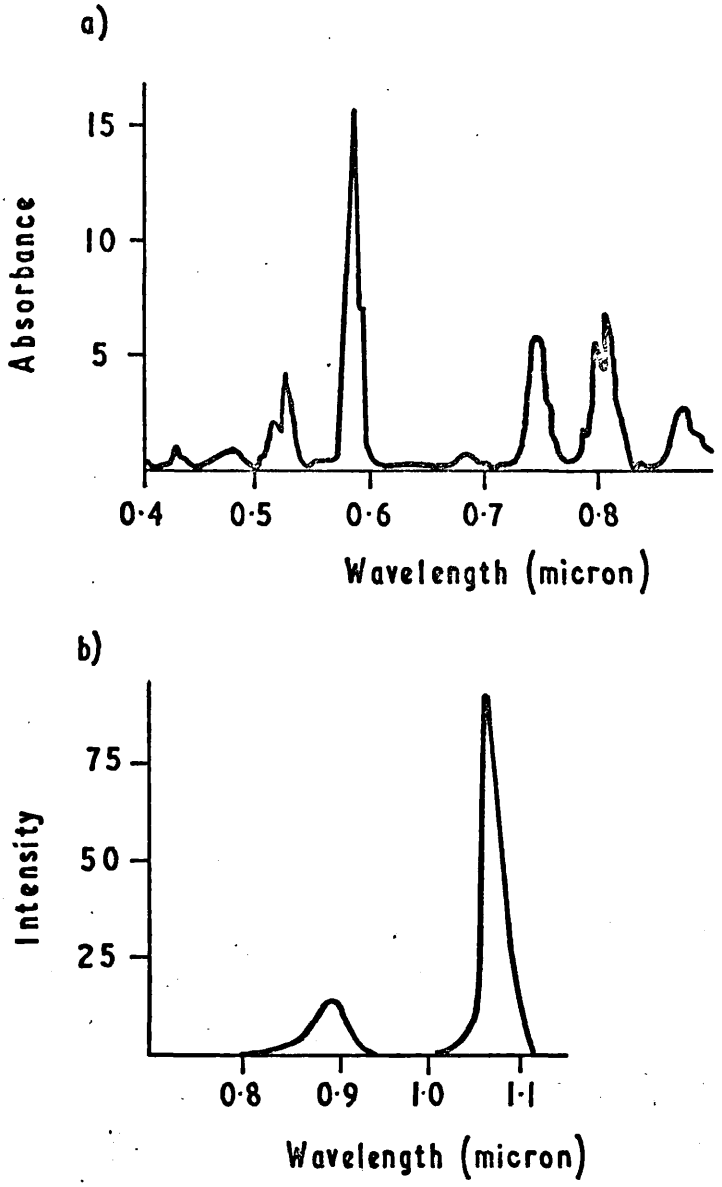

Fig. 3.1 Neodymium liquid laser spectra

a) Absorption spectrum of Nd:$SeOCl_2$-$SnCl_4$ (ref.107)

b) Emission spectrum of Nd:$POCl_3$-$SnCl_4$ (ref.122)

both the solution and the experimenter from harmful effects. An arrangement closely approaching the rod geometry of glass based lasers is achieved by sealing the ends of a Pyrex or silica tube with optical flats of the same material. A side tube is fused into the main body for filling purposes, and acts as an expansion chamber under flash pumping conditions. I50 mm. long cells of this construction, when filled with the laser solution, show characteristic laser spiking with external cavity mirrors. Threshold pumping energies are low and output pulse energies of several joules are obtained, with efficiencies of I% (I08,II0).

In the absence of external mirrors the neodymium selenyl chloride laser generates 'whispering modes' by total internal reflection at the liquid-glass interface, since the liquid has a higher refractive index, I.65, than that of the silica vessel, I.45. The laser emission emerges over a large solid angle, and exhibits limit cycle behaviour, a large amplitude modulation with slowly changing period, which extends over the greater part of the pumping pulse, typically several hundred microseconds long(I24). Examples obtained by the writer using a I50 mm. by 9.5 mm. cylindrical cell with plane parallel windows are shown in Fig. 3.2. Very similar behaviour is observed with neodymium glass cladded with clear glass of a lower refractive index(64). No such behaviour is found with neodymium phosphoryl chloride, presumably because its refractive index of I.460(I25) is close enough to silica to prevent

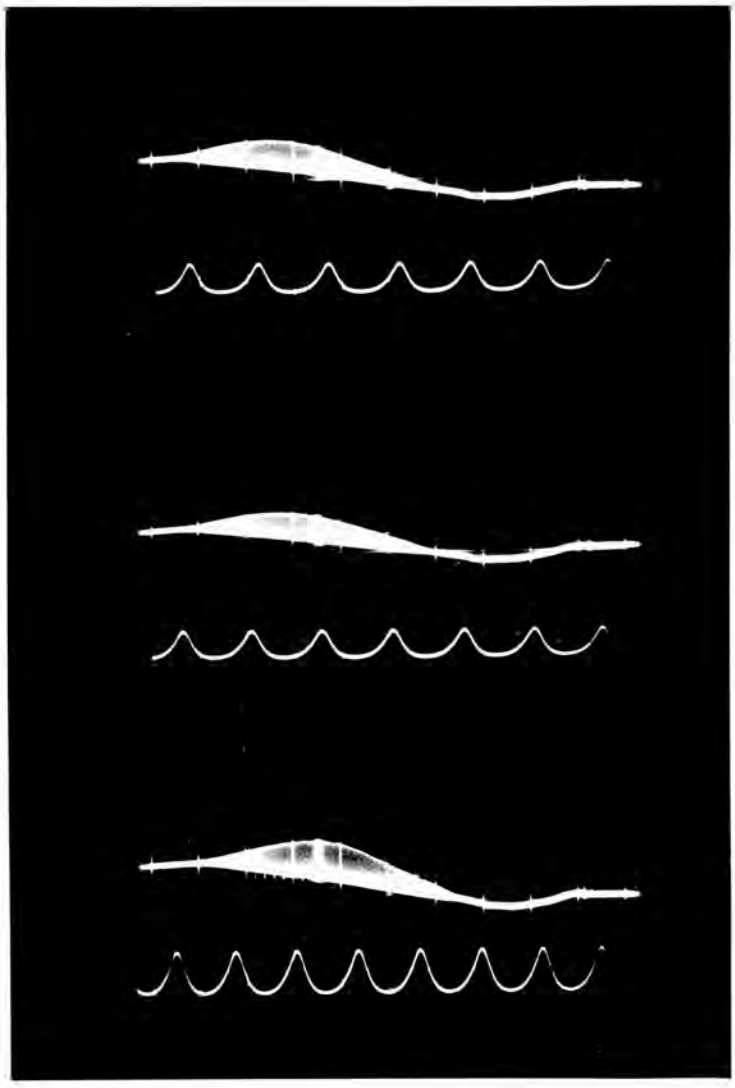

Fig. 3.2 Nd:$SeOCl_2$ limit cycle behaviour

Upper scale 50 μs/cm.

Lower scale 0.5 μs/cm.

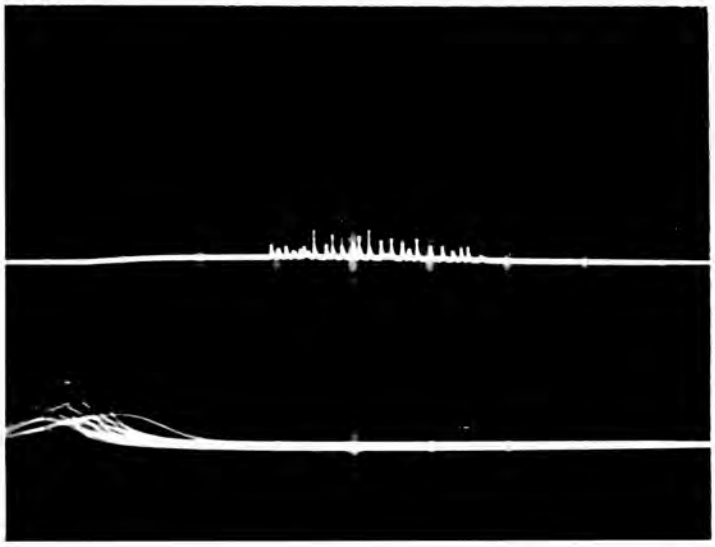

100 μs/cm

0.2 μs/cm

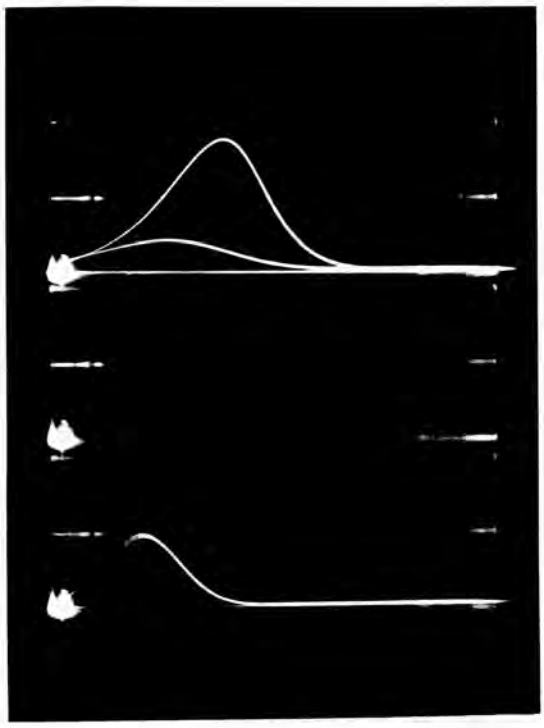

100 ns/cm

Fig. 3.3 Nd:$POCl_3$ oscillator spikes

significant reflection. Fig. 3.3 shows the normal spiking operation of a Nd:$POCl_3$-$SnCl_4$ liquid laser solution.

A practical problem in optical pumping of liquid lasers is thermally induced refractive index distortion. Since the volume coefficient of thermal expansion of normal liquids is of the order of a hundred times greater than that of amorphous solids, such as glass, the optical distortion resulting from quite modest pumping pulses can be severe, and the subsequent recovery of the initial condition through removal of heat by convection and conduction can take from 15 to 30 minutes for a cell 10 mm. in diameter[110]. This problem can be alleviated in two ways. For a static system the flash light may be filtered to admit only light in the spectral regions of the absorption bands, thus providing efficient excitation, and the cell may be externally cooled by a circulating liquid coolant. By using a coloured solution, the coolant may be made to perform both functions. However, the ultimate rate of recovery is set by the heat transport properties of the laser liquid itself, and for a cell of 10 mm. internal diameter the recovery time will be of the order of a few minutes, depending on the pumping energy. For more rapid operation than this allows the laser medium itself must be circulated. With a sufficient reservoir volume and an external heat exchanger, repetition rates of 1 pulse per second can be achieved[109].

In addition to normal spiking and limit cycle behaviour, mode-locked operation of the liquid laser can be obtained

using a saturable dye solution[61]. A self Q-switching phenomenon, producing peak powers of several hundred MW, is observed when the oscillator cavity Q is reduced to a low value by decreasing the reflective feedback[130]. This could be due to a dynamic increase in reflectivity by stimulated Rayleigh or Brillouin back-scattering of the laser light in the liquid medium[110].

CHAPTER 4 Laser Q-switching by organic solvents

4.I Introduction

In reviewing optical effects in liquids (Chapter I) we have seen how stimulated back-scattering of light can be sufficiently powerful to Q-switch the laser[I9]. The back-scattering grows by stimulated Brillouin scattering for example, and the liquid becomes a strong reflector for the incident light[I8]. Because of the non-linear interaction between the electromagnetic field and the liquid, the spatial periodicity in the field due to the superposition of the incident and scattered waves produces a spatially periodic modulation of refractive index in the liquid which may be observed by diffraction (Bragg reflection) of a second beam incident at the Bragg angle[39,I3I,I32]. Similarly, 90° scattering occurs when two strong opposing waves of equal frequency collide in a non-linear medium[I33]. These phenomena can be described in terms of the four-wave formalism of Bloembergen[42] since they involve the interaction of four electromagnetic waves, two incident and two scattered or diffracted, coupled by the non-linearity of the medium.

The refractive index of the liquid can be altered by a change in polarisability (the optical Kerr effect), in density(electrostriction), in extinction coefficient (saturable absorption), and in temperature (absorbing medium). Phase gratings formed by refractive index modulation through

one or more of these processes are conveniently observed in liquid samples inserted in the standing wave field present in the laser cavity[I32], where they may initiate or accompany Q-switching of the laser[I9,40,4I,I32]. The phase grating is spectrally selective due to its periodic structure, and favours the waves creating it. For example a laser resonator containing a non-linear medium is expected to be self-tuning due to the formation of a phase lattice by the standing wave[I34].

In this Chapter we discuss the experimental observations made on a group of organic solvents which Q-switch the neodymium laser, interpreting the results in terms of the formation of phase gratings, and consider what physical processes are responsible.

We begin with the theory of the phase grating, with particular reference to its reflectivity and dynamic behaviour.

4.2 Theory of the phase grating

The spectral properties of a periodic refractive index structure in a dielectric medium may be determined most generally by solving Maxwell's equations for the propagation of light in a periodic medium, with proper choice of boundary conditions. This method is applied by Iwata, Makabe and Katsube[I35] to the study of Lippman plates formed by standing light waves in photographic emulsion, which produce cosine squared refractive index modulation. However, by making

one or more approximations, some simple analytical expressions for the reflectivity may be obtained. Thus, for a standing wave A cos kz, the refractive index takes the form[134]:

$$n(z) = n_o + \delta n \cos^2 kz \qquad (4.2.1)$$

where δn is the modulation amplitude of the refractive index. The reflectance of the grating is a maximum for a wave with the same wave number k :

$$R = \left[\pi \frac{l}{\lambda} \delta n\right]^2 \qquad (4.2.2)$$

where l is the length of the grating, λ the wavelength, and it is assumed that $R \ll 1$.

An alternative expression valid for all values $0 \leq R \leq 1$, may be obtained on replacing the cosine squared modulation by an equivalent stratified medium of alternating high and low index layers, each $\frac{1}{4}\lambda$ thick. The reflectance for a stack of N pairs of quarter wave layers is[136]:

$$R_{2N} = \left[\frac{\mu^{2N} - 1}{\mu^{2N} + 1}\right]^2 \qquad (4.2.3)$$

where μ is the refractive index ratio of adjacent layers,

$$\mu = 1 + q \frac{\delta n}{n_o} \qquad (4.2.4)$$

and $q \sim 1$ is a shape factor accounting for the replacement

of a cosine squared modulation by a stack. Substitution of (4.2.4) in (4.2.3) gives:

$$R = \tanh^2 (2q \frac{1}{\lambda} \delta n) \qquad (4.2.5)$$

where it is assumed $\delta n \ll I$, a condition usually well satisfied in those liquid phase gratings observed experimentally, for which $\delta n \sim 10^{-7}$ to 10^{-5}. It can be seen that (4.2.5) meets the requirement for a physically real solution because for $1/\lambda \to \infty$, $R \to I$. In the case $R \ll I$, the approximate expression:

$$R = (2q \frac{1}{\lambda} \delta n)^2 \qquad (4.2.6)$$

may be used. The close similarity with (4.2.2), derived for the cosine squared modulation, suggests that the stack model is a satisfactory approximation.

The dynamics of a phase grating are determined by the nature of the optical effect producing the change δn in refractive index, and the associated relaxation time. The importance of any one mechanism is thus dependent on the choice of liquid and the time scale of events. As the thermal effect is somewhat greater and the relaxation time long compared with the Kerr effect and electrostriction in common solvents[134], we discuss it first.

For a weakly absorbing medium in the field of a standing wave of periodic intensity $I_o \cos^2 kz$, the steady state

amplitude δT of the induced temperature modulation with a spatial period I/2k is[134];

$$\delta T = g \frac{h}{2Kk^2} \qquad (4.2.7)$$

where h is the average absorbed power per unit volume, K is the thermal conductivity, and k the wave number, and g is a factor estimated to lie in the range $\frac{1}{2} < g < I$, for cylindrical symmetry. The corresponding thermal refractive index modulation:

$$\delta n = \delta T \left(\frac{\partial n}{\partial T} \right)_p \qquad (4.2.8)$$

and the thermal relaxation time τ is given by[134]:

$$\frac{I}{\tau} = 4k^2 D \qquad (4.2.9)$$

where D is the thermal diffusivity.

At an intensity of I MW/cm^2, corresponding to a power of I0 kW in a laser filament approximately I mm. in diameter, and a wavelength of I micron, we find $\delta n \sim I0^{-6}$ and $\tau \sim 30$ ns. for the common organic solvents[137,138,139]. For the same wavelength and light intensity, the corresponding quantities for the non-linear effects are: I) Kerr effect, $\delta n \sim I0^{-7}$ to $I0^{-9}$ (32,34,46), $\tau \sim I0^{-I0}$ to $I0^{-I2}$ sec.[1,7,14];

2) Electrostriction, $\delta n \sim 10^{-7}$ [46] and $\tau \sim 10^{-9}$ sec.[I,I8];
3) Saturable absorption, $\delta n \sim 10^{-5}$ at saturation[I40,I46], which occurs at 10^5 to 10^6 W/cm^2 in certain photo-sensitising dyes[I4I,I42], for which $\tau \sim 10^{-8}$ to 10^{-11} sec.[95,96,I42].

For weakly absorbing liquids with a non-saturable absorption it appears that the thermal effect will be dominant in the formation of a phase grating, but because of the relatively long thermal relaxation time it is necessary to consider the dynamics of the process.

For a plane standing wave of infinite extent established in an absorbing medium of length small compared with the absorption length and large compared with the wavelength, the temperature T(z,t) at point z and time t obeys the thermal diffusion equation[I43];

$$K \frac{\partial^2 T}{\partial z^2} + u(z,t) = c\rho \frac{\partial T}{\partial t} \qquad (4.2.10)$$

where K is the thermal conductivity, c the specific heat, ρ the density and u(z,t) the local rate of generation of heat:

$$u(z,t) = u_o f(t) \cos^2 kz \qquad (4.2.11)$$

It is assumed that the function f(t) is slowly varying compared with the relaxation rate of the molecular absorption process, which is typically 10^{11} sec.$^{-1}$ for organic solvents.[I44]

On solving (4.2.IO) for f(t) = I in (4.2.II), and extracting that part of the solution relating to the temperature modulation of period I/2k:

$$\delta T(t) = \frac{h}{2Kk^2} \left(I - e^{-t/\tau} \right) \qquad (4.2.I2)$$

where τ is the thermal relaxation time defined in (4.2.9), and $h = \frac{1}{2} u_o$, the mean power absorbed per unit volume. Thus $\delta T(t)$ approaches the steady state value given in (4.2.7), apart from a geometric factor g relevant to cylindrical geometry. The relative importance of the thermal refractive index modulation therefore depends on the time scale of the problem.

If the standing wave intensity increases at an exponential rate, then setting $f(t) = e^{at}$ in (4.2.II), we find the solution for the temperature modulation of period I/2k,

$$\delta T(t) = \frac{2h}{ac\rho + 4Kk^2} e^{at} \qquad (4.2.I3)$$

Thus δT increases exponentially with an amplitude factor determined by the ratio of the rate of rise of intensity to the thermal relaxation rate[I45].

4.3 Experimental Results

The use of photo-sensitive dye solutions for Q-switching and mode-locking lasers involves the introduction of solvents

in the laser cavity. In view of the variety of optical effects in liquids observed using laser light sources it is expected that there will be some interaction with the solvent itself which will affect the laser emission. Stimulated Raman scattering[20,21], Q-switching[19,40,41], suppression of spiking[147], and cut-off of emission[148] are each observed under appropriate conditions with pure liquids present in the laser cavity. However, each of these effects requires high intensity, achieved by Q-switching the laser or by focusing the light into the cell, or a long sample[148], whereas the dye cells used for passive Q-switching and for mode-locking are normally a few millimetres or a few centimetres thick and are placed in the unfocused beam. Here we describe the experimental results obtained for a range of pure solvents introduced in the cavity of a neodymium glass laser in a similar arrangement.

The experiments were performed with the simple arrangement of Figure 4.1, and consisted of observing the character of laser emission for each liquid placed in the cell shown. The neodymium laser used was a Schott LG 56 glass rod 153 mm. long and 9.5 mm. diameter, with the end faces cut at the Brewster angle and the cylinder surface lightly ground. The laser rod was mounted in a Pyrex water jacket and optically pumped by two linear xenon flashtubes mounted symmetrically on either side. A close-wrapped polished silver sheet reflector provided efficient coupling of the lamp with the laser. Dielectric mirrors of 95% and 50% reflectance were used to

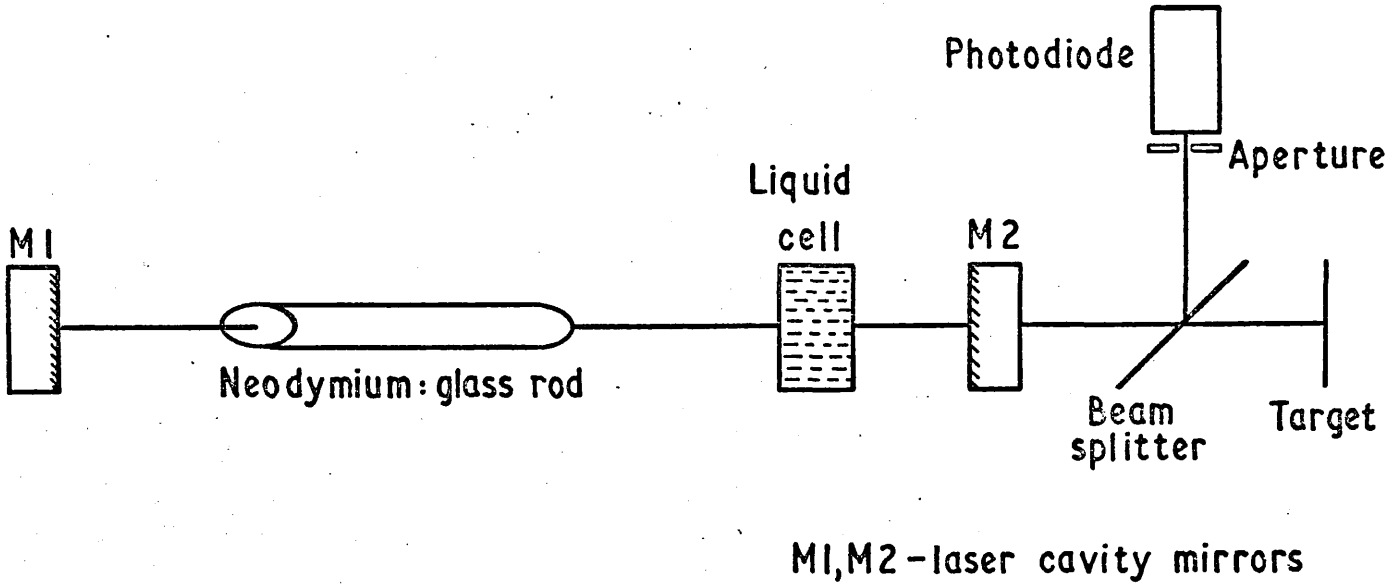

Fig. 4.1 Experimental arrangement for observing laser Q-switching by liquids.

form the laser cavity. These were aligned with an auto-collimator after inserting the liquid cell. 20 mm. path cells of Spectrosil B were used for the liquid samples, but later some observations were made with path lengths up to 76 mms. Laser emission was monitored with either an EMI 9713 B photo-diode and Tektronix 555 oscilloscope combination for general spiking display or an ITT F4000(SI) planar photo-diode and Tektronix 519 travelling wave oscilloscope for observing the profile of single pulses. The main beam was directed at a target for recording the intensity distribution. The energy could be measured by replacing the target with a calibrated calorimeter. All measurements were made at room temperature, 20° to 25° C.

The introduction of a liquid into the neodymium laser cavity resulted in pulse-sharpening behaviour, attributed to Q-switching through a non-linear interaction with the liquid. Peak power increased by a factor of 5 to 10, and pulse widths decreased by a corresponding amount. A series of sharp pulses varying in height and width was emitted during the pumping period, presenting a contrasting appearance with the normal laser spikes generated in the absence of the liquid, as shown in Figure 4.2 . The short duration of some individual pulses is illustrated in Figure 4.3 , and the experimental results are summarised in Table 4.I . Pulse widths of 20 to 25 ns. FWHM were occasionally observed in acetone and methanol, especially with a longer cell. This compares with the 300 to 500 ns. FWHM for normal spikes.

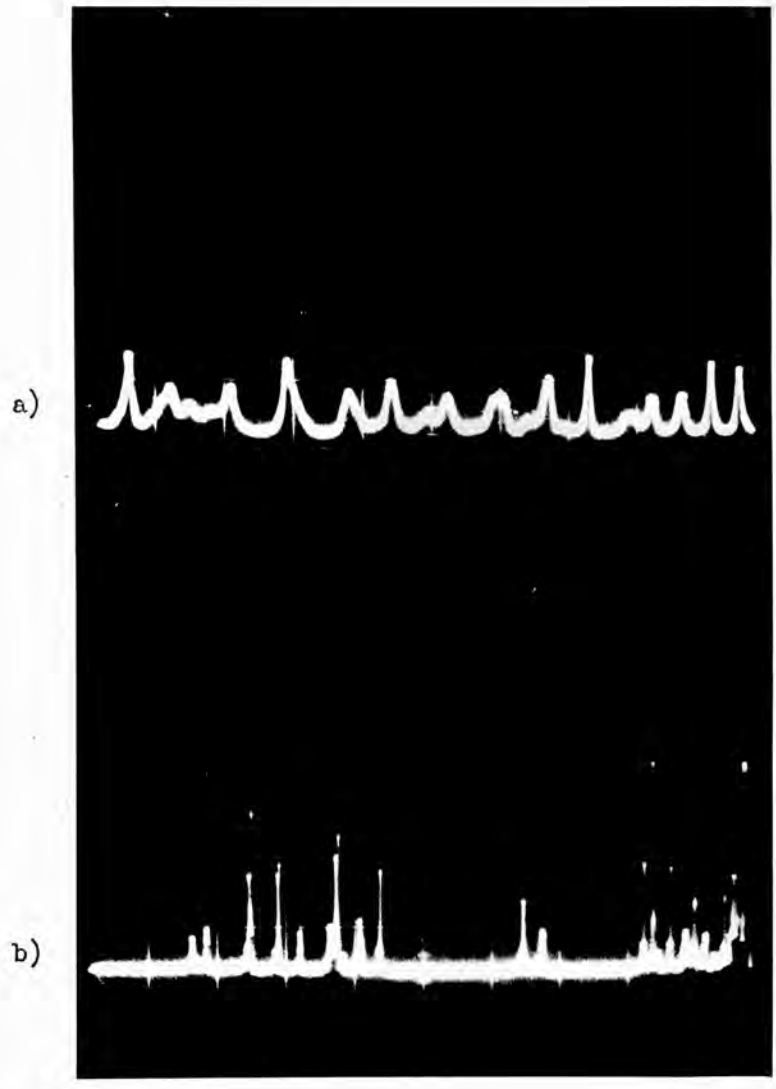

5 μs/cm

Fig. 4.2 Liquid pulse sharpening effect

a) Normal spiking

b) 20 mm. cell 1,2-dichloroethane in cavity

a)

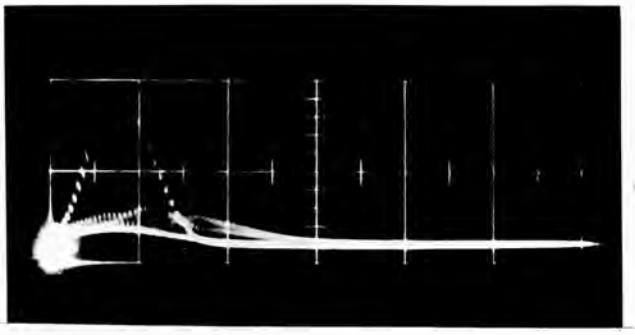

b)

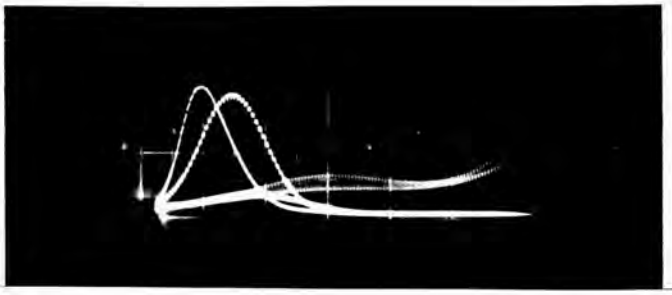

c)

50 ns/cm

Fig. 4.3 Liquid Q-switched pulses

a) Methanol 20 mm.

b) 1,2-dichloroethane 20 mm.

c) Acetone 76 mm.

Peak powers up to 100 kW were recorded, compared with 10 kW for the larger laser spikes in the absence of the liquid cell. A particularly strong effect is reported for the ruby laser when Q-switched with 1-chloronaphthalene, which produced 2 MW, 30 ns. pulses[145].

TABLE 4.I

Observed pulse widths for the neodymium laser with different Q-switching solvents. Cell length 20 mm.

Liquid	Pulse width ns.	Remarks
Acetone	35-100	
Benzene	75-150	
Carbon disulphide	300-500	No Q-switching
Carbon tetrachloride	200-300	Weak absorption
Chlorobenzene	100	
1-chloro-naphthalene	70-200	
1,2-dichloro-ethane	50-200	
Glycerol	150	
Methanol	20-100	
Nitrobenzene	200	
Water (distilled)	100-200	

All the common solvents found to Q-switch the neodymium laser have absorption bands in the near infra-red region (0.8 to 2.5 microns), caused by overtones or harmonics of the hydrogenic vibrations CH, NH, OH in the molecule. The resulting absorption at the laser wavelength, I.06 micron, ranges from I% to over 30% for 20 mm. path in the various liquids listed in Table 4.I [I39]. Carbon disulphide, a non-hydrogenic molecule with no absorption at I.06 micron, produced no pulse sharpening; carbon tetrachloride, a hygroscopic liquid with a measured absorption of the order of I% in the 20 mm. sample used in the experiment, gave a small reduction in pulse width and some increase in peak power. Mixing a small quantity of an active liquid e.g. acetone with carbon disulphide also caused a Q-switching effect, showing the phenomenon to be sensitive to even a slight amount of absorption.

In addition to the need for absorption it was found that pulse sharpening only occurred with the liquid cell placed in the standing wave field of the laser cavity. When the liquid was moved beyond the output mirror, or placed in a second cavity coupled to the first by a third aligned mirror, no pulse sharpening resulted. Modulation at the fundamental cavity frequency c/2L was observed with the cell near one mirror, changing to the corresponding harmonics when the cell was positioned at simple fractions of the cavity length, but this effect was subsequently established as arising from spectral channelling and spatial loss modulation due to the presence of the cell in the cavity, and is discussed further in Chapter 5.

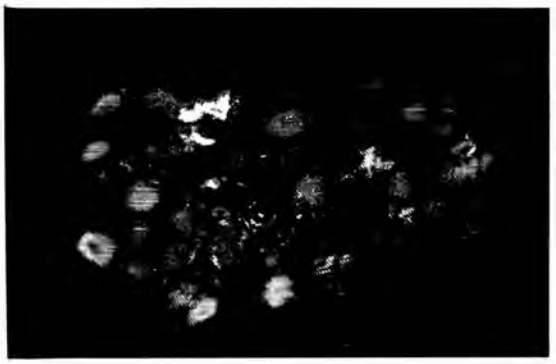

Fig. 4.4 Filaments in liquid Q-switched laser beam. Filament diameter approx. $\frac{3}{4}$ mm. Benzene

The liquid Q-switched laser beam pattern recorded on the target showed a distinct filamentary structure (Fig. 4.4), in contrast with the more uniform emission characteristic of normal spiking. The filaments were typically I mm. in diameter, with a more intense central component of $\sim$ I/3 mm. diameter observed on attenuating the beam. Pulse width and power measurements with a $\frac{1}{2}$ mm. aperture placed over the photo-diode showed that Q-switched pulses were associated with individual filaments, and that at least half the power was concentrated in this small area, indicating peak intensities in the liquid $\sim$ 50 MW/cm^2 for the most intense filaments. A small reduction in pulse width was also noted when observing this central region.

4.4 Discussion

The phenomenon of laser Q-switching by organic solvents described above can be interpreted in terms of the formation of phase gratings with the aid of the theory developed in Sec. 4.2 above, where it was shown that the induced refractive index modulation δn is proportional to the intensity of the standing wave producing it, and is established in a time of the order of the relaxation time for the physical process responsible. Because the thermal modulation is generally greater than those due to the optical Kerr effect or electrostriction for a given intensity, and because the experiments show that absorbing liquids Q-switch the neodymium laser, it is assumed that the effect is due to the development of a thermal phase grating during the growth of a laser spike. This view is supported by the experiment of Gires and Soep[40], who Q-switched a neodymium laser with a cuvette of ethanol at the focus of a lens in the cavity, and observed no Brillouin components in the emission spectrum. However, the long thermal relaxation time for common solvents, ~30 ns., means that the thermal grating develops relatively slowly and the modulation amplitude for a rapidly increasing intensity is correspondingly less than the steady state value. Further, the refractive index is <u>decreased</u> at points of high field intensity[37] because $(\frac{\partial n}{\partial T})_p$ is negative for these liquids at room temperature, 20 to 25 °C. This decrease

is opposed by both the optical Kerr effect and electrostriction, which tend to increase the refractive index at high field points, the former by changing the molecular polarisability at the anti-nodes of the standing wave, and the latter by a field induced increase in density. Thus electrostriction directly opposes thermal expansion, which tends to decrease the local density.

Whatever the process involved, the observed Q-switching is assumed to result from the dynamic increase in reflectivity of the phase grating during the growth of the pulse. This co-operative phenomenon arises from the coupling of the electromagnetic field with the liquid, and in the early stages the induced reflectivity is proportional to the square of the incident intensity, which leads to a rapidly increasing cavity Q and the evolution of a short pulse.

For a I mm. diameter filament with a power of I0 kW i.e. an intensity of I MW/cm^2, the thermal refractive index change is $\sim 10^{-6}$ (Sec. 4.2). For a grating 20 mm. long we find from (4.2.2) or (4.2.6) a reflectivity of 0.I to 0.2%. Already therefore the back reflected intensity is $\sim$ I kW/cm^2. If the Q-switched pulse grows exponentially with a rise time equal to the thermal relaxation time, the filament intensity reaches 20 MW/cm^2, about half the maximum observed, in $\sim$I00 ns. i.e. in three e-folding times. Taking an average absorption 0.05 cm^{-I} (I39) and a thermal relaxation time of 30 ns., we find from (4.2.I3) $\delta T = 0.0I5\ ^{o}C$ for $c\rho = 2\ J.cm^{-3}\ ^{o}C^{-I}$. Now $(\frac{\partial n}{\partial T})_P \sim -5.10^{-4}\ ^{o}C^{-I}$ for most of

these solvents at 20° C.[I38], so $\delta n \simeq -7.5.10^{-6}$, and the reflectivity of the thermal grating becomes R ~10%. Therefore the thermal effect is of sufficient magnitude at the observed intensity to increase the cavity Q significantly during the evolution of the pulse, and thus enable the liquid medium to produce a pulse sharpening or Q-switching effect. The electrostrictive increase in refractive index at 20 MW/cm^2 for a non-absorbing liquid is $\sim 10^{-6}$, too small to oppose thermal expansion in the absorbing liquid, and the increase due to the optical Kerr effect, $\sim 10^{-6}$ to 10^{-8}, is too small to be significant in most cases (Sec. 4.2). In the worst case, if these act together the thermal change in refractive index is reduced by 25%. It is significant in this context that carbon disulphide produces no Q-switching effect. Since it has negligible absorption at the laser wavelength of 1.06 micron[I39] and the largest optical Kerr and electrostrictive coefficients of the solvents tested[32, 34,36], with the possible exception of chloronaphthalene[32], this negative result suggests that it is the thermal effect which induces the observed Q-switching behaviour in the absorbing liquids.

From (4.2.7) and (4.2.8) the amplitude of the refractive index modulation due to the thermal effect is proportional to $\frac{\alpha}{K}\left(\frac{\partial n}{\partial T}\right)_P$, where α is the optical absorption coefficient. Table 4.2 shows that the Q-switching performance for several liquids, expressed as the ratio of the non-Q-switched to the Q-switched pulse width, increases with the magnitude of the

thermal coefficient. This is consistent with the thermal phase grating interpretation of the observed Q-switching behaviour. There are variations, the performance of acetone for example is somewhat stronger than predicted, but the trend is clear.

TABLE 4.2

Comparison of the thermal coefficients and Q-switching performance of several common solvents

Liquid	Thermal decay time ns. $\lambda = 1.06\,\mu$	$\frac{\alpha}{K}\left(\frac{\partial n}{\partial T}\right)_P$ $W^{-1} \times 10^{2}$	Max. obs. pulse sharpening
Methanol	40	3.5	15
1,2-dichloro-ethane	29	2	6
Benzene	30	1.8	4
Acetone	42	1.6	8.5
Carbon tetrachloride	43	0.2	1.5
Water	28	0.2	3
Carbon disulphide	23	< 0.1	1

CHAPTER 5 Influence of dielectric plates on laser emission

5.I Effect of subsidiary resonances in the cavity

We have seen in Chapter 2 that the emission of ideally mode-locked and random phase lasers with the same oscillating bandwidth is not easily distinguished by means of intensity correlation measurements. Furthermore, the noise generated in the random phase case has a periodicity imposed on it equal to the longitudinal mode spacing of the cavity, with the result that picosecond duration intensity fluctuations caused by interference of the random phase modes in broad band solid state lasers are emitted at regular intervals 2L/c. Therefore periodic picosecond pulse trains can be generated without mode-locking, although the signal to noise ratio differs greatly in the two cases[100]. The propensity of a laser of inhomogeneous construction to maximise emission and minimise losses by appropriate ordering of phase also results in modulation of the emission intensity[103,104, 105,106]. Similarly the frequency shift associated with stimulated Brillouin back scattering of laser light from a liquid in the cavity gives rise to mode interaction and beats in the emission intensity[17,19]. These three examples serve to show that laser oscillator emission is commonly periodic, with a frequency spectrum determined by the cavity resonances.

Where intensity modulation due to random phase effects differs from that caused by mode-locking is that the former is a linear process, whereas the latter is non-linear. The periodicity superimposed on random phase emission comes from the spatial modulation of the standing wave field in the cavity. Since the emission intensity is equivalent to the linear superposition of the normal modes, the impressed frequency is simply the Fourier transform of the spatial modulation imposed by the cavity boundaries, with a spatial period equal to twice the cavity length. In contrast, mode-locking involves coupling of the modes through a non-linear interaction in which mode amplitude and phase are no longer independent. Mode interactions are induced by frequency loss modulation[51,59] or spatial inhomogeneity in the cavity[103-106], and the effect is to generate beats between modes at the difference frequency and thereby frequency modulate the inversion, with the result that the gain by stimulated emission is a maximum for certain phase relations between modes. The phases are therefore determined by the generating condition, and mode-locking ensues.

In addition to the spatial modulation arising from the finite length of the cavity further resonances occur in practical laser oscillators. These correspond to various sub-cavity modulations imposed by the presence of optical elements in the main cavity, such as Q-switching dye cells or parallel-sided mirrors. Unless every dielectric surface, excepting one reflecting face on each of the two cavity

mirrors, is made strictly non-reflecting by setting it at the Brewster angle for the appropriate polarisation of the laser beam, then spatial modulation and spectral channelling result. Snitzer demonstrated this effect by using a thin glass plate as one of the cavity mirrors for a neodymium glass laser. The emission spectrum consisted of a series of equally spaced sharp lines[64]. Similarly dye mode-locked lasers with sub-cavity resonances emit multiply periodic groups of pulses whose several periods correspond to the various spatial modulations present[61,68,82,90,93,94]. The same is true of free running oscillators, although here the phase relations may alter from spike to spike[102]. The question is whether spatial and therefore spectral modulation of the oscillator cavity does more than impose spectral channelling and a characteristic frequency on the emission, whether in fact a static constraint in the form of a dielectric plate can induce mode-locking through the non-linearity of the amplifying medium.

A phenomenological description of mode-locking in the presence of absorption in the cavity has been given already for saturable absorption (Sec. 2.4); the phases are so ordered as to increase intensity fluctuations and reduce the loss by saturating the absorption. The modes therefore oscillate in phase, and absorption is minimised for a given mean power. If the absorption is non-saturable or increases with intensity, the modes tend to oscillate out of phase to achieve minimum loss, but at the same time they are favoured

by the intensity dependent stimulated emission process to oscillate in phase and so maximise emission in the laser medium[106]. This latter tendency reinforces mode-locking in the saturable dye case, but in the case of linear loss the two requirements are conflicting, and competition results. Although it is not clear which way the phases go in this situation, it seems unlikely that they can be random. Given the non-linearity of the amplifying medium it is more probable that they tend to oscillate in phase. Certainly the intensity of a free running laser is strongly modulated by the presence of dielectric plates in the cavity[149,150].

Experimental studies of this and other phenomena observed in the interaction of lasers with dielectric plates are described below, but first we discuss the relevant properties of both single and multiple plates, and give the theory for a practical multi-plate laser reflector.

5.2 Spectral properties of dielectric plates

The transmittance of a non-absorbing plane parallel-sided dielectric plate is[154]:

$$T = (1 + 4z^2 \sin^2\Delta)^{-1} \qquad (5.2.1)$$

where $$z = \frac{\sqrt{r}}{1 - r} \qquad (5.2.2)$$

and the phase $$\Delta = \frac{2\pi n d}{\lambda} \cos\theta \qquad (5.2.3)$$

Here n is the refractive index, Θ the internal angle which each refracted beam makes with the normal to the surface, λ the wavelength of the incident light, d the thickness of the plate, and r the reflectance of a single surface:

$$r = \left(\frac{n - I}{n + I}\right)^2 \qquad (5.2.4)$$

The transmittance is therefore modulated with the spectral period $\bar{\nu} = (2nd\cos\Theta)^{-I}$, and has a maximum value of unity, a minimum value $T_{min.} = \left(\frac{I-r}{I+r}\right)^2$, and a modulation depth $M = \frac{4r^2}{(I+r)^2}$. Maximum transmittance occurs for $\Delta = p\pi$, where p is an integer i.e. when the optical path in the plate is an integral number of half wavelengths, and minimum transmittance when $\Delta = (p+\frac{1}{2})\pi$ i.e. for an odd integral number of quarter wavelengths. Typical values for a glass plate at normal incidence are found on setting $n = I.5, \Theta = 0$, $d = I$ mm. ; whence $r = 0.04$, $\bar{\nu} = 3.3\ cm^{-I}$, $T_{min.} = 85\%$, $M = I5\%$.
The insertion of a tilted plate in a laser cavity modulates the gain sufficiently to restrict oscillation to narrow spectral bands centred on the peak transmitted wavelengths[I5I]. Similarly, a single plate reflector restricts oscillation to those wavelengths for which the reflectance is a maximum[64] i.e. for those satisfying the minimum transmittance condition $\Delta = (p+\frac{1}{2})\pi$. For $n = I.5$, the peak reflectance of a single plate is I5%.

The maximum reflectance of N regularly arranged plane parallel plates has been given already (4.2.3), and for air-spaced dielectric plates is[136]:

$$R_{2N} = \left(\frac{n^{2N} - I}{n^{2N} + I}\right)^2 \qquad (5.2.5)$$

Thus for two plates, with $n = I.5$, $R_4 = 45\%$.

For N randomly arranged plates it is not generally possible to satisfy the condition for constructive interference either for reflection or transmission, and so the reflectance R takes some intermediate value in the range $0 \leq R \leq R_{2N}$, with a mean $\bar{R}_{2N}$, which can be found by averaging with respect to phase over the range $0 \leq \Delta \leq \pi$. For a total of m surfaces the mean reflectance is[152]:

$$\phi(m) = \frac{mr}{I + (m-I)r} \qquad (5.2.6)$$

and since $m = 2N$ for N plates,

$$\bar{R}_{2N} = \left(I + \frac{4n}{2N(n - I)^2} \right)^{-I} \qquad (5.2.7)$$

where we have used (5.2.4) to eliminate r. For $n = I.5$, $\bar{R}_4 = I4.3\%$, which may be compared with $R_4 = 45\%$ for the case of constructive interference. Increasing the number of plates increases the mean reflectance, which is asymptotic to unity (for $N \to \infty$), but a lower limiting value than this is set by the accompanying increase in surface scattering loss and

bulk absorption. For a stack of I3 thin glass plates with n = I.5 the mean reflectance given by (5.2.7) is $\bar{R}_{26}$ = 52%. Such a stack, which is easily constructed with microscope cover slips for example, could be used as the output mirror of a laser oscillator, a suggestion first made and successfully demonstrated by Burch[I53]. A reflecting stack of this type in which the optical path varies over the aperture by several wavelengths has a reflectance whose mean is $\bar{R}_{2N}$, with higher local values in those regions where the arrangement of surfaces more nearly approaches the condition for constructive interference. The beam generated by a laser with a random stack cavity mirror has an irregular filamentary structure due to this random variation of reflectivity, with a minimum filament diameter presumably determined by the condition that the increased gain resulting from the local enhancement of reflectivity be balanced by the increase in diffraction loss.

The requirement that the peak reflectance of each plate in the stack fall within the same spectral band of the plate modulation places a stringent limit on allowed random variations in thickness about the condition for constructive interference. This may be shown as follows:

For normal incidence, the condition for peak reflectance of a single plate is:

$$2nd = (p+\tfrac{1}{2})\lambda_p \qquad (5.2.8)$$

where p is an integer and λ_p the wavelength. Increasing p

to p+I, and taking the difference in wavelength, we find the modulation period

$$\Delta\lambda = \frac{2nd}{p^2} \qquad (5.2.9)$$

for $p \gg I$. Similarly, the change of wavelength $\delta\lambda$ necessary to satisfy the peak reflectance condition (5.2.8) on a small change δd of plate thickness is:

$$\delta\lambda = \frac{2n\delta d}{p} \qquad (5.2.10)$$

again for $p \gg I$. We require $\delta\lambda < \Delta\lambda$, whence from (5.2.9) and (5.2.10), and eliminating p by means of (5.2.8),

$$\delta d < \frac{\lambda}{2n} \qquad (5.2.11)$$

For $n = I.5$, $\delta d < \frac{1}{3}\lambda$. Since this condition is unlikely to be met in a stack of thin glass plates, the random phase calculation for the mean reflectance of the stack suffices.

5.3 Self-modulation with multiple plates

The observation of intensity modulation due to beats between cavity modes in the free running laser and the creation of subsidiary resonances by the introduction of dielectric elements in the cavity have been discussed. The modulation amplitude is increased by restricting the number

of oscillating modes[I50]. An experimental study of intensity modulation of the neodymium laser with glass plates reveals a dependence of modulation amplitude on spectral period, number of plates, and surface reflectivity. This will now be described.

Experiments were performed with the neodymium glass laser described earlier (Sec. 4.3) operated in a cavity defined by a pair of thin film multi-layer dielectric mirrors, with surfaces flat to 0.I of the wavelength. The cavity length was variable over the range 0.5 to I.7 metre, and observations were made with various plates inserted in the cavity, or with one mirror replaced by a random stack reflector[I53]. The emission was recorded simultaneously by an EMI 97I3B photo-diode and Tektronix 555 oscilloscope combination for monitoring the overall spiking, and a fast ITT F4000 SI photo-diode and Tektronix 5I9 oscilloscope combination for observing the intensity modulation on individual spikes.

It was found that I00% modulation at the fundamental cavity frequency c/2L was imposed on the emission of the laser when using a stack reflector consisting of eight I mm. thick glass microscope slides. For a I.5 metre cavity this frequency is I00 MHz. Fig. 5.I shows three examples of such modulation observed on successive laser shots. Replacing the stack mirror with a thin film dielectric mirror reduced the modulation to the range I0 to 20%, this residual amount presumably arising from self-modulation within the active medium, as described earlier. Pulses with similar envelopes

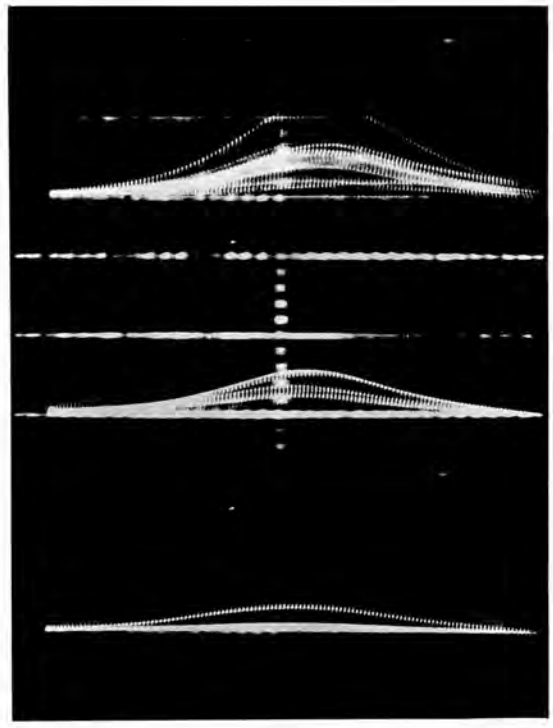

200 ns/cm.

Fig. 5.1 Pulse modulation with multi-plate stack mirror

8 x 1 mm. glass slides

are compared in Fig. 5.2 . Examination of single modulated waveforms generated by the laser with stack reflector revealed the frequent occurrence of periodic trains of sharp pulses of period 2L/c, with some background noise between pulses (Fig. 5.2). The observed pulse width to spacing ratio of ~0.I requires the simultaneous oscillation of at least I0 adjacent longitudinal cavity modes. For random phases the peak fluctuation intensity is expected to be approximately ln I0 (Sec. 2.5) i.e. a ratio of peak intensity to background of approximately 2.3: I [I00]. The observed ratios lie in the range 3:I to 5:I, corresponding to 20 to I50 (e^3 to e^5) modes in the random phase case, and requiring pulse widths less than the instrument limited width of 0.7 ns. for the cavity length used (L = I.7 metre, 2L/c = II.3 ns.). However, the recorded pulse widths of approximately I ns. exceeded this limiting value, and the observations suggest that partial mode-locking may have occurred in these cases.

Beats at the fundamental cavity frequency c/2L were also observed with a single glass plate inserted in a cavity formed between two wedged thin film multi-layer dielectric mirrors (Fig. 5.2) . This was true for minimum self-modulating configurations, with the laser rod at the centre of the cavity[I03,I04], or for short cavity lengths[I55,I56]. A series of observations were made for various plates inserted in the cavity, noting the average depth of the intensity modulation as a function of their number and thickness (recorded as equivalent spectral period). The results are shown in Table 5.I,

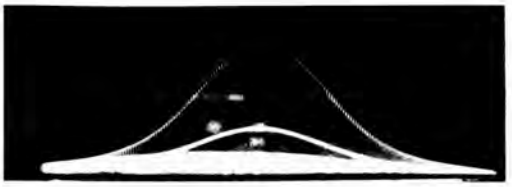

a) Stack mirror 200 ns/cm.

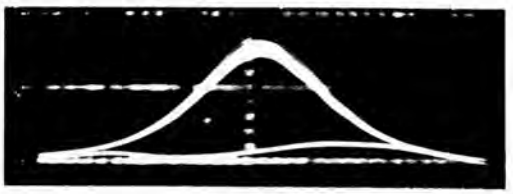

b) Dielectric mirror 200 ns/cm.

c) 1 mm. plate in cavity
20 ns/cm.

d) Wedged dielectric mirrors
20 ns/cm.

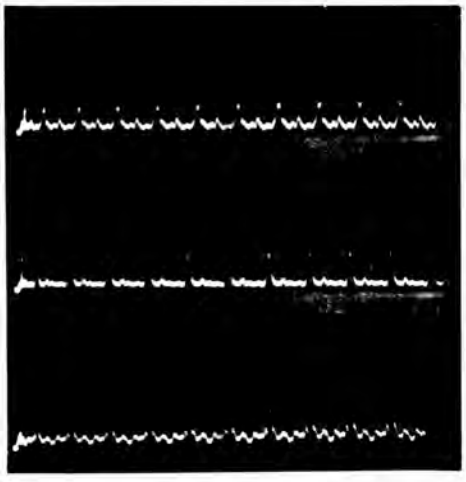

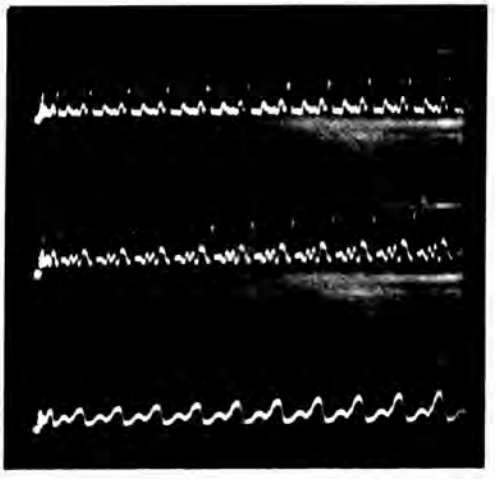

e) Pulse modulation with multi-plate stack mirror 20 ns/cm.

Fig. 5.2 Comparison of self-modulated waveforms

whence it is concluded that the modulation amplitude increases with the number of plates, and that those producing the greatest modulation have a spectral period in the range I to 20 cm^{-I}, comparable with the homogeneous linewidth of $\sim$ 20 cm^{-I} reported for neodymium glass[64,I57], within the overall inhomogeneously broadened bandwidth of 300 cm^{-I}.

TABLE 5.I

Intensity modulation observed with dielectric plates inserted in the neodymium laser cavity

Element	Thickness	Spectral period cm^{-I}	Number of elements	Mean obs. intensity modulation	Remarks
Pellicle (cellophane)	6 μm.	600	I	23%	On higher power pulses
Cover slip (glass)	0.I5 mm.	22	I	25%	
	..	..	4	45%	
Microscope slide (glass)	I mm.	3.3	I	33%	
	..	..	2	39%	
	..	..	4	60%	
Schott RG I000 glass	2 mm.	I.7	I	39%	Transmission 64%
Fabry-Perot etalon	I00 mm.	0.05	I	I5%	Uncoated wedged silica plates

Experimental evidence for the influence of transmission loss modulation on the intensity modulation was obtained by

inclining a set of 4 glass slides at angles ranging from normal incidence to the Brewster angle. The observed intensity modulation varied accordingly, from the tabulated value for normal incidence to zero at the Brewster angle, where the reflectivity and therefore the transmission modulation of the polarised laser beam vanish.

Although the observed modulation with a few plates in the cavity may be consistent with the random phase interpretation[I50], it appears that the larger number of plates and their random arrangement in the multi-plate stack reflector does induce some mode-locking between those modes generated in such a cavity, in accordance with the ideas referred to earlier[I05,I06].

Finally it may be remarked that the modulation observed on liquid Q-switched pulses (Sec. 4.3) arises from the presence of the liquid cell in the cavity, since the windows constitute a pair of dielectric plates. Removal of the liquid, leaving a dry cell, increases the intensity modulation because the interface reflectivity is increased, and tilting the cell at the Brewster angle removes the modulation. Thus a liquid cell orientated at this angle produces nearly modulation-free Q-switched pulses.

5.4 Operating characteristics of the laser with random stack mirror

The observation of 100% intensity modulated pulses generated by a laser with a reflector consisting of a stack

of randomly arranged dielectric plates has been described in the previous section. Here we consider further aspects of the random stack laser resonator.

In the free running case, the laser emits a series of random spikes bearing the intensity modulation discussed, their number and average separation depending on the pumping and the cavity length. In a short cavity the number of spikes so increases due to the high mean reflectivity and random structure of the multi-plate reflector, that quasi-continuous emission is observed. An example of this is shown in Fig. 5.3 for a 330 mm. cavity (of which 230 mm. constituted the optical path in the laser rod); the emission obtained with the stack reflector is compared with that observed for a thin film multi-layer dielectric mirror. This effect can be explained in terms of the high mode degeneracy(I58) of the short cavity with stack reflector, with the noise level arising from the poor optical quality of the latter, much as Berzing et al.(I59) found for poorer quality laser rods in a quasi-continuous system.

In the case of a dye mode-locked oscillator, the multi-plate stack mirror offers the advantage of improved damage resistance to the high intra-cavity light intensity(I60). However, the spectral modulation and mode selection effects of the plates produce pulse broadening(80). For example, with a stack reflector consisting of I3 cover slips each 0.I5 mm. thick the pulse widths inferred from two-photon fluorescence (TPF) intensity correlation measurements (Sec. 2.3) were

a)

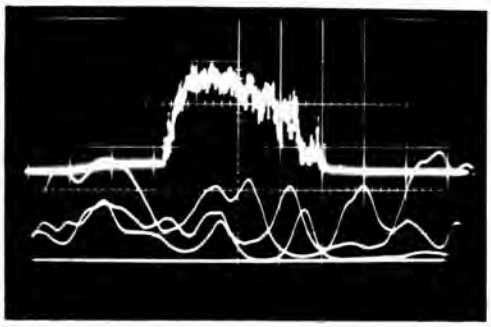

b)

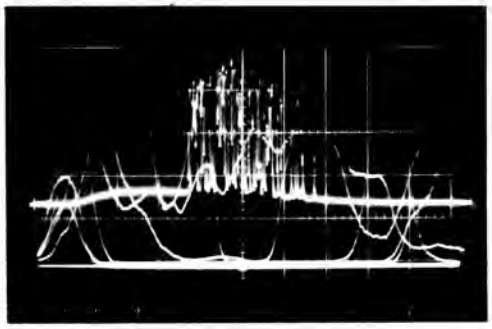

Upper 100 μs/cm

Lower 1 μs/cm

Fig. 5.3 Quasi-continuous emission with multi-plate stack mirror

a) 8 x 1 mm. stack

b) 50% reflectance wedged dielectric mirror

a)

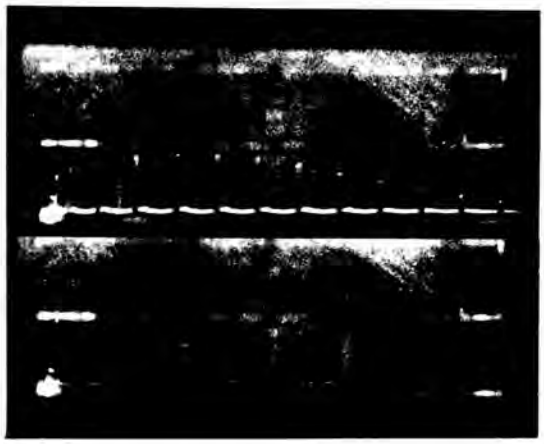

Upper 10 ns/cm

Lower 2 ns/cm

b)

Fig. 5.4 Dye mode-locked laser with random stack mirror

a) Mode-locked pulse train

b) Beam pattern on target distant 0.75 m. Aperture 5 mm. diam. 4 successive shots

20 to 50 psecs. for the neodymium glass laser. No such pulse broadening is reported for the ruby laser with similar reflector[160], nor is expected, since the spectral modulation period of the plates used is approximately 20 cm^{-1}, almost an order of magnitude larger than the ruby emission linewidth. Fig. 5.4 shows the instrument limited pulses obtained with the mode-locked neodymium laser with stack reflector, and the irregular intensity distribution in the laser beam, which changes with successive firings.

Comparison of the laser beam divergence with the stack reflector and with a thin film multi-layer dielectric mirror gave similar results for both the mode-locked and free running (random spiking) cases, provided the variation of plate inclination in the stack was less than the divergence observed with the thin film mirror, which amounted to I.3 milli-radian for the free-running neodymium laser.

Thus in some cases a simply constructed stack reflector, with its higher damage threshold and lower cost, may be used in a laser system in place of the conventional optically flat dielectric mirror.

CHAPTER 6 Experimental study of a liquid laser amplifier

6.I Design and construction

The potential of the neodymium liquid laser as an an amplifier for short optical pulses has already been remarked (Chapter 3). Briefly, it has a greater stimulated emission cross-section than neodymium glass, a comparable spectral bandwidth, and can be prepared with a similar concentration of neodymium ions. The performance of a neodymium phosphoryl chloride liquid laser amplifier is described below (Sec. 6.3). Here we discuss its design and construction.

The cell is shown in Fig. 6.I . It consists of a thick-walled silica tube, I53 mm. long and 8.5 mm. bore, terminated by optically flat windows which were attached by careful contacting and subsequent fusion of the mated surfaces. In contrast to the selenyl chloride laser, no self-oscillation occurs with neodymium phosphoryl chloride solution optically pumped in this configuration because of the near refractive index match with fused silica (Sec. 3.3). Since the refractive indices are I.460 and I.4495 for pure phosphoryl chloride[I25] and fused silica[I6I] respectively, the reflection coefficient for normal incidence at the interface is $\sim 10^{-5}$. That for the silica/air boundary at the outer face of each cell window is 3.4%, requiring a single pass gain G = 30 for self-oscillation, a high value not realised with the experimental system. For longer cells at high excitation it would be

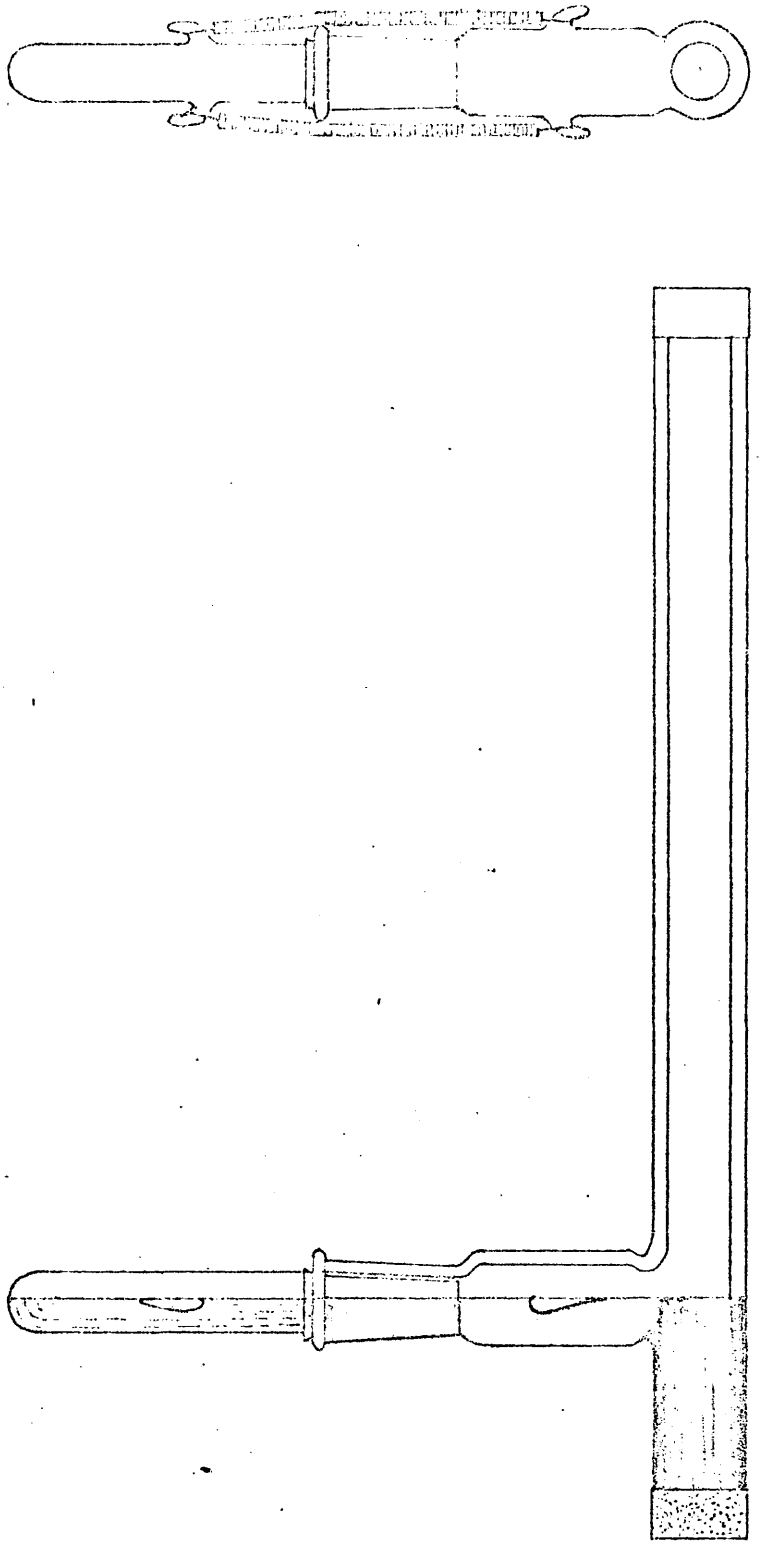

Fig. 6.1 Liquid laser cell

necessary to use tilted exit faces to avoid possible self-oscillation, preferably oriented at the Brewster angle to avoid reflection losses.

The cell is filled through the side tube attached near one end and closed by means of a cone and socket joint with a Teflon (PTFE) seal. A steady pressure is maintained by the springs attached to glass hooks on the tube and stopper. The air space left in the neck of the side tube after filling, and the further space in the hollow stopper, allow for thermal expansion of the solution and dissipation of the pump-induced shock wave. The springs provide a safety valve in the event of too great an over-pressure being generated. This design allows for flexibility, in that it is relatively easy to empty and re-fill with fresh solution, and yet is adequately sealed for use over a period of a few months.

Having evolved a suitable cell design, the next problem was to excite the laser medium efficiently, and with a minimum of optical distortion. Because the thermal expansion coefficient for liquids is of the order of 100 times that for solids, the refractive index distortion in the optically pumped liquid laser is correspondingly greater (Chapter 3). The temperature coefficient of refractive index for common liquids (Sec. 4.4) is $\sim -5.10^{-4}\ ^{o}C^{-1}$, so for a column 150 mm. long the change in optical path due to a temperature rise of 0.01 C.deg. is of the order of a wavelength (for $\lambda \sim 1\ \mu m.$). Now microscopic random fluctuations of temperature in a liquid

merely give rise to scattering losses (Chapter I), but a temperature variation of this magnitude on a macroscopic scale, such as a radial distribution resulting from non-uniform pumping, causes sufficient refraction to distort the beam propagating in a liquid amplifier of the given dimension. In the ideal case of circular symmetry and a monotonic temperature distribution this produces a lens effect of either positive or negative power, depending on whether the axial temperature is lower or higher than that at the circumference. In a practical system perfect circular symmetry is unlikely to be achieved and a distorting lens effect results, which produces an irregular intensity distribution in the transmitted beam.

The chosen cell design is equivalent in cross-section to a cladded laser rod[64,I62] when filled with the solution, in that it consists of an optically absorbing medium of circular cross-section surrounded by an annulus of transparent material of very nearly the same refractive index. By adjusting the internal and external radii of the cylinder and the optical absorption of the laser medium, the distribution of the pumping intensity can be optimised with respect to minimum thermal distortion and uniform gain profile[I63]. For an isotropic intensity distribution of pump light incident at the outer surface of the composite cylinder, the ratio of the radii should be equal to the refractive index of the medium[I62,I64]. The optimum absorption is dependent on the detailed absorption spectrum, and the

actual absorption may depart from the optimum because of practical constraints on the diameter of the amplifier and on the concentration of the laser solution. An optimum neodymium concentration, with respect to fluorescent efficiency, of 0.3 molar is reported for selenyl chloride[110], corresponding to a quoted Nd^{3+} ion concentration 1.8×10^{20} cm^{-3}. The neodymium phosphoryl chloride-tin tetrachloride solutions ($Nd:POCl_3-SnCl_4$) used in the amplifier experiments were prepared with Nd^{3+} ion concentrations in the range 0.7 to 1.0 $\times 10^{20}$ cm^{-3} i.e. 0.35 to 0.5 normal, the latter being a saturated solution.

A practical approach to the problem of achieving an isotropic intensity distribution for uniform pumping is to use a helical discharge lamp closely surrounding the cylindrical laser cell, with an external diffuse reflecting cylinder surrounding the lamp[164]. This method has two limitations: first, the large radiation volume leads to a low excitation efficiency; second, the pulse discharge time of helical lamps is inherently long, leading to excessive heating and consequent distortion of the laser solution. Since the radiative lifetime of the metastable Nd^{3+} ion is of the order of 100 μs. in solution (Chapter 3), it is desirable to pump on this time scale. Pulse durations of this order are more easily achieved with linear flashlamps; further, the pumping volume is significantly less than that associated with helical lamps. The problem of isotropy in the pumping intensity reasserts itself however, and has only been successfully

overcome by mounting both lamp and laser end to end on the axis of a rotationally symmetric reflector[I64,I65]. This arrangement limits access to one end of the laser only, and is more suited to small oscillator applications. Returning to the conventional parallel arrangement of lamp and laser, since the use of a single lamp produces asymmetric pumping and a thermal wedge effect, it is necessary to use several lamps symmetrically disposed to achieve better uniformity. The optimum number is $N \simeq \frac{D}{d}$, where D and d are respectively the apparent diameters of the laser rod and the luminous column in the lamp, allowing for refractive index immersion effects[I66]. For the cell shown in Fig. 6.I, D = I2.4 mm., and the internal diameter of the flashlamp d = 9.5 mm., whence $\frac{D}{d}$ = I.3, and the next larger integer is N = 2. Therefore two linear xenon lamps were used for pumping the liquid laser. These were placed symmetrically on either side of the cell, and a polished silver sheet was wrapped closely round the assembly to provide good optical coupling in a symmetric afocal arrangement[I64]. This geometry combined reasonably uniform pumping with a short pump pulse duration.

A final consideration relevant to minimising optical distortion of the laser medium is the need for filtering the pump light such that only that portion of the lamp spectrum corresponding to the neodymium absorption bands is incident on the liquid. As pure phosphoryl chloride is colourless, the striking lilac colour of the neodymium solution is entirely due to the Nd^{3+} ion absorption bands, and so only

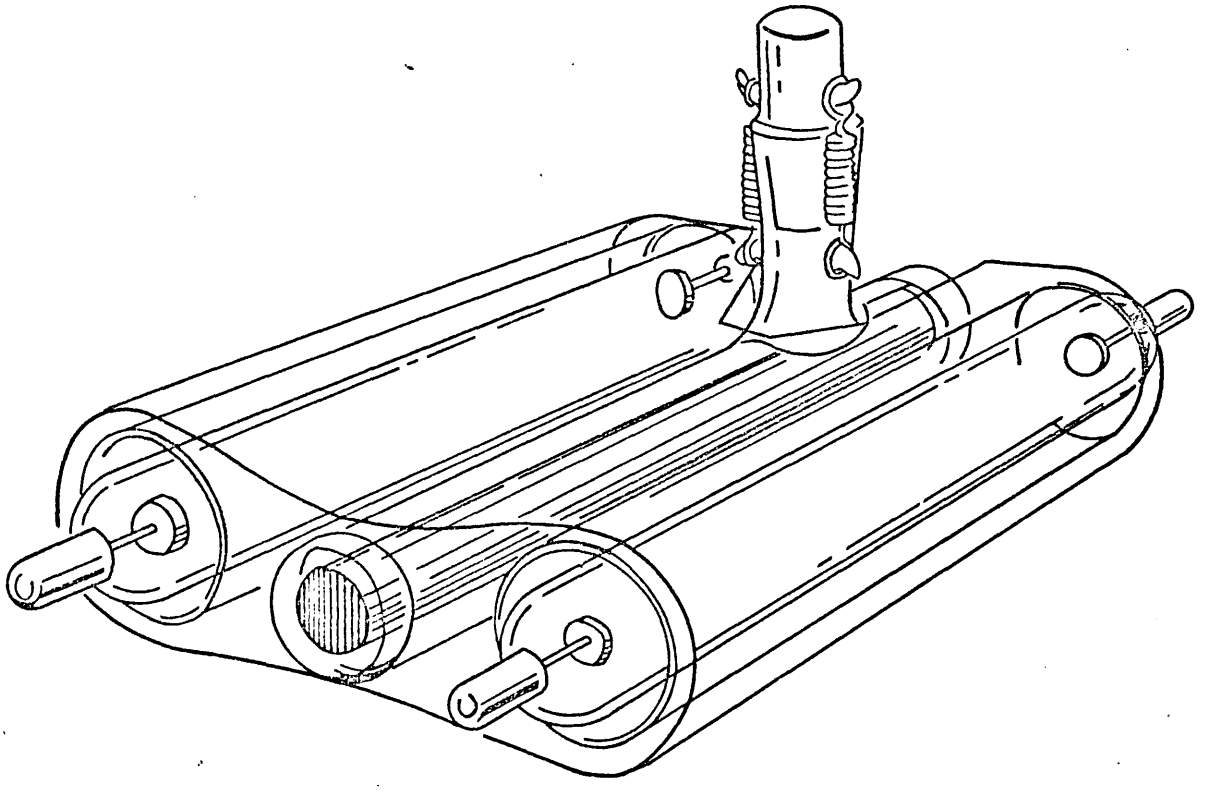

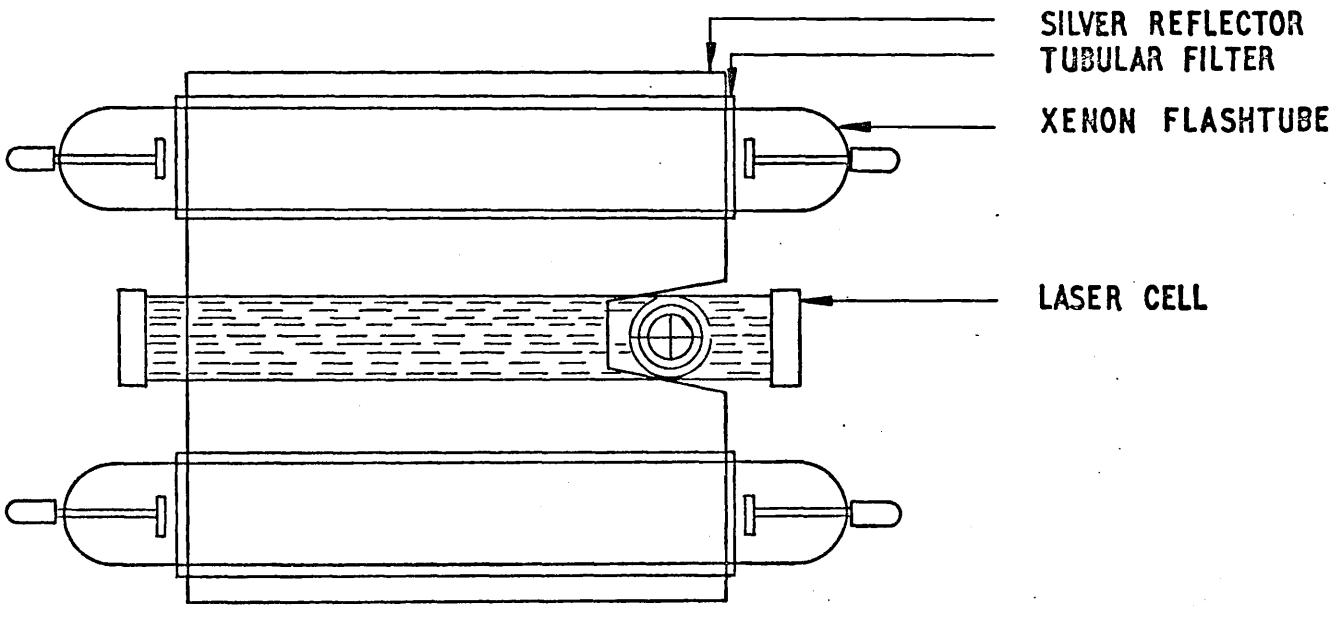

Fig. 6.2 Liquid laser assembly

the ultra-violet and blue regions of the spectrum ($\lambda < 0.4$ μm.) need be filtered out, since it is here that the peak lamp brightness occurs and thus induces excessive heating of the liquid. Tubular filters of Pyrex or uranyl glass were used for the purpose, provision being made to fit them either over the lamps or the liquid cell. The liquid laser assembly is shown in Fig. 6.2 .

6.2 Behaviour of neodymium oscillators

6.2.I Neodymium phosphoryl chloride laser

Prior to the amplifier experiments, some observations were made on the behaviour of the neodymium liquid laser oscillator. Information was obtained on beam divergence and intensity distribution, the maximum available gain, and pump induced distortion of the laser medium. In addition, the efficiency of various neodymium solutions was compared as a guide to selection for the liquid amplifier experiments.

Fig. 6.3 shows some typical intensity distributions. In a) the beam was photographed through four neutral density quadrants to obtain a measure of the divergence, which amounted to approximately 6 milli-radians full angle between half power points. The speckle pattern associated with the use of a random plate reflector (Chapter 5) as one of the cavity mirrors can be seen in b) and c). Several small filaments of 0.5 to I mm. diameter were observed in the near

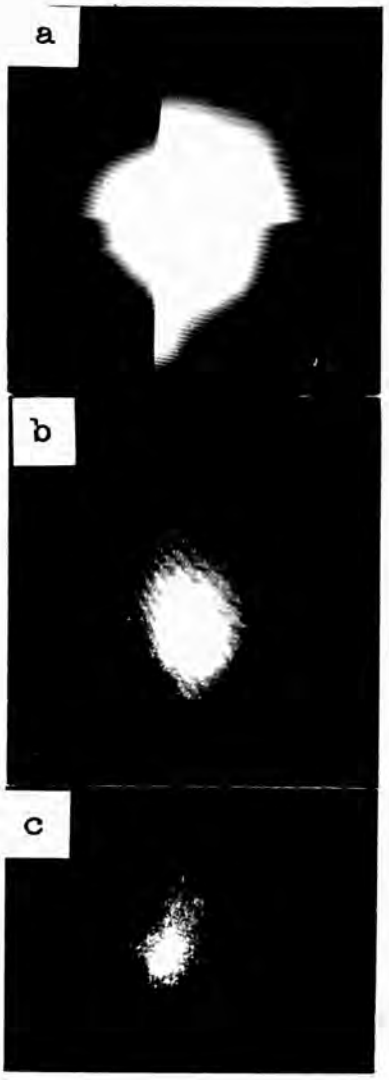

Fig. 6.3 Nd:$POCl_3$ oscillator beam patterns

a) Divergence

b) 15 x 0.15 mm. stack reflector

c) As b).

field when using thin film multi-layer dielectric cavity mirrors and uranyl glass flashlamp filters.

Optical distortion of the liquid after pumping was displayed by passing the beam of a helium-neon gas laser through the laser cell, as in ref. 110, and observing the flare patterns on a white card a few metres distant. In this way the efficacy of the optical filtering of the pump light could be examined, and the use of the uranyl glass filters was found to greatly reduce the distortion. Pump-induced refractive index variations within the liquid in the range I to 5.10^{-5}, depending on the filtering arrangements, were inferred from the steady deflection of the beam after firing. Thus the maximum radial temperature variation reached during the pumping pulse was $\lesssim$ 0.I ^{o}C., and the variation of optical path amounted to several wavelengths across the aperture. If the laser was fired again before the recovery of thermal equilibrium, the beam pattern obtained closely resembled the flare pattern seen with the helium-neon laser, showing that refractive index distortion largely determined the intensity distribution of the generated beam, as in the case of the ruby laser[167].

The maximum small signal gain attainable was readily determined by reducing the reflectivity of the oscillator cavity mirrors until laser threshold coincided with the maximum available pumping intensity. For a 0.44N solution of Nd:$POCl_3$-$SnCl_4$ pumped in the arrangement shown in Fig. 6.2, laser spiking was observed using an external gold mirror

aligned with the exit face of the window at the far end of the cell, the Fresnel reflection from the window providing sufficient feedback for oscillation at the maximum pumping energy of I kilojoule, using unfiltered pumplight. The duration of the pumping pulse was 300 μs, and the time to peak intensity I00 μs., at which point the first spikes appeared. For a reflectivity of 3.4% (Sec. 6.I) the occurrence of self-oscillation indicated a single pass small signal gain G = 5.4, assuming a reflectance of unity for the gold mirror. Since the cell length was I53 mm., the measured gain required an exponential gain coefficient of 0.II cm^{-I}. For a stimulated emission cross-section of $I0^{-I9}$ cm^2 (I23), and a Nd ion concentration of 8.8 $I0^{I9}$ cm^{-3} (0.44N), this corresponds to an inversion of I½%. With the tubular filters fitted over the flashlamps the maximum gain was reduced, presumably due to the increased reflection losses at the extra glass surfaces, and probably some absorption loss in the case of uranyl glass.

6.2.2 Mode-locked neodymium glass laser

A mode-locked neodymium glass oscillator was constructed to provide a signal source for the liquid amplifier. The laser head, described earlier (Sec. 4.3), contained a water-jacketed laser rod and a pair of linear xenon flashtubes. The pumping geometry closely resembled that used for the liquid amplifier, with the Pyrex water-jacket providing a

combined refracting sheath and ultra-violet filter for the immersed laser rod, which had a lightly ground surface to diffuse the pumping light. Under pulsed (random spiking) operation, a uniform far field intensity distribution was obtained with this geometry. In view of the multiple pulsing effects caused by introducing subsidiary resonances in the oscillator cavity (Chapter 5), care was taken to employ Brewster angle orientation of dielectric surfaces for mode-locked operation. The mode-locking dye cell was constructed from two silica discs with a 1 mm. spacer, and filled through a small opening with Eastman 9860 dye solution conveniently dispensed from a hypodermic syringe. Hard dielectric coatings were used on the cavity mirrors to reduce the damage caused by the high light intensities generated by mode-locking, and the exterior face of each mirror was wedged with respect to the reflecting face to avoid spectral channelling effects[79]. The dye cell, oriented at the Brewster angle in its swivel mount, was placed near the non-transmitting mirror, and a 5 mm. diameter circular aperture near the output mirror. The purpose of the aperture was to limit the diameter and divergence of the beam by increasing the loss for non-axial modes. A sketch of the oscillator is included in Fig. 6.7 .

A typical pulse train emitted by the mode-locked laser is shown in Fig. 6.4a . The pulse spacing corresponds to the cavity round trip time 2L/c. The emission was monitored with a fast planar photo-diode (ITT F4000) mounted in a co-axial tapered holder designed to provide impedance matching to the

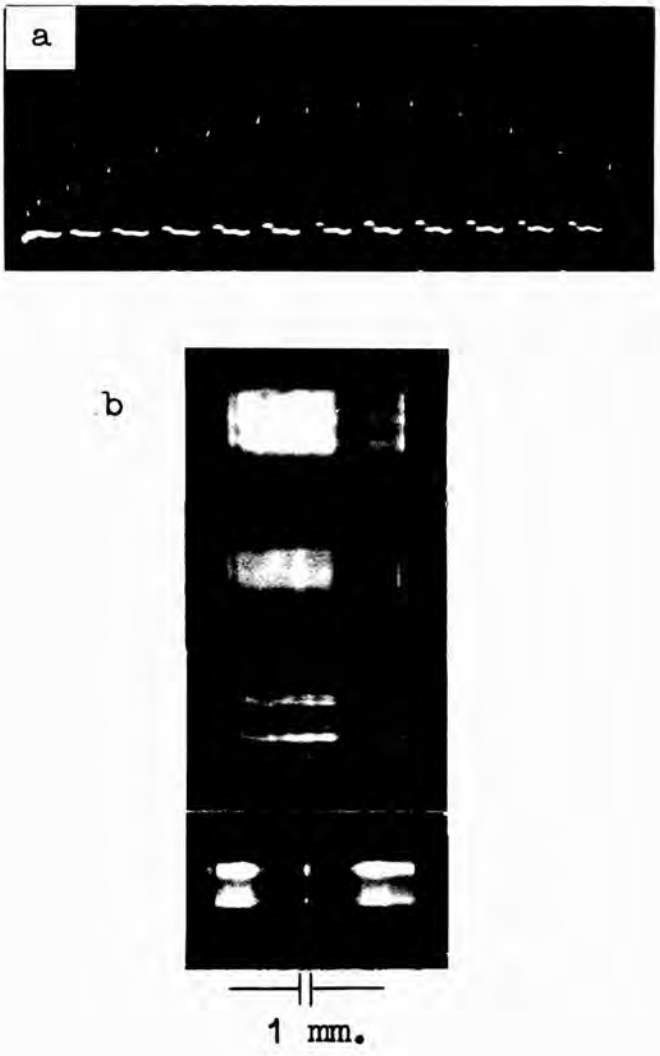

Fig. 6.4 Mode-locked Nd:glass laser

a) Mode-locked pulse train 10 ns/cm

b) TPF intensity records - wedged mirror
- parallel mirror
- parallel dye cell
- cross correlation with neutral density filter

Tektronix 519 oscilloscope[168]. The small after pulses reflect the electrical response of the system[71]. The beam divergence was approximately I milli-radian for a pumping energy of I.2 kilojoule and pump pulse duration 700 μs. With cavity mirrors of 99.5% and 50% reflectance respectively, and a 0.95 metre cavity length, single picosecond pulses were obtained, spaced at the double cavity transit time of 6.3 ns. Auto-correlation (Sec. 2.3) was performed by reflecting the pulses at the surface of a mirror immersed in rhodamine dye solution, and the intensity ratio estimated by covering part of the field with a neutral density filter[63]. Pulse widths ~5 ps. and contrast ratios ~2 were observed. Replacing the wedged laser output mirror with a parallel sided one produced additional pulses separated by the optical thickness of the element, and setting the mode-locking dye cell normal to the beam had a similar result, with pulses spaced only I to 2 mm. apart. Examples of these two-photon correlation patterns are shown in Fig. 6.4b. More precise measurements of pulse duration and contrast ratio obtained for both oscillator and amplifier by microdensitometry are described in Sec. 6.3 .

Because of the high instantaneous intensity of picosecond pulses generated by the mode-locked laser several higher order multi-photon experiments are possible, in addition to the two-photon fluorescence measurements just described. Such observations also serve as a check on the nature of the laser emission, that it is truly mode-locked and not random phase, since the yield of a k-th order process is dependent on the k-th power of the incident intensity, and therefore the

discrimination becomes increasingly sensitive as the order k is increased.

Fig. 6.5a shows intense scattered third harmonic light generated by focusing the mode-locked laser beam in a stack of fused silica discs[63], using a 250 mm. focal length lens. A check on the wavelength and intensity of the incident light was provided by first passing the beam through a weak rhodamine 6G dye solution, where it produced two-photon fluorescence, and a Schott RG 1000 infra-red filter. The scattered light was photographed through a Wratten 18A filter (transmission band 0.3 to 0.4 micron) on blue-sensitive film (Polaroid 4IO), indicating an approximate wavelength of 0.35 micron, consistent with it being the third harmonic of the incident light ($\lambda = 1.06\mu$).

Fig. 6.5b shows the luminosity generated in a 50 mm. cell of 1-chloronaphthalene at the focus of a 1 metre focal length lens. Using a combination of Wratten filters (Nos. 8 and 18A) it was found that the maximum luminosity occurred at a wavelength near 0.4 μ., with none beyond 0.46 μ. and fainter emission in the 0.35 μ. region. This blue emission is presumably identical with that generated by two-photon absorption of ruby laser light in chloronaphthalene[169,170]. Thin filaments $\sim$50 microns in diameter and extending for a few tens of millimetres in the luminous channel were frequently observed (Fig. 6.5c), indicating self-trapping of the incident picosecond pulsed laser beam.[48,49] The stability of the filaments showed that the blue luminosity probably resulted from three-photon fluorescence, rather than by electric breakdown of the liquid in the strong light field.

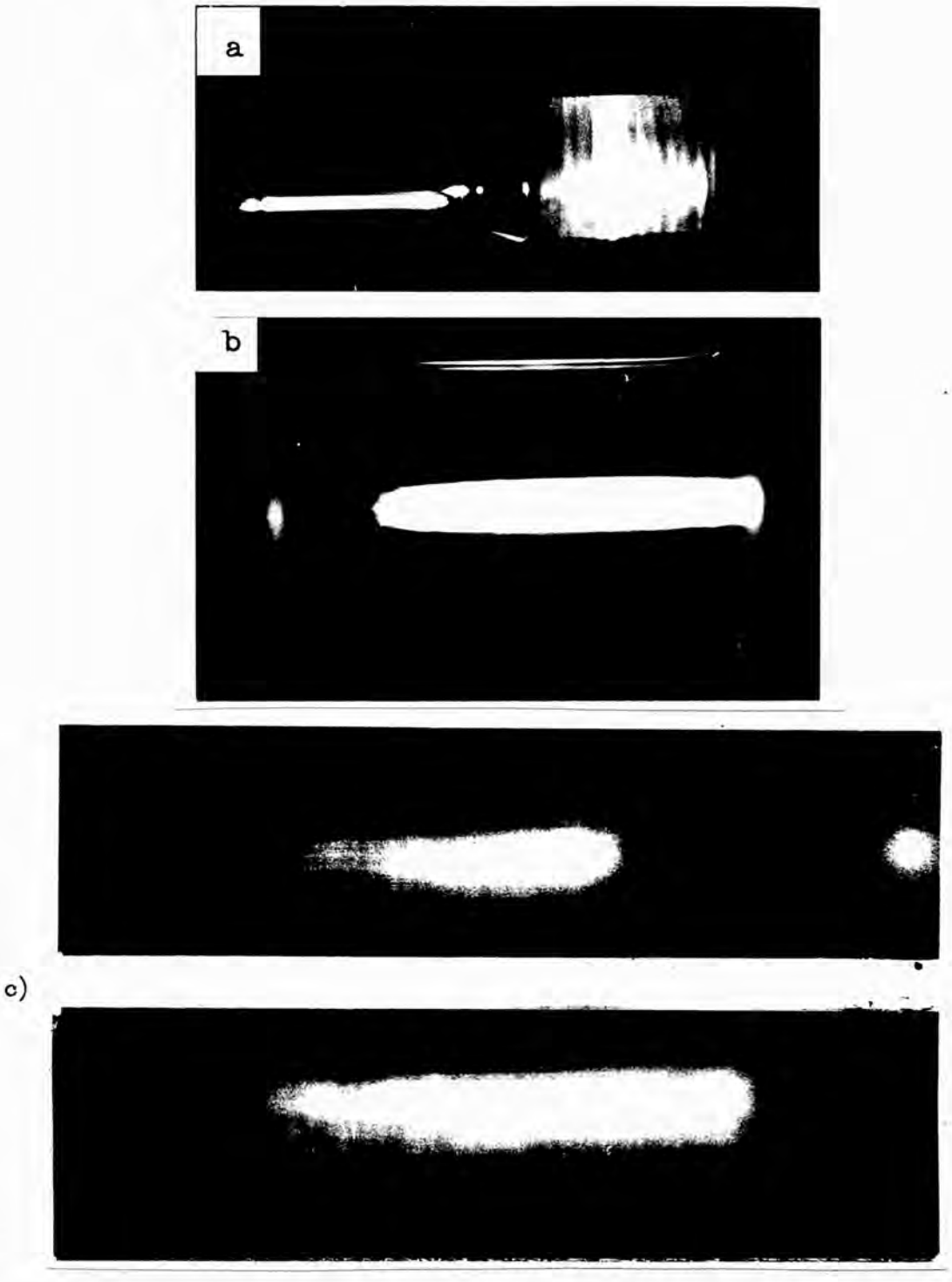

Fig. 6.5 Multi-photon effects observed with a mode-locked Nd:glass laser

a) TPF in rhodamine and third harmonic in silica

b) Blue fluorescence in 1-chloronaphthalene (CLNP)

c) Filamentary structure of fluorescence in CLNP ; dark space: yellow filter - Wratten No. 8

6.3 Liquid laser amplification of picosecond pulses

The inorganic liquid laser has several physical features which make it an attractive proposition as a high power amplifier, but certain disadvantages, such as the problem of thermal distortion, make it important to evaluate its performance experimentally. A practical difficulty encountered in attempting to do so is that the emission bands of neodymium glass and neodymium phosphoryl chloride are not coincident (Fig. 6.6), so that the gain of a hybrid system could fall short of the theoretical maximum. However, a neodymium selenyl chloride laser has been successfully used in this way[171], and the broad overlap of the emission bands indicates the potential of the liquid laser for amplifying short optical pulses to the limiting duration set by the inverse bandwidth. Since the use of picosecond pulses also avoids many of the non-linear interactions of high intensity light with liquids (Sec. I.6), the logical method of approach is to examine the performance of the amplifier in conjunction with a mode-locked neodymium glass oscillator as the signal source. Using this method, the gain and saturation of a liquid amplifier were measured and compared with a glass amplifier operating under similar conditions. Observations were made of the divergence and optical distortion of the amplified beam, the passive transmission of the liquid at intensities in the region of 10^9 $W.cm^{-2}$, the pulse width, energy and peak power of the amplified pulses, and the physical behaviour of the laser solutions. Note was taken of any reversible or irreversible changes (Sec. 6.4),

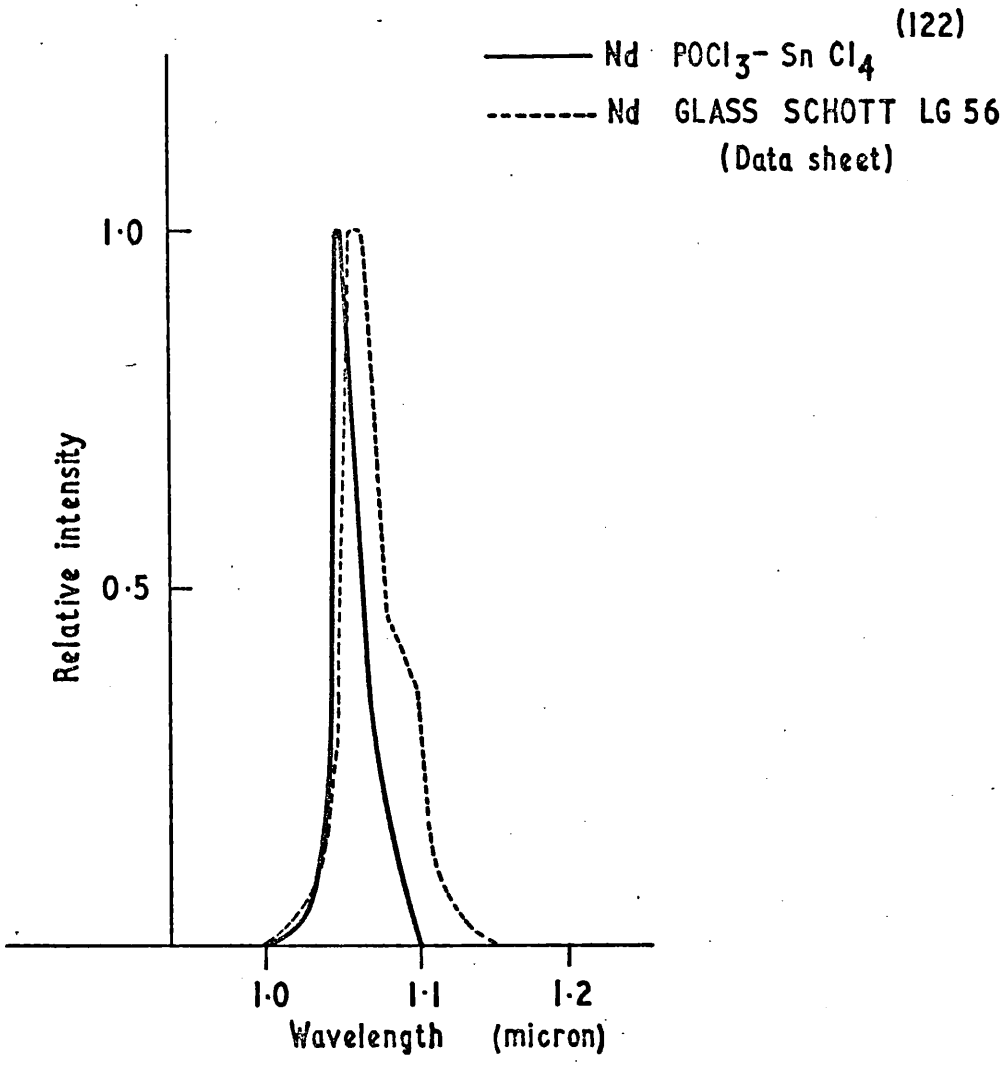

Fig. 6.6 Comparison of spectral emission profiles

Half intensity spectral width { glass 300 Å; liquid 200 Å

and of its storage properties in the chosen cell design (Fig.6.I). The experimental arrangement for measuring the gain of the amplifier and simultaneously recording the second order intensity correlation function (Sec. 2.3) of the amplified pulses is shown in Fig. 6.7 .

The procedure for setting up the experiment was as follows: first the optic axis was defined by directing the beam from a I mW helium-neon laser through a pair of pin-holes PI, P2 set at opposite ends of the optical system; all optical components were subsequently centred on this axis. Reflections of the gas laser beam were then used to align the system; the oscillator mirrors were set parallel to one another and normal to the optic axis by passing the reflected beam back through PI and observing the images on an optical target approximately 5 metres distant. The mode-locking dye cell was set at the Brewster angle by rotating it to the position at which the reflected image of the polarised beam vanished. This was made quite sensitive by viewing the reflection on a white card. The error in setting the silica cell at the Brewster angle for 0.6328 micron wavelength instead of I.06 micron (the neodymium wavelength) is 2.6 mrad.[I6I], well within the accuracy of the method. A 5 mm. diameter aperture AI was used to limit the oscillator beam divergence and diameter for transmission through the liquid amplifier. A similar aperture A2 defined the beam width at the TPF dye cell DC2. Sharp cut-off filters FI and F2, transmitting for $\lambda > 0.8\ \mu$. and $\lambda > I\ \mu$. respectively, served to isolate the laser beam and block stray visible light emitted

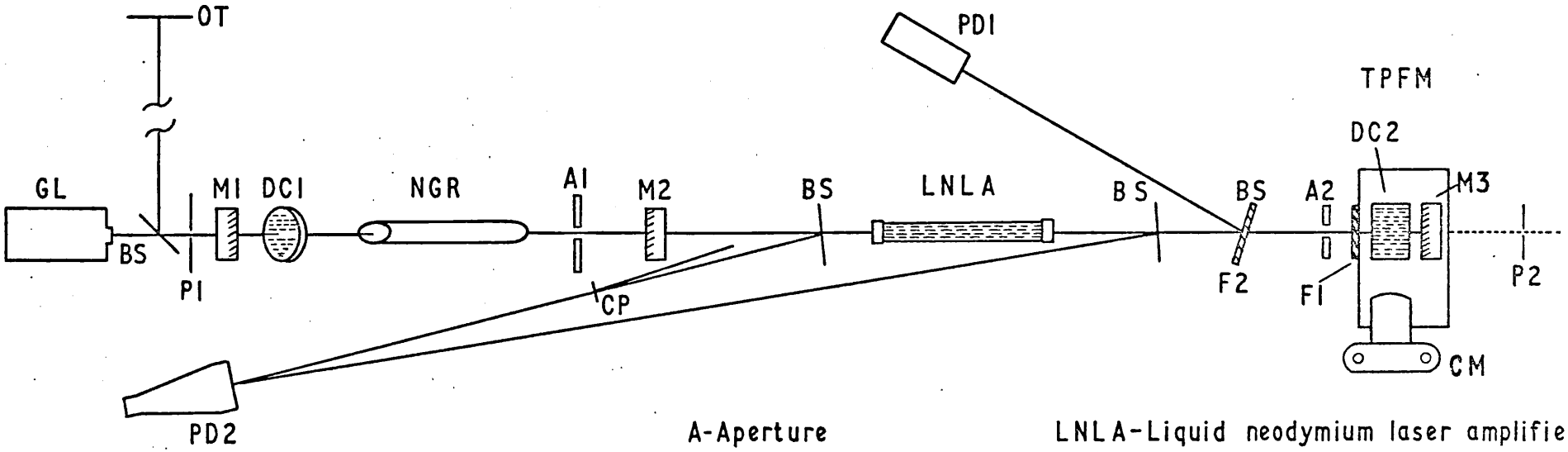

A-Aperture
BS-Beam splitter
CM-Camera
CP-Compensating plate
DC-Dye cell
F-Filter
GL-Gas laser
LNLA-Liquid neodymium laser amplifier
M-Mirror
NGR-Neodymium glass rod
OT-Optical target
P-Pinhole
PD-Photo-diode
TPFM-Two-photon fluorescence measurement

Fig. 6.7 Mode-locked oscillator/amplifier experiment
Measurement of gain and pulse width.

by the flashlamps. F2, a 2mm. thick disc of Schott glass RG I000, also acted as beam splitter for the monitoring photo-diode PDI. Two further beam splitters allowed the input and output of the amplifier to be sampled by photo-diode PD2. The compensating plate or plates CP could be adjusted to allow measurement of the intrinsic gain. All optical surfaces nominally perpendicular to the incident laser beam, such as the amplifier windows, the filter FI, the TPF dye cell DC2 and the mirror M3, were carefully misaligned by the angles necessary to prevent reflective feedback into the oscillator cavity and consequent disruption of mode-locking. That this was important was shown by deliberately reflecting back a fraction $I.5 .10^{-3}$ of the oscillator emission intensity. Emission of the familiar periodic pulse trains characteristic of mode-locking was immediately suppressed, and only resumed on removing the small reflectivity introduced.

With all components correctly adjusted the system was fired and the signals recorded. Since the amplifier pump pulse duration was shorter than that of the oscillator (Secs. 6.2.I and 6.2.2), the firing of the flashlamps on the amplifier was delayed such that peak excitation coincided with the passage of the mode-locked pulse train emitted by the oscillator. The necessary delay was typically 200 μs. The signal gain was found from the ratio of the pulse heights of the input and output signals monitored by an ITT F4000 fast photo-diode in the impedance matched mounting described earlier (Sec. 6.2.2), and displayed on a Tektronix 5I9 oscilloscope. The optical delay

resulting from the extra distance travelled by the amplified pulses, about I.3 m., made it possible to display corresponding pairs of pulses on the same sweep for direct comparison, and to use the one detector for both signals. Ambiguity was avoided by spacing the pulses asymmetrically, with an optical delay greater than half the pulse repetition period 2L/c. Examples of amplified pulse trains are shown in Fig. 6.8 .

Care was taken in obtaining these measurements with the setting of the two beam splitters and the illumination of the photo-diode. A white PTFE disc, 3 mm. thick, was mounted at the entrance window to diffuse the incident light over the photo-cathode area and compensate for variations in cathode sensitivity. The beam splitters were adjusted to produce coincidence of the two beams at the centre of the disc, with the normal to the surface bisecting the angle between them. Possible calibration errors due to changes in reflectivity of the beam splitters with polarisation were reduced by making the angles of incidence sufficiently small(Appendix III).

Since the instrument limited width of the recorded pulses, approximately 0.7 ns. (Fig. 5.4), was much greater than the actual width of the optical pulses, the observed pulse height ratios define the energy gain of the amplifier under the experimental conditions. The maximum gain observed was 3.2, achieved using unfiltered pump light at an input energy of I kilojoule, the same conditions under which a self-oscillation (threshold) gain of 5.4 was observed previously (Sec. 6.2.I). Assuming an identical inversion and exponential

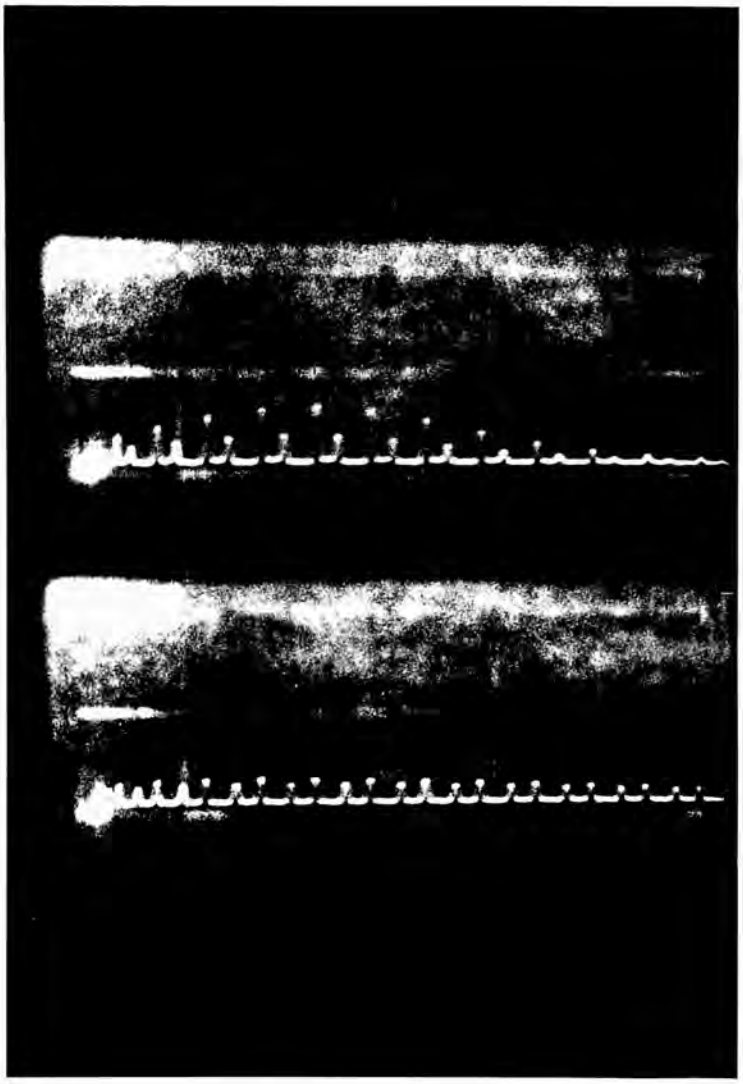

10 ns/cm

Fig. 6.8 Liquid laser amplification of mode-locked pulse trains

a) Amplified pulse train

b) Passive transmission

gain in both cases, the corresponding gain coefficients are 0.076 and 0.II cm^{-I} respectively, which implies an amplifying efficiency for the mode-locked oscillator pulses of 70%. This can be attributed to two factors: spectral mis-match (Fig. 6.6), and partial gain saturation. Comparison with a neodymium glass amplifier (Owens-Illinois ED-2) of similar dimensions showed the liquid to have a 30 to 40% greater intrinsic gain coefficient for the same excitation.

Gain saturation of the liquid amplifier, representing the transition from exponential small signal gain to linear large signal gain at sufficient intensity and pulse energy, caused the amplification of succeeding pulses in the train to decrease. Measurements of this were made for a range of initial values of the gain. Examples are shown in Fig. 6.9 . From a nearly constant value observed for the first few low energy input pulses i.e. the initial small signal gain, the gain is rapidly depleted by the more intense pulses occurring later in the train, and finally approaches a lower limit as the end of the pulse train is reached i.e. the final small signal gain provided by the remaining inversion. Calorimeter measurements showed the onset of saturation to occur for pulse energy density in the region of 25 $mJ.cm^{-2}$.

For the TPF intensity correlation measurements a parallel-sided output mirror M2 was used on the oscillator to produce repetitive pulsing (Sec. 5.I) and facilitate cross-correlation of the pulses emitted. This approach overcame the difficulty of achieving meaningful records with auto-correlation in the case where the pulse was made to overlap with itself

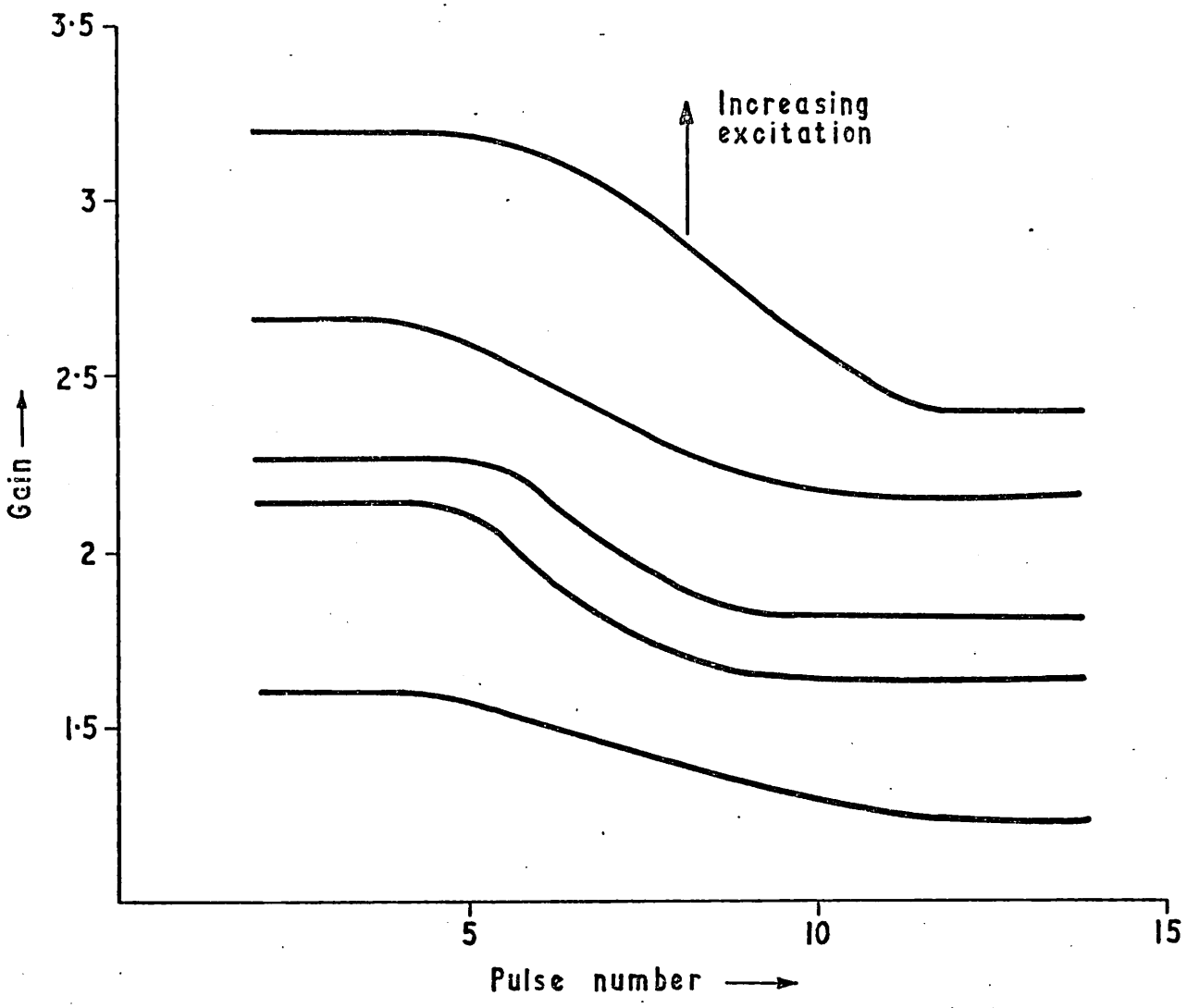

Fig. 6.9 Gain saturation of Nd:$POCl_3$-$SnCl_4$ liquid laser amplifier.

The curves show the progressive decrease of gain with pulse number in a mode-locked pulse train

at the surface of an immersed mirror (Fig. 6.4), and avoided the long optical paths and isolation problem associated with the pulse collision method involving a triangular configuration[79]. TPF intensity profiles were obtained, and the amplifier gain recorded simultaneously, using the arrangement shown earlier (Fig. 6.7). The pulses were crossed in a 20 mm. cell of rhodamine 6G in acetone, and the resulting fluorescence intensity profile was photographed on Ilford HP4 film, using a 75 mm. Zeiss Biotar lens at f/2.8 . The film was subsequently developed in Microphen or Promicrol. A neutral density strip filter, calibrated in the wavelength range of the fluorescence, was arranged to cover the bright central band caused by the pulse overlap in the dye solution and provide a comparison of its intensity with that of the background trail photographed on either side[63]. Fig. 6.10 shows the calibrated TPF intensity profile obtained by microdensitometry of the photographic negative. The profile is symmetric, a property of the second order correlation function, and therefore only the pulse duration and not the pulse shape can be inferred from it[81]. The contrast ratio in this example is 1.9 and the pulse width 5 psec. This result is typical; records obtained with the oscillator emission alone, and when amplified by the liquid laser, yielded contrast ratios in the range 1.6 to 2.0 and pulse widths of 3 to 6 psec. No apparent pulse shortening was observed for amplifier gains between 1.2 and 2. The narrow peak approaching the theoretical contrast ratio of 3 [73], reported with sub-picosecond components in the laser emission[62,63], was not observed. The reported width of 50 to 75 microns

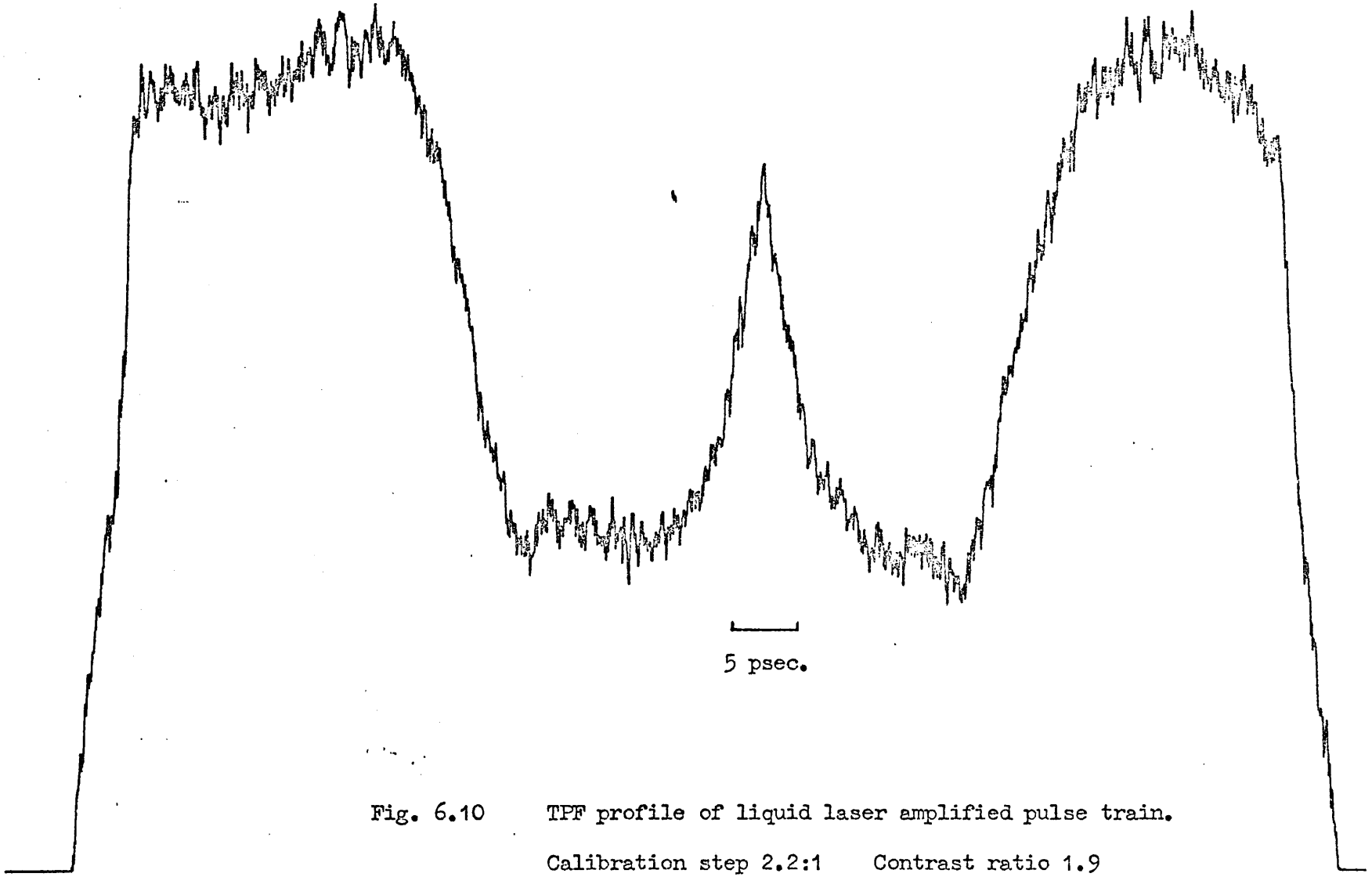

Fig. 6.10 TPF profile of liquid laser amplified pulse train.

Calibration step 2.2:1 Contrast ratio 1.9

above a contrast level of 2 [62,63] is comparable with the grain noise of approximately 50 microns found in the writer's experimental records, and it is likely that the spike was not resolved. What can be deduced without ambiguity from the TPF records is that the input to the liquid amplifier consisted of bursts of light of 3 to 6 picoseconds duration, and that these were then amplified by the observed amount and emerged with a similar duration.

Measurements were also made of the total laser emission energy as a basis for inferring the energy and intensity of individual picosecond pulses and relating these to the levels required for non-linear effects. The emergent laser beam was intercepted by a simple cone calorimeter (Laser Associates) and the absorbed energy recorded. At the same time the emission was monitored by the two photo-diodes PDI and PD2 (Fig. 6.7), an EMI 9713B and an ITT F4000 respectively, to ensure that no subsidiary pulses were emitted, and the measured energy referred to one mode-locked pulse train only. A series of such records were obtained both with and without amplification to check for consistency. With some confidence that measurements meeting these requirements represented the total energy of a train of picosecond pulses, it was then necessary to determine their number. A lower limit was obtained from the oscilloscope record (Fig. 6.4), and usually amounted to I5 to 20 pulses. Each of these represented the electrical response of the detection system to one or more picosecond bursts. The TPF records showed only one such short burst per cavity round trip 2L/c with the wedged output mirror, and more than two with the

parallel sided mirror (Fig. 6.4). An upper limit was set by the requirement that each recorded pulse be instrument limited i.e. 0.7 ns. FWHM. Thus for the parallel mirror the number n of picosecond pulses per recorded pulse was found to be $2 \leq n < 10$, and for the wedged mirror n=1. The mode-locked oscillator emitted pulse trains of energy 60 to 80 millijoules in a beam of 0.2 cm^2 cross-section, with an average energy of 4 mJ per electronically detected pulse and a maximum of 8 mJ. For optical pulses of 5 psec. duration these figures give a peak intensity 8 $GW.cm^{-2}$ for the wedged mirror and ~ 1 $GW.cm^{-2}$ for the parallel mirror. Thus the observed performance of the liquid amplifier as described here refers to its response on the picosecond time scale to pulse intensities in the region of 10^9 $W.cm^{-2}$.

At these intensities it was necessary to discover whether non-linear optical effects had any significant effect on the propagation of picosecond pulses in the liquid amplifier. To this end observations were made of the divergence and detailed intensity structure of the transmitted beam for both active and passive transmission i.e. with and without optical pumping of the amplifier. The intensity distribution of the mode-locked oscillator beam was recorded simultaneously for direct comparison. Fine detail in the more intense areas was recorded by ablation of developed (black) Polaroid roll film, and the overall distribution obtained by infra-red photography with Polaroid type 413 film. It was found that no apparent distortion occurred for passive transmission in the laser liquid;

the symmetry of the beam pattern was preserved, and only minor changes due to divergence were observed (Fig. 6.IIA). Also the oscilloscope records showed constant pulse transmittance throughout the mode-locked pulse train, thus supporting the earlier observations on gain saturation in the pumped amplifier (Fig. 6.9). Distortion and increased beam divergence were however observed for active transmission (Fig. 6.IIB). Some rippling of the amplified beam intensity occurred where there was none in the oscillator beam, and with uranyl glass filters on the amplifier flashlamps a diffuse periphery and small vertical flare were seen outside the bright central region. In this case the measured beam divergence was I.5 milliradian for an amplifier gain of I.8, compared with a divergence of I milliradian for the incident oscillator beam. Without filters large vertical distortion occurred with a divergence of I5 milliradian in the vertical plane, and the intensity distribution took the form of a large striped flare.

In view of the negative results for passive transmission it was concluded that optical distortion occurring in the pumped amplifier resulted from thermal distortion of the liquid medium, as found for the liquid laser oscillator (Sec. 6.2.I), and not from non-linear optical effects. On delaying the emission of the oscillator signal past the peak of the amplifier pumping pulse the beam divergence was found to increase linearly with increasing delay. Since the duration of the oscillator pulse train was short enough ($\sim$ I00 ns.) to provide an effectively instantaneous sampling of the active transmission of the liquid, this result was consistent with the conclusion

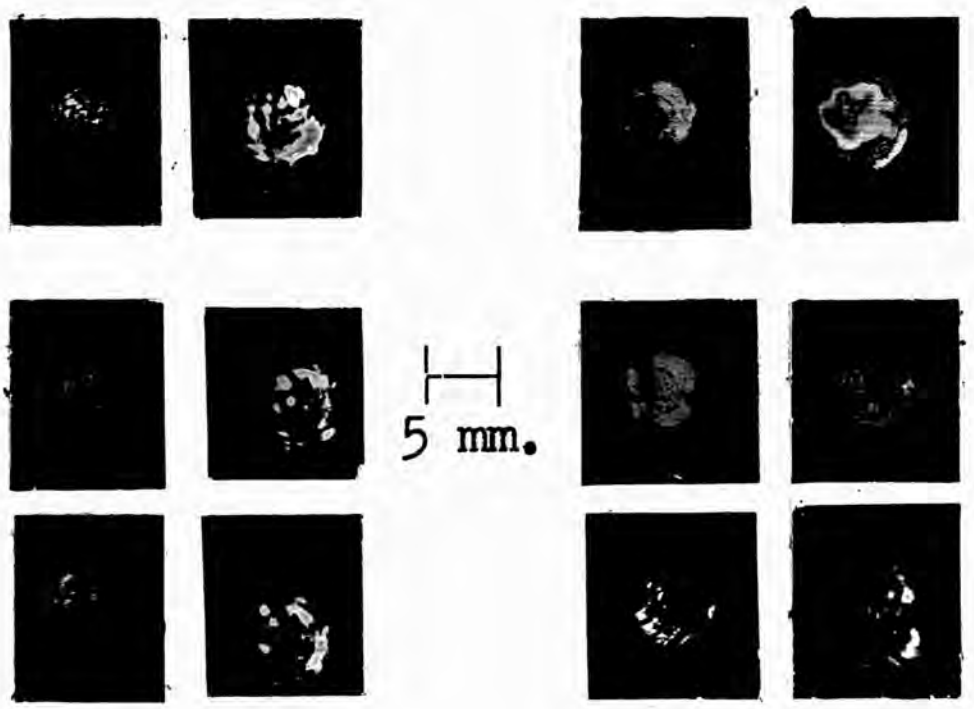

Fig. 6.11A Passive transmission of liquid amplifier

150 mm. cell Nd:$POCl_3$-$SnCl_4$

Columns 1 and 3 - oscillator beam structure

.. 2 .. 4 - transmitted beam structure

Target distant 2 m.

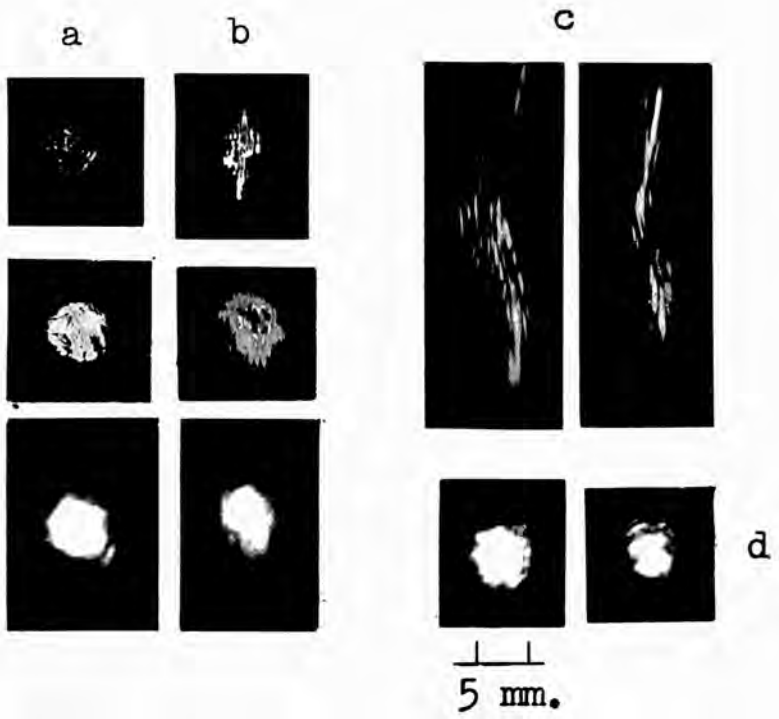

Fig. 6.11B Amplified beam structure - 150 mm. cell Nd:$POCl_3$-$SnCl_4$

a) oscillator beam structure

b) amplified beam - uranyl glass filter - gain 1.5 to 1.8

c) amplified beam - no filter - gain 3.

d) oscillator beam structure

Target distant 2 m.

that the divergence depended on the integrated thermal distortion of the amplifier.

6.4 Physical changes in liquid laser solutions

In view of the practical importance of liquid lasers, it seems worth recording here the various physical changes noted in the experimental samples, together with their cause where determined, and the steps taken to remedy them. The main factors found to influence the physical state of the solution are temperature, optical pumping, and chemical contamination.

Lowering the temperature of a stable phosphoryl or selenyl chloride solution promotes rapid crystallisation through the formation of chemical complexes with the added metal chlorides[I72]. The optical path in the liquid becomes blocked and laser action ceases. Since the temperature below which crystallisation occurs depends on the nature and proportions of the metal chlorides[I72], the problem is overcome by choosing an appropriate liquid mixture possessing sufficient solubility to achieve the desired neodymium concentration and which does not crystallise at the chosen laser operating temperature.

Optical pumping at high intensity levels without the use of ultra-violet filters produced bubbles and colour changes in some solutions. The small bubbles may have been released through the shock heating of solutions containing dissolved gases, whereas the colour changes were interpreted as the result

of flash photolysis on hydroxyl contaminated solutions[I73]. Since the Nd^{3+} ion laser is based on optical transitions, the solutions have a characteristic colour, which may be pale blue or deep lilac depending on the optical depth viewed by eye, and any changes in this colour provide a sensitive indication of chemical change. The colours observed were a wine red or pale brown in some cases. These changes were avoided by preparing purer solutions[II3] and by mounting ultra-violet filters on the flash tubes (Fig. 6.2).

Chemical contamination took the form of hydroxyl groups entering the hygroscopic solution, and caused a flocculent precipitate in one of the brown solutions. This was overcome by preparing solutions under strictly dry conditions.

Thus, the physical changes described above can all be avoided by careful preparation and storage of solutions, and such solutions may then be used over periods of several months with little change in performance.

CHAPTER 7 Concluding remarks

It was our thesis, adopted from the extensive work of others on optical effects in liquids, that liquid media placed in the beam can influence both laser emission and laser beam propagation, and that this may take the form of either active or passive behaviour, resulting in temporal and spatial changes of intensity. This contention is largely supported by the experimental results, and it is relevant to the study of high power laser systems, where such effects can lead to increased losses through stimulated scattering processes, and to beam instability through field dependent change of refractive index. Passive behaviour is usually ascribed to thermal effects, and leads to distortion of the propagating beam in a liquid laser amplifier. However, active thermal effects can also be important, as exemplified by liquid Q-switching, where we have shown that several common organic solvents Q-switch the neodymium laser by virtue of a weak absorption in the region of the laser emission wavelength (I.06 μ), which gives rise to the formation of a reflecting thermal phase grating.

Self-modulation of a laser oscillator has been studied in connection with understanding mode-locking and short, high power pulse generation, and periodic pulse trains observed with a passive arrangement of dielectric plates in the cavity. This represents I00% self-modulation of the emission intensity at frequencies in the range I00 to I50 MHz achieved with an entirely static system, and underlines the peculiarly active

behaviour of a physical device employing stimulated emission.

Useful gains have been obtained with an inorganic liquid laser, Nd:$POCl_3$-$SnCl_4$, used to amplify picosecond laser pulses in the 10^9 W.cm^{-2} intensity range. A study of laser beam propagation in the amplifier has shown that no overt non-linear optical effects occur under these conditions, and that the observed changes in intensity structure and divergence are caused by pump induced thermal distortion of the liquid medium, which may be reduced by spectral filtering of the pump light. The absence of non-linear effects is not unexpected because only the electronic polarisability of the medium and the Rayleigh wing scattering process can respond on the picosecond time scale, and neither self-focusing nor intensity dependent transmission were observed. The onset of gain saturation in the liquid amplifier was found for picosecond pulses with energy density in the region of 25 mJ cm^{-2}.

As to future work, the present technique can clearly be extended to the investigation of non-linear optical effects at higher intensities and on different time scales in a more powerful liquid amplifier, with a view to determining the maximum operating conditions of this device, including the approach to a limit pulse, and the nature of the physical limitations imposed. Application of this development could be made to the study of non-linear optics in other media on the 10^{-12} to 10^{-13} sec. time scale, and to continuing studies of thermonuclear fusion with pulses of longer duration, preferably in the region of 10^{-10} sec.(80)

APPENDIX I Notation

I. Roman symbols

a - rate constant, amplitude, dispersion constant

b - dispersion constant

c - velocity of light, specific heat

c'- velocity of light in dielectric medium

d - thickness, diameter

D - thermal diffusivity, diameter

E - electric field amplitude

f - function, fraction

g - factor

G - correlation function

h - mean absorbed power

I - intensity

j - integer

k - wave number = $2\pi/\lambda$

K - thermal conductivity

l - length

L - cavity length

m - integer

M - modulation

n - refractive index, integer

N - integer

p - integer

q - factor

Q - cavity 'Q' - quality

r,R - reflectivity

t - time

T - cavity period, temperature, transmittance

u - source function, group velocity

v - velocity

V - function

x - space coordinate

z - reflectivity function, space coordinate

2. Greek symbols

α - polarisability, absorption coefficient, spectral bandwidth

β - factor, group velocity dispersion

Γ - linewidth

δ - small quantity

Δ - finite difference, phase

ε - dielectric constant

θ - angle

λ - wavelength

μ - refractive index ratio

ν - frequency

ρ - density

τ - relaxation time, pulse width

ϕ - reflectance, angle of incidence

ϕ' - angle of refraction

χ - susceptibility

ψ - function

ω - angular frequency

3. Subscripts

B - Brillouin

cr. - critical

ijkl - tensor components

L - laser

max. - maximum

min. - minimum

o - scalar, initial value

obs. - observed value

p - pulse, p-th, p-polarisation

P - constant pressure

R - Rayleigh

s - saturable absorber, s-polarisation

$\parallel$ - parallel

4. Abbreviations

CLNP - chloronaphthalene

FWHM - full width at half maximum

PTFE - polytetrafluorethylene

SBS - stimulated Brillouin scattering

SCRS - .. central Rayleigh scattering

SRWS - .. Rayleigh wing ..

STBS - Stimulated thermal Brillouin scattering

STRS - .. .. Rayleigh ..

TPF - two photon fluorescence

APPENDIX II Pulse propagation and mode spectrum in a dispersive medium

A propagating pulse $\psi(z,t)$ can be expressed as an integral over an infinite number of plane waves:

$$\psi(z,t) = \int_{-\infty}^{\infty} a(k)\, e^{i(kz - \omega t)}\, dk \qquad (A.2.I)$$

Assuming a Gaussian amplitude function:

$$a(k) = a_o\, e^{-\alpha(k - k_o)^2} \qquad (A.2.2)$$

and expanding the angular frequency ω as a function of wave number k in a Taylor series about k_o :

$$\omega(k) = \omega_o + u(k - k_o) + \beta(k - k_o)^2 + \ldots\ldots \qquad (A.2.3)$$

where the group velocity $u = \left.\frac{d\omega}{dk}\right|_{k_o}$

and the group velocity dispersion $2\beta = \left.\frac{du}{dk}\right|_{k_o}$

and retaining terms to the second order in the expansion of $\omega(k)$, we find the solution of (A.2.I) for the intensity $\psi\psi^*$

to be[97]:

$$I(z,t) = \frac{\pi a_o^2}{(\alpha^2 + \beta^2 t^2)^{\frac{1}{2}}} \; e^{-\frac{\alpha(z - ut)^2}{2(\alpha^2 + \beta^2 t^2)}} \qquad (A.2.4)$$

which is a pulse travelling with the group velocity u and broadening at a rate determined by the group velocity dispersion 2β. The pulse width τ_p at time t is given by:

$$\tau_p^2 = \frac{2}{\alpha}(\alpha^2 + \beta^2 t^2) \qquad (A.2.5)$$

The resonant frequencies of a cavity containing a dispersive medium are:

$$\nu_p = \frac{cp}{2n(\nu_p)L} \qquad (A.2.6)$$

where L is the geometrical length of the cavity, p is a large integer (cavity dimension large compared with the wavelength) and the refractive index n is a function of frequency ν.
For a non-dispersive medium the frequency difference of adjacent longitudinal modes (2.I.I)

$$\Delta\nu^o = \frac{c}{2nL} \qquad (A.2.7)$$

The frequency difference of the p-th and (p + j)-th modes in a dispersive cavity can be expressed as a power series in the integer j by expanding $n(\nu_{p+j})$ as a Taylor series about $n(\nu_p)$ and substituting in (A.2.6).

Thus:

$$\frac{\Delta\nu_j}{\Delta\nu^o} = (1-a)j + bj^2 + \ldots. \qquad (A.2.8)$$

where $$a = \nu_p \frac{n'(\nu_p)}{n(\nu_p)} \qquad (A.2.9)$$

and $$b = \Delta\nu^o f(n_p, n'_p, n''_p) \qquad (A.2.10)$$

Thus linear dispersion merely changes the mode frequency difference by a constant amount $a\Delta\nu^o$ compared with the non-dispersive case, and the pulse width of a mode-locked laser is not affected by this term. It is the quadratic term in the expansion which is responsible for the linear frequency sweep in the mode spectrum and for the broadening of a propagating pulse.

APPENDIX III Variation of reflectivity with polarisation

In considering the calibration of beam splitters for energy gain measurements obtained from the ratio of two reflected signals (Sec. 6.3), it is important to know how the calibration varies with the state of polarisation of the incident light.

The amplitude reflectivity of a dielectric surface for light polarised with the E-vector perpendicular to the plane of incidence is[174]:

$$r_s = -\frac{\sin(\phi - \phi')}{\sin(\phi + \phi')} \qquad (A.3.1)$$

and for light polarised with the E-vector in the plane of incidence,

$$r_p = \frac{\tan(\phi - \phi')}{\tan(\phi + \phi')} \qquad (A.3.2)$$

where ϕ is the angle of incidence and ϕ' the angle of refraction. If a fraction f of the incident light intensity is composed of s vibrations and the rest of p vibrations, the effective reflectivity of the surface is:

$$R(f,\phi) = fr_s^2 + (I - f)\, r_p^2 \qquad (A.3.3)$$

For two surfaces, and differing angles of incidence, the ratio of their reflectivities is a function of f, the degree of polarisation of the incident light. The calibration of a pair of beam splitters fixes this ratio for the particular value of f corresponding to the polarisation state of the calibrating beam. It is desirable to minimise the possible range of variation with changing polarisation, so that the calibration remains valid at least within experimental error.

Since $r_p^2 < r_s^2$ for $0 < \phi < \pi/2$, the points f=0 and f=I are extrema of the function $R(f,\phi)$, and therefore the maximum variation of reflectivity ratio for two surfaces is represented by the function:

$$V(\phi_1,\phi_2) = \frac{R(I,\phi_1)\, R(0,\phi_2)}{R(I,\phi_2)\, R(0,\phi_1)} \qquad (A.3.4)$$

assuming no significant change of polarisation to occur in

passing from the first surface to the second.

For the experimental conditions (Fig. 6.7), the angles involved in the Fresnel equations (A.3.I) and (A.3.2) took the values:

$$\phi_1 = 8.5^\circ \qquad \phi_1' = 5.6^\circ$$
$$\phi_2 = 11.5^\circ \qquad \phi_2' = 7.6^\circ$$

assuming the refractive index for the glass plates n = I.5 . Evaluating (A.3.4) for these angles yields:

$$V(\,8.5^\circ,\ 11.5^\circ\,) = 0.95$$

Thus the maximum possible calibration error is of the order of 5%. Although real beam splitters consist of dielectric plates, each having two surfaces, the V-function can provide a reasonable estimate of the likely error in a practical case. In fact it is probably less than this because the experiments involved the use of a nominally plane polarised beam.

REFERENCES

I. M.Denariez, G.Bret Phys. Rev. I7I, I60 (I968)

2. Lord Rayleigh 'Scientific papers' 4, 397 C.U.P New York I903

3. L.D.Landau, E.M.Lifshitz 'Electrodynamics of continuous media' 387-393 Pergamon Press I960

4. V.S.Starunov Opt. Spectrosc. I8, I65 (I965)

5. R.D.Mountain Rev. Mod. Phys. 38, 205 (I966)

6. R.G.Harrison, P.Key, V.I.Little, J.Katzenstein IEEE J. Quant. Electron. QE-6 (in press)

7. S.L.Shapiro, H.P.Broida Phys. Rev. I54, I29 (I967)

8. A.J.DeMaria, R.Gagosz, H.A.Heynau, A.W.Penney, G.Wisner J.Appl. Phys. 38, 2693 (I967)

9. T.A.Wiggins, R.V.Wick, N.D.Foltz, C.W.Cho, D.H.Rank J. Opt. Soc. Am. 57, 66I (I967)

I0. D.I.Mash, V.S.Starunov, E.V.Tiganov, I.I.Fabelinskii ZhETF 49, I764 (I965) (Sov. Phys. JETP 22, I205 (I966))

II. C.V.Raman Ind. J. Phys. 2, 3; ibid. 87 (I928)

I2. J.C.Evans 'Infra-red spectroscopy and molecular structure' I99-225 ed. Mansel Davies Elsevier I963

I3. C.W.Cho, N.D.Foltz, D.H.Rank, T.A.Wiggins Phys. Rev. Letters I8, I07 (I967)

I4. N.D.Foltz, C.W.Cho, D.H.Rank, T.A.Wiggins Phys. Rev. I65, 396 (I968)

I5. D.I.Mash, V.V.Morozov, V.S.Starunov, I.I.Fabelinskii ZhETF Pis'ma 2, 4I (I965) (JETP Letters 2, 25 (I965))

I6. V.I.Bespalov, A.M.Kubarev ZhETF Pis'ma 6, 500 (I967) (JETP Letters 6, 3I (I967))

I7. A.J.Alcock, C.DeMichelis Appl. Phys. Letters II, 42; II, I85 (I967)

I8. M.Maier, W.Rother, W.Kaiser Appl. Phys. Letters IO, 80 (I967)

I9. D.Pohl Phys. Letters 24A, 239 (I967)

20. E.J.Woodbury, W.K.Ng Proc. IRE 50, 2367 (I962)

2I. G.Eckhardt, R.W.Hellwarth, F.J.McClung, S.E.Schwarz, D.Weiner, E.J.Woodbury Phys. Rev. Letters 9, 455 (I962)

22. M.Maier, W.Kaiser, J.A.Giordmaine Phys. Rev. Letters I7, I275 (I966)

23. A.Z.Grasiuk, V.F.Mulikov, L.Csillag Nuovo Cimento 64B, 300 (I969)

24. J.Kerr Phil. Mag. (4) 50: 337, 446 (I875); J.W.Beams Rev. Mod. Phys. 4, I33 (I932); L.D.Landau, E.M.Lifshitz 'Electrodynamics of continuous media' 329 Pergamon Press I960

25. V.I.Talanov ZhETF Pis'ma 2, 2I8 (I965) (JETP Letters 2, I38 (I965))

26. P.L.Kelley Phys. Rev. Letters I5, I005 (I965)

27. R.Y.Chiao, E.Garmire, C.H.Townes Phys. Rev. Letters I3, 479 (I964)

28. C.C.Wang Phys. Rev. Letters I6, 344 (I966)

29. R.G.Brewer, J.R.Lifsitz Phys. Letters 23, 79 (I966)

30. V.V.Korobkin, R.V.Serov ZhETF Pis'ma 6, 642 (I967) (JETP Letters 6, I35 (I967))

3I. A.V.Butenin, V.V.Korobkin, A.A.Malyutin, M.Ya.Shchelev ZhETF Pis'ma 6, 687 (I967) (JETP Letters 6, I73 (I967))

32. R.W.Hellwarth Phys. Rev. I52, I56 (I966)

33. F.DeMartini, C.H.Townes, T.K.Gustafson, P.L.Kelley Phys. Rev. I64, 3I2 (I967)

34. Y.R.Shen, Y.J.Shaham Phys. Rev. I63, 224 (I967)

35. J.A.Fleck, P.L.Kelley Appl. Phys. Letters I5, 3I3 (I969)

36. H.C.Craddock, D.A.Jackson J. Phys. D (Appl. Phys.) I, I575 (I968)

37. R.M.Herman, M.A.Gray Phys. Rev. Letters I9, 824 (I967)

38. D.H.Rank, C.W.Cho, N.D.Foltz, T.A.Wiggins Phys. Rev. Letters I9, 828 (I967); C.W.Cho, N.D.Foltz, D.H.Rank, T.A.Wiggins Phys. Rev. I75, 27I (I968)

39. M.E.Mack Phys. Rev. Letters 22, I3 (I969)

40. F.Gires, B.Soep Proc. IEEE 56, I6I3 (I968)

4I. E.A.Tikhonov, M.T.Shpak ZhETF Pis'ma 8, 282 (I968) (JETP Letters 8, I73 (I968))

42. N.Bloembergen Am. J. Appl. Phys. 35, 989 (I967)

43. W.E.Lamb Phys. Rev. I34, AI429 (I964)

44. J.P.Wittke, P.J.Warter J. Appl. Phys. 35, I668 (I964)

45. A.Icsevgi, W.E.Lamb Phys. Rev. I85, 5I7 (I969)

46. Y.R.Shen Phys. Letters 20, 378 (I966)

47. D.Pohl, I.Reinhold, W.Kaiser Phys. Rev. Letters 20, II4I (I968)

48. F.Shimizu, B.P.Stoicheff IEEE J. Quant. Electron. QE-5, 544 (I969)

49. R.G.Brewer, CH.Lee Phys. Rev. Letters 2I, 267 (I968)

50. M.DiDomenico Jr. J. Appl. Phys. 35, 2870 (I964)

5I. L.E.Hargrove, R.L.Fork, M.A.Pollack Appl. Phys. Letters 5, 4 (I964)

52. M.H.Crowell IEEE J.Quant. Electron. QE-I, I2 (I965)

53. A.Yariv J. Appl. Phys. 36, 388 (I965)

54. T.Deutsch Appl. Phys. Letters 7, 80 (I965)

55. H.W.Mocker, R.J.Collins Appl. Phys. Letters 7, 270 (I965)

56. P.Kafalas, J.I.Masters, E.M.E.Murray J. Appl. Phys. 35, 2349 (I964)

57. M.DiDomenico, J.E.Geusic, H.M.Marcos, R.G.Smith Appl. Phys. Letters 8, I80 (I966)

58. A.J.DeMaria, C.M.Ferrar, G.E.Danielson Jr. Appl. Phys. Letters 8, 22 (I966)

59. A.J.DeMaria, D.A.Stetser, H.Heynau Appl. Phys. Letters 8, I74 (I966)

60. D.A.Stetser, A.J.DeMaria Appl. Phys. Letters 9, II8 (I966)

6I. H.Samelson, A.Lempicki J.Appl.Phys. 39, 6II5 (I968)

62. S.L.Shapiro, M.A.Duguay Phys. Letters 28A, 698 (I969)

63. D.J.Bradley, G.H.C.New, S.J.Caughey Phys. Letters 30A, 78 (I969)

64. E.Snitzer 'Quantum Electronics III' 999 ed. P.Grivet, N.Bloembergen Columbia Univ. Press (I964)

65. R.A.Fisher, P.L.Kelley Appl. Phys. Letters I4, I40 (I969)

66. T.H.Maiman Phys. Rev. I23, II45 (I96I)

67. J.A.Armstrong Appl. Phys. Letters I0, I6 (I967)

68. J.A.Giordmaine, P.M.Rentzepis, S.L.Shapiro, K.W.Wecht Appl. Phys. Letters II, 2I6 (I967)

69. P.M.Rentzepis, M.A.Duguay Appl. Phys. Letters II, 2I8 (I967)

70. W.H.Glenn Bull. Am. Phys. Soc. I3, I63 (I968)

7I. A.J.DeMaria, W.H.Glenn, M.J.Brienza, M.E.Mack Proc. IEEE 57, 2 (I969)

72. M.E.Mack IEEE J. Quant. Electron, QE-4, 1015 (1968)

73. H.P.Weber Phys. Letters 27A, 321 (1968)

74. J.R.Klauder, M.A.Duguay, J.A.Giordmaine, S.L.Shapiro Appl. Phys. Letters 13, 174 (1968)

75. R.Hanbury Brown, R.Q.Twiss Proc. Roy. Soc. A242, 300; A243, 291 (1958)

76. R.J.Harrach Phys. Letters 28A, 393 (1968)

77. J.R.Klauder Appl. Phys. Letters 14, 147 (1969)

78. E.B.Treacy Phys. Letters 28A, 34 (1968)

79. G.Kachen, L.Steinmetz, J.Kysilka Appl. Phys. Letters 13, 229 (1968)

80. G.Kachen, J.Kysilka IEEE J. Quant. Electron. QE-6, 84 (1970)

81. H.P.Weber, R.Dändliker Phys. Letters 28A, 77 (1968)

82. A.A.Malyutin, M.Ya.Shchelev ZhETF Pis'ma 9, 445 (1969) (JETP Letters 9, 266 (1969))

83. W.H.Glenn, M.J.Brienza Appl. Phys. Letters 10, 221 (1967)

84. M.A.Duguay, J.W.Hansen Appl. Phys. Letters 13, 178 (1968)

85. E.B.Treacy Appl. Phys. Letters 14, 112 (1969)

86. A.J.DeMaria, W.H.Glenn, D.A.Stetser Appl. Opt. 7, 1405 (1968)

87. E.I.Blount, J.R.Klauder J. Appl. Phys. 40, 2874 (1969)

88. N.G.Basov, P.G.Kriukov, V.S.Letokhov, Yu.V.Senatskii IEEE J. Quant. Electron. QE-4, 606 (1968)

89. V.S.Letokhov ZhETF 55, 1077 (1968) (JETP 28, 562 (1969))

90. J.A.Fleck Appl. Phys. Letters 12, 178 (1968)

91. S.E.Schwarz IEEE J. Quant. Electron. QE-4, 509 (1968)

92. V.S.Letokhov ZhETF 54, 1392 (1968) (JETP 27, 746 (1968))

93. R.Harrach, G.Kachen J. Appl. Phys. 39, 2482 (1968)

94. A.Schmackpfeffer, H.Weber Phys. Letters 24A, 190 (1967)

95. M.M.Malley, P.M.Rentzepis Chem. Phys. Letters 3, 534 (I969)

96. M.Hercher, W.Chu, D.L.Stockman IEEE J. Quant. Electron. QE-4, 954 (I968)

97. V.V.Batygin, I.N.Toptygin 'Problems in Electrodynamics' 327 Academic Press I964

98. A.W.Smith Appl. Phys. Letters I5, I94 (I969)

99. R.Cubeddu, O.Svelto Phys. Letters 29A, 78 (I969)

I00. V.S.Letokhov ZhETF 55, I943 (I968) (JETP 28, I026 (I969))

I0I. J.A.Fleck Appl. Phys. Letters I3, 365 (I968)

I02. M.A.Duguay, S.L.Shapiro, P.M.Rentzepis Phys. Rev. Letters I9, I0I4 (I967); S.L.Shapiro, M.A.Duguay, L.B.Kreuzer Appl. Phys. Letters I2, 36 (I968); D.J.Bradley, G.H.C.New, B.Sutherland, S.J.Caughey Phys. Letters 28A, 532 (I969)

I03. S.Singh, M.DiDomenico, R.G.Smith Proc. IEEE 53, 507 (I965)

I04. H.Statz, C.L.Tang J. Appl. Phys. 36, 3923 (I965)

I05. H.Statz, G.A.DeMars, C.L.Tang J. Appl. Phys. 38, 22I2 (I967); C.L.Tang, H.Statz ibid. 38, 2963 (I967); H.Statz, M.Bass ibid. 40, 377 (I969)

I06. K.Kaufmann, W.Weidlich Z. Phys. 2I7, II3 (I968)

I07. A.Heller Appl. Phys. Letters 9, I06 (I966); A.Lempicki, A.Heller Appl. Phys. Letters 9, I08 (I966)

I08. N.Blumenthal, C.B.Ellis, D.Grafstein J. Chem. Phys. 48, 5726 (I968); E.J.Schimitschek J. Appl. Phys. 39, 6I20 (I968)

I09. W.Watson, S.Reich, A.Lempicki, J.Lech,IEEE J. Quant. Electron. QE-4, 842 (I968)

II0. H.Samelson, A.Lempicki, V.A.Brophy IEEE J. Quant. Electron. QE-4, 849 (I968)

III. A.A.Grütter, H.P.Weber, R.Dändliker Phys. Rev. I85, 629 (I969)

II2. A.Heller Physics Today 20, 34 (I967)

II3. Personal communication from Mr. F. Hudswell and Miss B.Maude, Chemical Preparative Group, Harwell, who kindly supplied the laser solutions.

II4. C.G.Young IEEE Proc. 57, I267 (I969)

II5. O.K.Deutschbein, C.C.Pautrat IEEE J. Quant. Electron. QE-4, 48 (I968)

II6. D. Röss 'Laser Lichtverstärker und Oszillatoren' Table I6-2 Akademische Verlag Frankfurt I966

II7. K.H.Hellwege 'Quantum Electronics III' 623 ed. P.Grivet, N. Bloembergen Columbia Univ. Press I964

II8. D.K.Rice, L.G.DeShazer Phys. Rev. I86, 387 (I969)

II9. L.G.DeShazer, L.G.Komai J. Opt. Soc. Am. 55, 940 (I965)

I20. 'Non-aqueous solvent systems' 332 ed. T.C.Waddington Academic Press I965

I2I. H.Samelson, C.Brecher, A.Heller J. Opt. Soc. Am. 58, I054 (I968)

I22. G.Raoult, F.Collier, H.Dubost Comptes Rendus 267, I420 (I968)

I23. V.R.Belan, V.V.Grigoryants, M.E.Zhabotinskii Opto-Electronics I, 33 (I969)

I24. T.M.Shepherd Nature 2I6, I200 (I967)

I25. International Critical Tables I: I09, I65 McGraw-Hill I926

I26. Physics Today 22, 55 (Nov. I969)

I27. F.Floux, D.Cognard, J-L. Bobin, F.Delobeau, C.Fauquignon Comptes Rendus 269 Ser.B, 697 (I969)

I28. Physics Today 22, 60 (June I969)

I29. R.C.Eckardt, C.H.Lee Appl. Phys. Letters I5, 425 (I969)

I30. H.Samelson, A.Lempicki, V.A.Brophy J. Appl. Phys. 39, 4029 (I968)

I3I. R.Y.Chiao, P.L.Kelley, E.Garmire Phys. Rev. Letters I7, II58 (I966); R.L.Carman, R.Y.Chiao, P.L.Kelley ibid. I28I(I966)

I32. R.G.Harrison, P.Key, V.I.Little, G.Magyar, J.Katzenstein Appl. Phys. Letters I3, 253 (I968)

I33. A.P.Veduta, B.P.Kirsanov ZhETF Pis'ma 7, 22I (I968) (JETP Letters 7, I69 (I968))

I34. V.S.Letokhov, B.D.Pavlik Zh. Tekhn. Fiz. 38, 343 (I968) (Sov. Phys. Tech. Phys. I3, 25I (I968))

I35. M.Iwata, R.Makabe, S.Katsube Jap. J. Appl. Phys. 4 Suppl.I, 347 (I965)

I36. M.Born, E.Wolf 'Principles of Optics' 68 Pergamon Press I959

I37. N.V.Tsederberg 'Thermal conductivity of gases and liquids' I99, 204 Edward Arnold I965

I38. International Critical Tables 3: 28,33; 5: I07, 227; 7: I2,35 McGraw-Hill I928-30

I39. A.Visapää Valt. Tekn. Tutkim. Tied. Ser.4 No.76 (I965)

I40. A.Javan, P.L.Kelley IEEE J. Quant. Electron, QE-2, 470 (I966)

I4I. W.F.Kosonocky, S.E.Harrison J. Appl. Phys. 37, 4789 (I966)

I42. F.Gires IEEE J. Quant.Electron. QE-2, 624 (I966)

I43. H.Margenau, G.M.Murphy 'The Mathematics of Physics and Chemistry' 237 D.Van Nostrand Princeton I956

I44. Communication from Dr. D.G.Wilkinson, King's College London.

I45. J.Katzenstein, G.Magyar, A.C.Selden Opto-Electronics I, I3 (I969)

I46. R.W.Ditchburn 'Light' 569 2nd edn. Blackie I963

I47. R.H.Pantell, J.Warszawski Appl. Phys. Letters II, 2I3 (I967)

I48. V.L.Broude, V.I.Kravchenko, P.P.Pogoretskii, E.N.Salkova, M.S.Soskin Doklady Akad. Nauk SSSR I73, 64 (I967) (Sov. Phys. Doklady I2, 2I4 (I967))

I49. G.Magyar, A.C.Selden Paper presented at the IERE Joint conference on 'Lasers and Opto-electronics' Southampton University March 25-28 I969

I50. V.I.Malyshev, A.S.Markin, A.V.Masalov, A.A.Sychov ZhETF 57, 827 (I969)

I5I. S.A.Collins, C.R.White 'Quantum Electronics III' I29I ed. P.Grivet, N.Bloembergen Columbia Univ. Press I964

I52. G.G.Stokes Proc. Roy. Soc. II, 545 (I862)

I53. J.M.Burch 'Quantum Electronics III' II87 ed. P.Grivet, N.Bloembergen Columbia Univ. Press I964

I54. F.A.Jenkins, H.E.White 'Fundamentals of Optics' 258 2nd edn. McGraw-Hill I950

I55. R.E.McClure Appl. Phys. Letters 7, I48 (I965)

I56. P.W.Smith IEEE J. Quant. Electron, QE-3, 627 (I967)

I57. M.Michon IEEE J. Quant. Electron. QE-2, 6I2 (I966)

I58. R.V.Pole, H.Wieder Appl. Opt. 3, I086 (I964)

I59. E.G.Berzing, Yu.V.Naboikin, I.A.Rom-Krichevskaya,Yu.A.Tiunov Opt. i Spektrosk. 22, 503 (I967) (Opt.Spectrosc. 22, 274 (I967))

I60. V.I.Little, D.Rowley J.Phys. E (Sci, Instrum.) 3 (I970 in press)

I6I. G.W.C.Kaye, T.H.Laby 'Tables of physical and chemical constants' 85 I3th edn. Longmans I966

I62. G.E.Devlin, J.McKenna, A.D.May, A.L.Schawlow Appl. Opt. I, II (I962)

I63. W.F.Hagen, P.C.Magnante J.Appl. Phys. 40, 2I9 (I969)

I64. D.Röss 'Laser Lichtverstärker und Oszillatoren' 405 ff. Akademische Verlag. Frankfurt I966

I65. C.J.Fan, C.B.Smoyer, J.Nuñez Appl. Opt. 3, I277 (I964); K.I.Krilov, N.E.Averianov, A.S.Mitrofanov, A.S.Ter-Pogosyan, S.E.Sharlai VUZ. Izvestiya 4, 9 (I967)

I66. Yu.A.Anan'yev, I.M.Buzhinskiy, M.P.Vanyukov, E.F.Dauengauer, O.A.Shorokhov Opt. Mekh. Prom. 35 (I968) (Sov. J. Opt. Techn. 35, 56I (I968))

I67. Yu.K.Danileiko, V.Ya.Khaimov-Mal'kov, A.A.Manenkov, A.M.Prokhorov IEEE J. Quant. Electron. QE-5, 87 (I969)

I68. M.J.Lubin, W.Leising Rev. Sci. Instrum. 38, II57 (I967); J.G.Edwards Opto-Electronics I, I (I969)

I69. W.E.K.Gibbs Appl. Phys. Letters II, II3 (I967)

I70. R.G.Harrison, P.Y.Key, V.I.Little J.Phys.D (Appl. Phys.) 3, 758 (I970)

I7I. T.Sasaki, T.Yamanaka, G.Yamaguchi, C.Yamanaka Jap.J.Appl. Phys. 8, I037 (I969)

I72. I.A.Sheka Russ. J. Inorg. Chem. 3, 343 (I958); B.A.Voitovich ibid. 5, 965 (I960); B.F.Markov ibid. 6, 6I6 (I96I)

I73. Communication from A.M.Deane, Chemistry Div. Harwell, who kindly performed the spectroscopic analysis.

I74. F.A.Jenkins, H.E.White 'Fundamentals of Optics' 562 2nd edn. McGraw-Hill I950

Laser Q-Switching by Organic Solvents

J. KATZENSTEIN, G. MAGYAR,* A. C. SELDEN†
UKAEA Research Group, Culham Laboratory, Abingdon, Berks, UK

Received 3 October 1968

The role of the solvent in the passive Q-switching of lasers by solutions of organic dyes has been examined in detail. It was found that several pure organic solvents could themselves partially Q-switch the laser, in the absence of the dye. This behaviour was observed for both ruby and neodymium : glass lasers. Pulse-widths as short as 20 nsec were occasionally recorded. Peak powers up to 2 MW have been observed using 1-chloronaphthalene to switch a ruby laser. It is proposed that Q-switching arises from an enhancement of reflectivity of the liquid, during the evolution of the laser pulse, through the formation of a periodic refractive index modulation in the liquid by the action of standing waves.

Offprint from:

Journal of Opto-electronics

CHAPMAN AND HALL
11 New Fetter Lane
London EC4

OPTO-ELECTRONICS 1 (1969) 13–19

Laser Q-Switching by Organic Solvents

J. KATZENSTEIN, G. MAGYAR,* A. C. SELDEN†
UKAEA Research Group, Culham Laboratory, Abingdon, Berks, UK

Received 3 October 1968

The role of the solvent in the passive Q-switching of lasers by solutions of organic dyes has been examined in detail. It was found that several pure organic solvents could themselves partially Q-switch the laser, in the absence of the dye. This behaviour was observed for both ruby and neodymium : glass lasers. Pulse-widths as short as 20 nsec were occasionally recorded. Peak powers up to 2 MW have been observed using 1-chloronaphthalene to switch a ruby laser. It is proposed that Q-switching arises from an enhancement of reflectivity of the liquid, during the evolution of the laser pulse, through the formation of a periodic refractive index modulation in the liquid by the action of standing waves.

1. Introduction

There has been much interest in the passive Q-switching of lasers by the saturable absorption of solutions of organic dyes [1-4]. Rate equation analyses of the laser pulse evolution and the bleaching of the dye [5, 6] have been made and compared with experiment. Mode locking [7, 8] has been achieved using dyes with a relaxation time less than the cavity round trip time, giving periodic pulse trains.

Less attention has been paid to solvent behaviour, the initial interest being to choose a particular solvent which produced the best match between the absorption peak of a given dye and the laser emission wavelength [6, 9]. More recently two effects of intracavity liquid cells on laser spiking operations have been reported [10, 11].

During the course of experiments aimed at achieving a better understanding of the passive Q-switching process and particularly the role of the solvent, we have discovered that in certain cases the pure solvent, itself, acts as a rudimentary passive Q-switch when placed in the laser cavity. Spiking behaviour is still observed, but the spikes become fewer, narrower in width, and enhanced in power. Typical values are an increase of peak power by a factor of 5 to 10 times compared with ordinary spiking, and pulse-widths in the range 50 to 200 nsec, compared with 500 nsec for the normal laser spikes. Pulse-widths as small as 20 nsec have been observed in particular cases. Both neodymium: glass and ruby lasers show this pulse-sharpening behaviour.

2. Experiments

The experiments were carried out with a simple arrangement consisting of a laser head housing the rod and one or more linear xenon flashtubes in a common reflector, and a pair of external plane dielectric coated mirrors which formed the optical cavity. The laser rods had Brewster angle faces and lightly ground sides. The ruby rod (154 × 12 mm) was pumped by a single flashlamp in an exfocal elliptical cylinder, and the neodymium : glass rod (154 × 9.5 mm Schott LG56 glass) was mounted in a Pyrex water-jacket and pumped by two lamps symmetrically disposed in a close-coupled arrangement. Liquid samples, contained in 2 cm optical quality cells of Spectrosil B were inserted in the cavity, and the mirrors aligned subsequently, using either an autocollimator or a helium: neon gas laser.

Part of the laser output was deflected for monitoring photoelectrically, using a fast planar photodiode (ITT F4000 or FW114A) and travelling wave oscilloscope (Tektronix 519). The main beam was used for measuring the energy calorimetrically, or for photographic recording of the near:field pattern. All measurements were made at room temperature (20 to 25° C).

The introduction of a liquid sample into the laser cavity (with the cell usually tilted a few degrees off-axis, although Brewster angle orientation was also used) resulted in pulse-sharpening behaviour in which the normal laser spikes, generated in the absence of the liquid cell, were replaced by narrower pulses of larger amplitude. The peak power was increased by 5 to 10 times, accompanied by a pulse-narrowing from the normal width of 500 nsec to the range 50 to 200 nsec, indicating a strong interaction between the active medium and the liquid during the generation of the laser spike. In the course of the pumping pulse (about 700 μsec duration) a series of

*Current address: Royal Holloway College, Englefield Green, Surrey, UK.
†Research Fellow, attached from Royal Holloway College.

such pulses is emitted, varying in height and width in a random manner from pulse to pulse over the range indicated, but always presenting a sharper appearance than the normal laser pulses, as can be seen in fig. 1. The behaviour for the various liquids is summarised in the accompanying table.

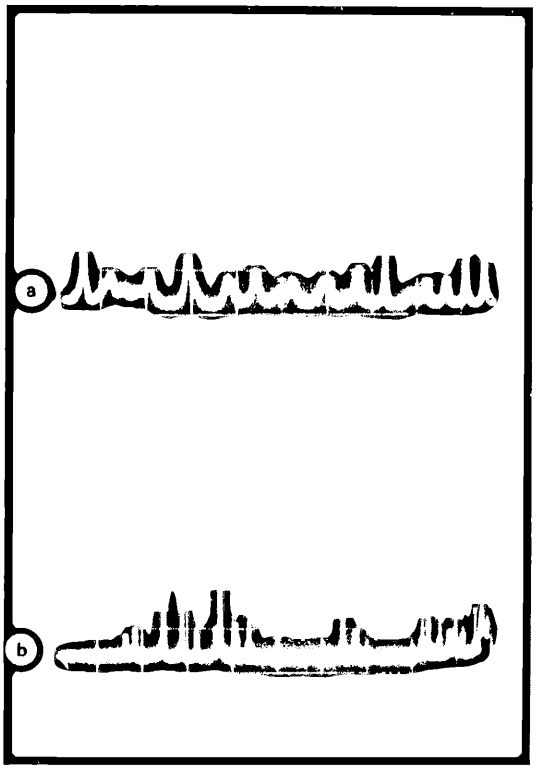

Figure 1 Pulse sharpening behaviour – neodymium: glass laser. (a) Normal spiking. (b) 2 cm cell of 1,2-dichloroethane in cavity, both 5 μsec/div.

Pulse widths as short as 20 nsec (methanol/neodymium : glass) and peak powers up to 2 MW (1-chloronaphthalene/ruby) were observed (fig. 2). With the notable exception of carbon disulphide, all the liquids tested were found to produce pulse sharpening with the neodymium : glass laser. A more restricted class showed this behaviour with the ruby laser.

Replacing the dielectric mirror with a resonant reflector (etalon) destroyed the effect in the case of ruby, presumably because the selective reflectivity prevented mode-locking, with its inherently greater peak power.

The near infra-red spectra of the common solvents [12] show that all the liquids which Q-switch the neodymium laser have an absorption band at the laser emission wavelength (1.06 μm). Measured transmission losses for a 2 cm cell ranged from

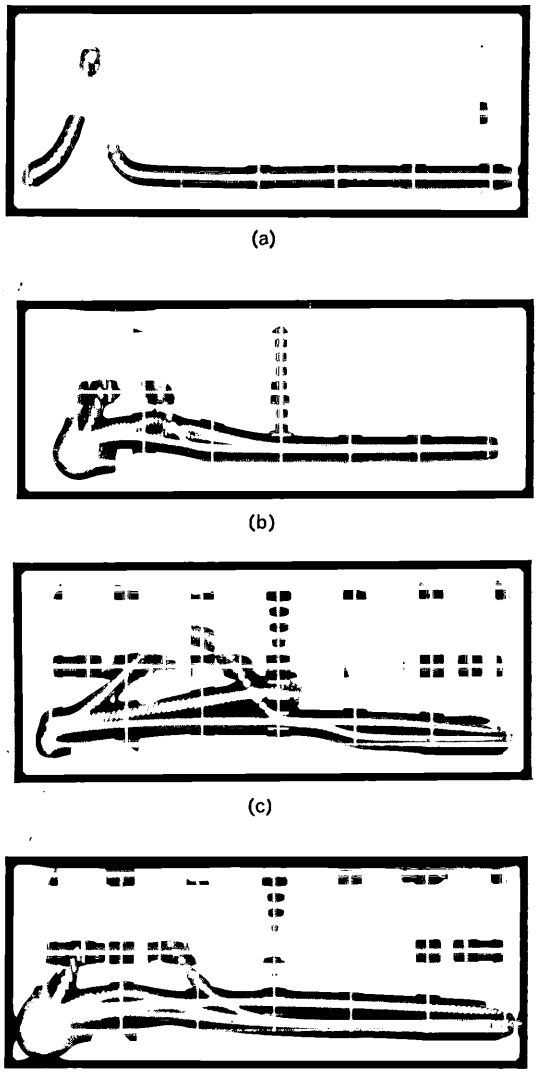

Figure 2 Pulse profiles. (a) 1-chloronaphthalene: ruby laser; 100 nsec/division. Vertical scale 1 M W/division approx. (b) Methanol:neodymium laser; 50 nsec/division. (c) Benzene:neodymium laser; 50 nsec/division. (d) Acetone:neodymium laser; 50 nsec/division.

approximately 1% to over 30%, depending on the liquid. These absorption bands correspond to overtones and combination tones of fundamental vibrations in the molecule, and are generally weak in the 1 μm region. Carbon disulphide, a non-hydrogenic molecule, has no measurable absorption at 1.06 μm and no switching action. Dry carbon tetrachloride, another non-hydrogenic molecule, also has zero absorption at the wavelength of the neodymium laser [12], but is hygroscopic and for this reason, or due to some other impurity, the experimental sample was found to have a very weak absorption band at

TABLE I Observed behaviour of Q-switching solvents.

Laser	Liquid	Pulse-width nsec	Remarks
Ruby	1-chloronaphthalene	35 to 50	2 MW pulse. 2-photon absorption
	methanol	50 to 100	Slightly impure
	methanol	No pulse sharpening	Pure (Analar)
	carbon disulphide	No pulse sharpening	
	n-phenyl-2-naphthylamine in absolute alcohol	50 to 100	Strong 2-photon absorption
	trans-trans-1,4-diphenyl-1,3-butadiene in absolute alcohol	100 to 150	2-photon absorption. Pulse-sharpening at elevated temperature
Nd:glass	acetone	35 to 100	
	benzene	75 to 150	
	carbon disulphide	No pulse sharpening	Zero absorption
	carbon tetrachloride	200 to 300	
	chlorobenzene	100	
	1-chloronaphthalene	70 to 200	
	1,2-dichloroethane	50 to 200	
	glycerol	150	
	methanol	20 to 100	Heavy modulation
	nitrobenzene	200	
	water (Analar distilled)	100 to 200	

the laser wavelength, producing approximately 1% absorption in the 2 cm cell. This was a borderline case, producing some enhancement of peak power but only a small reduction in pulse width. Benzene also has a very weak absorption band near 1 μm [12] but produces sharper pulses (75 to 150 nsec) than carbon tetrachloride.

The evidence suggests that the presence of an absorption band, even a very weak one, at the laser emission wavelength is a necessary condition for pulse sharpening in the case of the neodymium laser. Where it is strictly absent, as in the case of carbon disulphide, this behaviour is not observed. The laser then operates in the ordinary spiking mode. That the pulse sharpening phenomenon is a very sensitive indicator of the presence of a weak absorption band is shown by the carbon tetrachloride result.

In the case of the ruby laser the Q-switching liquids do not show any absorption at the laser wavelength (6943 Å), though the fact that pulse sharpening was observed with slightly impure methanol may be explicable in terms of a weak impurity absorption, as in the case of carbon tetrachloride with the neodymium laser, and underlines the importance of using pure materials in investigating these phenomena (Analar quality solvents were used wherever possible). The pulse sharpening action of 1-chloronaphthalene is so remarkable (2 MW, 35 nsec pulse) that the possibility of two photon absorption was considered, because this liquid has a strong absorption edge in the region of 3470 Å, half the ruby laser wavelength, and the cross-section for a transition from a bound state to the continuum is greatest at the absorption edge [26]. To test this idea, two dye solutions were made up, each with negligible absorption at 6943 Å but with a strong absorption edge corresponding to twice the fundamental frequency. They each produced pulse sharpening of the ruby laser emission. Hence in the case of ruby we have to consider a switching process initially involving loss at the harmonic of the laser frequency.

The necessity for a discrete transition coinciding with the harmonic of the ruby laser line received further confirmation on testing carbon disulphide, which did not produce pulse-sharpening although it is completely absorbing at 3470 Å, but the absorption edge lies in the region of 4000 Å.

It was also found that the same was true at the fundamental, a weak aqueous solution of copper sulphate, which absorbs in the red end of the spectrum, producing no pulse-sharpening. It is noteworthy in this connection that all the neodymium laser Q-switching liquids have a discrete absorption band coinciding with the emission wavelength.

That two photon absorption can produce a loss in the cavity was shown by inserting a cell of chloronaphthalene in the cavity of a single mode ruby laser, which suppressed laser action at the same pump power. The same cell placed in the output beam of the laser showed no appreciable absorption.

1-Chloronaphthalene is a sufficiently strong pulse-sharpening liquid to improve the performance of a passive Q-switching dye. For the same pumping level and output power the pulse width was less ($\sim$ 20 nsec) when the ruby was switched with vanadium phthalocyanine in 1-chloronaphthalene than with *o*-dichlorobenzene as the solvent ($\sim$ 30 nsec), and equalled the performance with cryptocyanine in methanol as the passive switching element.

In addition to the absorption requirement it was

found that the presence of standing waves in the liquid medium was a necessary condition for the pulse sharpening effect. This was observed by comparing laser spiking behaviour with the cell in the cavity with that for the cell placed external to the cavity but still in the path of the laser beam, beyond a 50% transmittance output mirror. The latter arrangement had no effect on the laser output, even for the best Q-switching liquids.

Similarly, when the liquid cell was incorporated in a second cavity coupled to the first, made by aligning a third mirror on the optic axis of the laser cavity beyond the output mirror, and placing the cell between the two, no pulse sharpening was observed.

A corollary of the necessity for standing waves was the observation of amplitude modulation of each pulse envelope at the fundamental frequency of the laser cavity, $\nu_L = c/2L$, where L is the optical path between the cavity mirrors. The modulation depth varied between approximately 10 and 50% of the total pulse amplitude, with little dependence on the liquid used. Carbon disulphide produced a small modulation of the pulse, although not acting as a Q-switching liquid. The amplitude of modulation was found to increase slowly on the rising edge of the pulse and decrease on the trailing edge. No modulation was observed for the ordinary laser spikes (neodymium laser). With the cell placed at successive distances L/m, m integral, from one cavity mirror the modulation frequency was measured. For $m = 1$ the modulation was regular and corresponded to the fundamental calculated from the measured optical path. For $m = 2$ modulation at twice this frequency was observed. However, the waveform differed from pulse to pulse, as though the relative phases assumed a different relation for each laser spike.

This was equally true for values of m up to 5, corresponding multiples of the fundamental frequency being observed in most cases. The waveforms presented a large variety of complex patterns, but were always repeated with the period of the fundamental [13]. These results imply that the liquid cell creates partial mode-locking in the laser cavity.

The insertion of a liquid cell in the laser produces a filamentary emission pattern in the beam. In ruby which already emits in filaments there is no marked difference, but the neodymium : glass laser near field pattern is changed from a uniformly intense emission over the rod cross-section to a mosaic of bright filaments. These are generally of the order of 1 mm diameter, but studies with the attenuated beam, and with small apertures placed over the photodetector show them to have brighter central regions of the order of $\frac{1}{3}$ mm diameter, in which at least half the total power is concentrated. As the emitted peak powers are several tens of kW, this implies intracavity intensities of $\gtrsim$ 50 MW/cm^2 acting on the liquid at the peak of the pulse. This figure could be higher if mode-locking were taken into account. Use of a $\frac{1}{2}$ mm aperture over the detector reduced the pulse width for benzene from 80 to 150 nsec to 60 to 100 nsec range.

3. Theory

A standing wave acts on an absorbing liquid to produce a stationary periodic modulation of the refractive index. Such a structure has been observed by Bragg reflection obtained in the dye cell of a giant pulse ruby laser [14]. This periodicity of refractive index will act as a spectrally selective reflector in exact analogy with the Lippmann plate, thus providing a dynamic increase in the cavity Q. Those modes which are in phase with the first standing wave set up in the cavity can successfully compete with neighbouring out of phase modes and therefore be amplified preferentially, leading to the observed modulation of the pulse envelope. A simple experiment to test for induced reflectivity in the liquid cell was devised on the assumption that the cell, the ruby and the output mirror form a sub-cavity during the evolution of the pulse.

When a second cell with a weak dye solution having a small absorption at the laser wavelength is inserted in this sub-cavity and the laser pumped a little above the normal threshold level, pulse generation is inhibited. If this cell is now moved to a position beyond the first cell, but still within the main cavity defined by the mirrors, sharp pulses are emitted at the same pumping power. This happens with both the two photon absorbers, and a cryptocyanine dye cell as the laser Q-switching element, suggesting that the induced reflectivity in the liquid cell is of the order of a few per cent.

The reflectivity of a periodic refractive index structure is a function of the index modulation amplitude, the number of periods and the detailed form of the periodic function. A study of the spectral reflectance of the Lippmann plate [15] has shown that a reasonable approximation to the reflectivity for a sinusoidal modulation can be calculated on a multi-layer stack model, alternate layers being assigned an appropriate mean refractive index value. The reflectivity of a stack of N double quarter-wave layers, of alternating index, is [16]:

$$R_{2N} = \left(\frac{\mu^{2N} - 1}{\mu^{2N} + 1}\right)^2 \qquad (1)$$

where μ is the ratio of refractive indices.

If the index modulation amplitude Δn is small compared with the unperturbed index n_0, then

$$\mu = 1 + \tfrac{1}{2}\frac{\Delta n}{n_0} \qquad (2)$$

approximately, assuming a gentle modulation

function (e.g. sinusoidal). Because μ is very close to unity ($\Delta n \ll n_0$), we may write for the reflectivity,

$$R_{2N} = \tanh^2 N\delta \tag{3}$$

where $$\delta = \tfrac{1}{2}\frac{\Delta n}{n_0}$$

For $N\delta \lesssim 0.3$, we can employ the approximate formula,

$$R_{2N} = (N\delta)^2 \tag{4}$$

with an error of less than 6%.

(Note that for $N\delta \to \infty$, R_{2N} calculated from equation 3 is asymptotic to unity, thus satisfying the requirement for a physically real solution.)

The period of spatial modulation due to a standing electromagnetic wave is $\frac{1}{2}\lambda$, where λ is the wavelength in the medium, and the effective number of double layers in a length L is therefore,

$$N = \frac{2n_0 L}{\lambda_0} \tag{5}$$

where λ_0 is the wavelength in vacuo.

Inserting the values: $L = 2$ cm, $n_0 = 1.5$, $\lambda_0 = 10^{-4}$ cm and $\Delta n = 10^{-5}$ in equations 3 and 5 we obtain the result $R_{2N} = 4\%$, which is of the order of the reflectance value deduced experimentally.

A standing wave in an absorbing dielectric medium can induce a periodicity in refractive index in two ways, (i) through non-linear intensity-dependent effects – optical Kerr effect, saturable absorption, electrostriction [17, 18], or (ii) thermally, whereby energy absorbed at the antinodes and dissipated as heat raises the local temperature above that at the nodes, where the rate of energy deposition is zero. The saturable absorption process appears to be ruled out for the solvents because of the intrinsically low absorption cross-section per molecule ($\sim 10^{-23}$ cm^2) and short lifetime [19] ($\tau_{vib} \sim 10^{-2}$ nsec), but is not negligible in the Q-switching dyes, where $\Delta n \sim 10^{-5}$ at saturation for a 3 mm cell with initial transmittance of 35%. In this case the actual Q-switching is due to removal of the large absorption loss, but the spectral selectivity introduced by the periodic structure may explain the observed line-narrowing in dye-cell switched lasers [20], and can also account for the phenomenon of mode-locking in cavities where all other mode-selective elements have been removed.

The intensity-dependent refractive index change [17, 18] will be proportional to the instantaneous value of the intensity and will therefore keep step with the pulse profile. The dynamic behaviour provides a regenerative feedback mechanism for Q-switching the laser cavity. Taking molecular redistribution effects into account [21], we find $\Delta n \sim 10^{-6}$ to 10^{-5} for a peak intensity of 50 MW/cm^2 in the filament, depending on the liquid. The presence of a molecular transition coinciding with the laser wavelength (vibrational level) or the 2nd harmonic (electronic level) will make a contribution to the intensity-dependent refractive index through the enhanced polarisability of the molecule. This may explain, in part, the experimental observation on the necessity of such a coincidence for pulse-sharpening.

For the thermally-induced refractive index modulation we have to consider the thermal diffusion equation driven by a source function varying in space and time. In one dimension:

$$K\frac{\partial^2\theta}{\partial x^2} + u(x,t) = c\rho\frac{\partial\theta}{\partial t} \tag{6}$$

where K is the thermal conductivity, c the specific heat and ρ the density of the medium, and $u(x, t)$ the local rate of heat generation, θ the local temperature rise.

For a standing wave, periodic in the x-direction, if we assume the local rate of energy absorption to be proportional to the local intensity, we may write:

$$u(x,t) = u_0 f(t)\cos^2 kx \tag{7}$$

Considering the rising front of the pulse to be of exponential form, we may solve equation 6 with:

$$f(t) = e^{at} \tag{8}$$

to obtain the development of the thermal lattice during the Q-switching process. Thereafter, the behaviour of the thermal modulation will follow the pulse, but the interaction between the front of the laser pulse and the medium is of chief interest here.

The solution for θ, with $u(x, t)$ defined by equations 7 and 8 is:

$$\theta(x,t) = \frac{u_0}{2ac\rho}e^{at}\left\{1 - \left(1 + \frac{4Kk^2}{ac\rho}\right)^{-1}\cos 2kx\right\} \tag{9}$$

as may be seen on inspection. The competition between the heat input rate and loss by thermal diffusion is clearly indicated by the coefficient of the cosine term (the modulation amplitude). The amplitude of the temperature variation is therefore,

$$\Delta\theta(t) = \frac{u_0 e^{at}}{ac\rho + 4Kk^2} \tag{10}$$

For a mean intra-cavity intensity $I_0 e^{at}$, the absorption rate at the anti-nodes of the standing wave,

$$u_0 = 2\alpha I_0 \tag{11}$$

where α is the linear absorption coefficient in the medium. (For the ruby laser liquids we require the theory of two-photon absorption, itself an intensity-dependent process.) The thermal refractive index modulation corresponding to equation 10 would be:

$$\Delta n_{th} = \left(\frac{\partial n}{\partial\theta}\right)_{\theta_0}\Delta\theta(t) \tag{12}$$

approximately, for a small overall increase in temperature. For the liquids investigated $10^{-2} \lesssim \alpha \lesssim 0.15$ cm^{-1}. Taking an average value $\alpha = 0.05$ cm^{-1} and the beam intensity $I = 25$ MW/cm^2 at half-peak, beyond which the rise rate is no longer exponential, and recognising that this point is reached after many e-folding times, we may set $a \sim 10^8$ sec^{-1} for an observed rise time of 50 nsec. With $K/\rho c \sim 10^{-3}$ cm^2/sec, $k = 2\pi.10^4$ cm^{-1} (for a wavelength of 10^{-4} cm), and $\rho c \sim 2$ j/cm^3 (°C)$^{-1}$, we find $\Delta\theta \sim 10^{-2}$ °C. The temperature coefficient for many of these liquids at 20° C at the wavelength of the sodium D-line is $\partial n/\partial\theta \simeq -0.0005$ (°C)$^{-1}$. Employing this value we would get $\Delta n_{\text{th}} \sim -5.10^{-6}$. Thus the thermal effect appears to produce the same order of magnitude change in refractive index as the intensity-dependent effects, but of opposite sign. However, unlike field effects which have a rapid response ($\tau \sim 10^{-11}$ to 10^{-13} sec) to the electromagnetic wave, the thermal modulation relies on the establishment of a density wave, driven by the local dissipation of heat. This is an inherently slower process which will in addition be opposed by electro-striction tending to create a density *increase* at the anti-nodes of the standing light wave, and hence retard the thermal expansion (since the latter produces a *decrease* in density).

Therefore it is expected that the Q-switching of the initial loss in the laser cavity will be initiated by intensity-dependent effects and subsequently taken over by the thermal lattice, probably near or after the peak of the emitted pulse. The resultant phase grating will then decay by thermal diffusion, with a decay time $\tau \sim 10^{-7}$ sec (for $\lambda = 10^{-4}$ cm, $n_0 = 1.5$ and diffusivity $D \sim 10^{-3}$ cm^2 sec^{-1}). Experimental evidence lending support for these conclusions is provided by the Bragg reflection studies with variable time delay [14].

4. Summary and Conclusions

The observed pulse-sharpening behaviour of organic solvents placed in the laser cavity can be explained on the basis of an induced phase grating in the liquid serving to increase the cavity Q during the evolution of the pulse. The stationary periodic refractive index structure, with a spatial period of half the optical wavelength in the medium, will decay thermally with a characteristic time $\tau \sim 10^{-7}$ sec and should be observable both during and after the pulse by Bragg reflection techniques [14].

The remarkable behaviour of 1-chloronaphthalene in Q-switching the ruby laser may be attributed to its larger optical Kerr coefficient and high two photon absorption. By contrast, distilled water, which absorbs the neodymium laser radiation at 1.06 μm quite strongly, has a small optical Kerr constant and a variation of refractive index with temperature some seven times smaller than average, and consequently a relatively weak Q-switching behaviour.

The pulse-sharpening process is very sensitive to residual absorption present in the solvent, as shown by carbon tetrachloride and slightly impure methanol, and may prove a delicate test of the existence of a weak absorption band.

Carbon disulphide does not produce pulse narrowing, a fact which argues against Brillouin scattering as the explanation because this is one of the best scattering liquids [23], and has been used to Q-switch both the ruby and neodymium : glass lasers by backward stimulated Brillouin scattering [22]. No studies of the dependence of pulse-sharpening on the temperature of the liquid have been made in this connection [18]. The fact that Bragg reflection from the postulated periodic structure is observed below the threshold for stimulated Brillouin scattering [14] is further evidence in support of this conclusion.

Stimulated thermal Rayleigh scattering [24] may provide an alternative explanation for pulse-sharpening behaviour. In this process the back-scattered intensity of laser light incident on an absorbing liquid is enhanced through interaction with large, coherent density fluctuations produced by local heating. If such a liquid were present in the laser cavity a dynamic increase in feedback would be expected. A 2 cm cell containing a solution of iodine in carbon tetrachloride (as used for the reported observation of stimulated thermal Rayleigh scattering [25]) when placed in the ruby laser cavity did show some pulse sharpening (width approximately 150 nsec). However, solutions having an absorption coefficient greater than 0.1 cm^{-1} were required for observing the stimulated Rayleigh effect [24, 25], whereas pulse sharpening behaviour occurs in liquids with an absorption as low as 0.01 cm^{-1} (using the neodymium laser).

The organic solvents used in the neodymium : glass laser experiments have absorption bandwidths of the same order as the Nd^{3+} fluorescence emission at 1.06 μm, and the induced lattice structure possesses mode-selection properties. It follows that the emission spectra of the laser incorporating a liquid cell in the cavity should be modified, and therefore worth investigating. It is hoped to undertake such spectral studies in the near future.

Acknowledgements

One of us (A.C.S.) is grateful to the UKAEA for the support of a fellowship, and G.M. acknowledges financial support by the SRC.

References

1. P. P. SOROKIN, J. J. LUZZI, J. R. LANKARD, and G. D. PETTIT, *IBM Journ. Res. Dev.* **8** (1964) 182-184.
2. P. KAFALAS, J. I. MASTERS, and E. M. E. MURRAY, *J. Appl. Phys.* **35** (1964) 2349-2350.
3. B. H. SOFFER and R. H. HOSKINS, *Nature* **204** (1964) 276.

4. V. I. MALYSHEV, A. S. MARKIN, V. S. PETROV, I. I. LEVKOEV, and A. F. VOMPE, *JETP Lett.* **1** (1965) 159-160.
5. A. SZABO and R. A. STEIN, *J. Appl. Phys.* **36** (1965) 1562-1566.
6. F. GIRES and F. COMBAUD, *J. de Phys.* **26** (1965) 325-330.
7. A. J. DEMARIA, D. A. STETSER, and H. HEYNAU, *Appl. Phys. Lett.* **8** (1966) 174-176.
8. M. DIDOMENICO, J. E. GEUSIC, H. M. MARCOS, and R. G. SMITH, *Appl. Phys. Lett.* **8** (1966) 180-183.
9. D. RÖSS, *Z. Naturforschg.* **20a** (1965) 696-700.
10. V. L. BROUDE *et al*, *Sov. Phys. Doklady* **12** (1967) 214-216.
11. R. H. PANTELL and J. WARSZAWSKI, *Appl. Phys. Lett.* **11** (1967) 213-215.
12. A. VISAPAA, *Valt. Tekn. Tutkim. Tied*, Series 4, No. 76 (1965).
13. R. HARRACH and G. KACHEN, *J. Appl. Phys.* **39** (1968) 2482-2483.
14. R. HARRISON, P. KEY, V. I. LITTLE, G. MAGYAR, and J. KATZENSTEIN, *Appl. Phys. Lett.* (to be published).
15. M. IWATA, R. MAKABE, and S. KATSUBE, *Jap. J. Appl. Phys.* **4**, Suppl. 1 (1965) 347-351.
16. M. BORN and E. WOLF, "Principles of Optics", (Pergamon Press, Oxford, 1959) p. 68.
17. N. BLOEMBERGEN, *Amer. J. Phys.* **35** (1967) 989-1023.
18. Y. R. SHEN and Y. J. SHAHAM, *Phys. Rev.* **163** (1967) 224-231.
19. D. G. WILKINSON, Physics Department, King's College, London WC2 (private communication).
20. B. B. MCFARLAND, R. H. HOSKINS, and B. H. SOFFER, *Nature* **207** (1965) 1180-1181.
21. R. W. HELLWARTH, *Phys. Rev.* **152** (1966) 156-165.
22. D. POHL, *Phys. Lett.* **24A** (1967) 239-240.
23. E. GARMIRE and C. H. TOWNES, *Appl. Phys. Lett.* **5** (1964) 84-86.
24. R. M. HERMAN and M. A. GRAY, *Phys. Rev. Lett.* **19** (1967) 824-828.
25. D. H. RANK, C. W. CHO, N. D. FOLTZ, and T. A. WIGGINS, *Phys. Rev. Lett.*, **19** (1967) 828-830.
26. W. HEITLER, "Quantum Theory of Radiation", 3rd edition (Oxford University Press, Oxford, 1954) p. 204.